IMPROVING PERFORMANCE OF BODY SENSOR NETWORKS IN MODERATE-SCALE DEPLOYMENT SCENARIOS

SUN WEN

(*B. Eng., Harbin Institute of Technology, China*)

A THESIS SUBMITTED FOR THE DEGREE OF

DOCTOR OF PHILOSOPHY

DEPARTMENT OF ELECTRICAL AND COMPUTER ENGINEERING

NATIONAL UNIVERSITY OF SINGAPORE

2014

Declaration

I hereby declare that this thesis is my original work and it has been written by me in its entirety.

I have duly acknowledged all the sources of information which have been used in the thesis.

This thesis has also not been submitted for any degree in any university previously.

Sun Wen

SUN WEN
28/05/2014

To my parents.

Acknowledgements

I would like to thank several people who have contributed in different ways towards the work accomplished in this thesis.

First and foremost, I would like to express my utmost gratitude to my supervisor, Prof. Wong Wai-Choong, Lawrence, for his constant encouragement, guidance, and support. His wide knowledge and insightful comments have made my candidature a truly enriching experience.

I would also like to express my sincerest appreciation to my co-supervisor, Dr. Ge Yu. Her patience, motivation, and guidance have benefitted me immensely. This thesis work would not have been possible without her insightful thoughts.

My sincere thanks also goes to Prof. Mehul Motani and Prof. Soh Wee-Seng, for their time and efforts in assessing my research work, for the valuable suggestions and critical questions during my qualification examination.

I would like to thank my colleagues and lab mates, Ji Lianying, Zhang Zhiqiang, Lu Yu, Chen Qian, Jin Yunye, Wang Lei, and Wang Xiaoqiong for the stimulating discussions, for the accompany when we were working together, and for all the fun we have had in the last four years.

Finally, I am deeply indebted to my parents for their love and support, which provide me the motivation for everything.

Contents

Summary

Body Sensor Networks (BSNs) have been attracting intense research interest over the recent years due to their potential in practical applications such as healthcare monitoring, sports training, and interactive gaming. A BSN comprises multiple sensor nodes and a coordinator worn on a human body. The physiological information of the human body collected by the sensor nodes is first delivered to the coordinator, which then forwards the information to a remote server through a network interface for further processing. In a moderate-scale BSN deployment scenario, the performance of a BSN may deteriorate due to a number of factors, including handover failure and inter-user interference. In particular, a handover is required to maintain network connectivity, when a BSN that is linked to the backbone via a wireless network interface moves from one coverage zone to another. Inter-user interference is incurred by simultaneous transmissions of BSNs in the same vicinity. This thesis makes a fourfold contribution to the investigation of handover scheme and inter-user interference in BSNs.

Firstly, we present an improved handover scheme with movement trend awareness for BSNs. Handover initiation time is optimized to minimize the outage probability while the handover rate is estimated to meet the requirement. Simulation results show that the proposed scheme reduces the outage probability by 21% as compared with the existing hysteresis-based handover scheme under the constraint

of acceptable handover rate.

Secondly, we investigate the prevalence and severity level of inter-user interference in a realistic BSN deployment scenario in a hospital. The effects of multiple factors are considered, including BSN density, traffic load, and transmission power. Simulation results show that only 68.5% of data transmission in BSNs meets the reliability requirement even in the off-peak period.

Thirdly, we propose a lightweight and distributed inter-user interference mitigation (IIM) scheme. The proposed scheme takes into consideration the generic property of low channel utilization in BSNs and enables affected BSNs to adaptively reschedule their transmission time or switch channels. Based on the detected information from neighboring BSNs, BSNs reschedule their transmissions in a distributed and coordinated manner, so that wireless channels can be effectively utilized by multiple BSNs. Simulation results show that the proposed scheme improves the network throughput by 18% and reduces the energy consumption by 22% as compared with the existing beacon schedule scheme.

Fourthly, we present a stochastic geometry analysis of inter-user interference in BSNs. In the analysis, we evaluate the performance of BSNs in terms of outage probability and spatial throughput by averaging over all potential geometrical realizations for the BSN interferers. The effects of the IEEE 802.15.6 medium access control (MAC) are considered, where multiple MAC states, either contention-free or contention-based, coexist in the BSN application area at a given time. Based on the analysis, the interference detection range is optimized to achieve the maximum spatial throughput while the reliable transmission requirement is met. Moreover, implications are provided on the design of MAC protocol for BSNs based on the specific BSN applications.

List of Tables

List of Figures

List of Symbols

Symbol	Meaning
$X_k = [s, v, a]^T$	state vector of Kalman filter
$s = [s_x, s_y]^T$	BSN position along x-axis and y-axis
$v = [v_x, v_y]^T$	BSN velocity along x-axis and y-axis
$a = [a_x, a_y]^T$	BSN acceleration along x-axis and y-axis
$z_k = [s, a]^T$	measurement vector of Kalman filter
F_k	state transition matrix of Kalman filter
w_k	process noise
n_k	measurement noise
$\bar{v}$	average velocity of the historical trajectory
σ	the standard deviation
τ	prediction period
θ	target outage probability in handover
ξ	target unnecessary handover rate
$t,\ i,\ j,\ k,\ n$	indices
P_{con}	confidence probability
P_{out}	outage probability in handover scheme
$\hat{s}$	mean of predicted position
$\tilde{s}$	the distance along the orthogonal direction of the AP boundary

Symbol	Meaning
$\Delta\tilde{s}$	mean of $\tilde{s}$ along the orthogonal direction of the AP boundary
i_{opt}	the optimal handover initiation time
$\hat{s}_{i,opt}$	the optimal handover initiation position
$Q(\cdot)$	complementary function of standard Gaussian random variable
Ω_0	transmit power
Ω	received power
Ω_n	noise power
Ω_I	interference power
$l(\cdot)$	path loss function
α_o	on-body path loss exponent
α_I	inter-body path loss exponent
h	multi-path fading component
γ	shadow fading component
G	system loss
d_0	reference distance
d	distance
$\mathbb{1}$	transmission indicator of a BSN
$erfc(\cdot)$	complementary error function
$\lfloor\cdot\rfloor$	integer floor function
P_{BER}	bit error rate
P_{PER}	packet error rate
P_{SINR}	signal to interference noise ratio (SINR)
SD	superframe duration
BI	beacon interval
$(b_1, ..., b_n)$	the set of time slots

Symbol	Meaning
$(c_1, ..., c_m)$	available channel set
t^i_{temp}	possible transmission time for BSN i
$N_{\max}$	the maximum number of BSNs that can be supported by IIM
$N^{UB}_{\max}$	the upper bound of $N_{\max}$
$N^{LB}_{\max}$	the lower bound of $N_{\max}$
W	backoff window size
T_{delay}	rescheduling delay
T_{listen}	listening delay
T_{wait}	waiting delay
$T_{compete}$	competition delay
$T_{backoff}$	backoff delay
Φ_0	the set of BSNs which actually deployed in application area with intensity of λ_0
Φ_1	the set of BSNs which intend to transmit under contention-free scheme with intensity of λ_1
Φ_2	the set of BSNs which intend to transmit under contention-based scheme with intensity of λ_2
Φ_m	the set of BSNs in modified Matern point process with intensity of λ_m
Φ	the set of the interfering BSNs with intensity of λ
r	the distance between coordinator and sensor node in a BSN
R	interference detection range
u	the distance between two BSNs
$\{Y_1, Y_2, ..., Y_k, ...\}$	the set of BSN locations
$B(Y_k, R)$	the observation area at Y_k with radium R

Symbol	Meaning
φ	throughput
$m(\cdot)$	the Matern mark
$Q(\cdot)$	complementary function of standard Gaussian random variable
$f(\cdot)$	probability density function
$\exp(\cdot)$	exponential function
$\log(\cdot)$	logarithm function
$E[\cdot]$	expected value
β	the acceptable SINR threshold
η	duty cycle of a BSN
P_o	outage probability
ψ	spatial throughput
κ	the target outage probability in a BSN
w_1	the ratio of contention-free traffic to the total traffic in a superframe
w_2	the ratio of contention-based traffic to the total traffic in a superframe

Chapter 1

Introduction

1.1 Background

Advances in wireless communication technologies and recent developments in miniaturized computing devices have empowered the implementation of body sensor networks (BSNs) [1]. BSNs provide remote and continuous health monitoring for users without constraining their movements, and thus serve in a wide spectrum of applications, such as rehabilitation supervision, sports training, interactive gaming, and personal information sharing [2, 3].

Fig. 1.1 illustrates the common architecture of BSNs. A BSN comprises multiple sensor nodes and a coordinator worn on a human body. Sensor nodes measure the physiological information of the BSN user (e.g., heart rate, blood pressure, body and skin temperature, oxygen saturation, respiration rate). The sensory data is delivered to the coordinator on the body (e.g., a personal digital assistant, a smart phone, or a micro-controller board), which then in turn displays the corresponding information on a user interface or transmits the aggregated vital signs to a remote server through a network interface for further processing [4, 5]. As

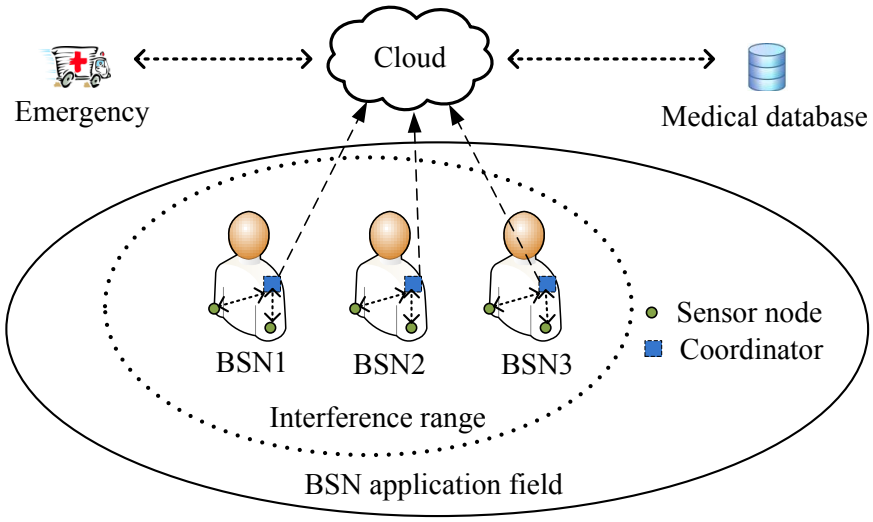

Fig. 1.1: The common architecture of BSNs.

in BSN application area, e.g., inpatient department or emergency department in a hospital, wireless local area network (WLAN) access points (APs) are commonly deployed for public Internet services, a BSN always connects to an applicable WLAN AP (as the network interface) when multiple interfaces, e.g., cellular network and WLAN, may be available.

Due to the presence of the human body, BSNs have some stringent requirements for communication systems:

- **Quality of service (QoS)**: QoS measures the overall performance of a wireless network in terms of throughput, transmission delay, error rates, bandwidth, etc [6, 7]. In BSNs, where health and motion information are monitored in real-time, QoS requirements are strict.

- **Energy efficiency**: Sensor nodes in BSNs are typically battery-powered, and difficult to charge especially for implanted sensor nodes [8]. An energy efficient communication protocol conserves energy by reducing protocol overhead, retransmission, and collisions, and thus extends the lifetime of a

BSN [9, 10].

- **Heterogeneous data rate**: Heterogeneous sensor nodes are employed in BSNs with various data rate requirements (e.g., 5 kbps for Electrocardiograph (ECG) and Electroencephalography (EEG), and 1 kbps for temperature sensor, respiratory sensor, and pulse sensor [11]). A flexible communication system for BSNs should accommodate the traffic with heterogeneous data rate requirement.

1.2 Motivation

In a moderate-scale BSN deployment scenario, the performance of a BSN may deteriorate due to a number of factors, including data packet collisions among sensor nodes in a BSN, dynamic channel condition, network connectivity failure, and inter-user interference. As extensive works have been done on the first two issues in the recent years [12–14], we focus on the network connectivity issue (handover scheme) and inter-user interference in BSNs in this thesis. In particular, we first conduct a preliminary study on and propose a handover scheme, and then perform an in-depth investigation on inter-user interference and its mitigation in BSNs.

1.2.1 Handover scheme

When a BSN that is linked to Internet via a WLAN AP moves from one coverage zone to another, a handover is required to maintain network connectivity. Handover schemes have been widely studied in wireless networks where received signal strength indicator (RSSI) is utilized as a common metric. However, fluctuations of RSSI associated with shadow fading and multipath fading

cause a call to be repeatedly handed over between neighboring APs, increasing handover rate (consuming additional network resources). To reduce the handover rate, several location-based handover schemes have been proposed using timers or hysteresis [15, 16]. Lin et al. [15] proposed a handover scheme based on the estimated location and velocity of mobile station to identify correlation among shadowing components, so that the number of unnecessary handover is reduced under the constraint of acceptable outage probability. Inzerilli et al. [16] proposed a location-based vertical handover scheme, where handover is carried out by following a goodput estimation phase in order to maximize goodput and limit the unnecessary handover. Note that handover performance is not only related with the current location of a mobile station but also with the movement trend (movement pattern, direction, and velocity) of the mobile station [17]. Mechaelis et al. [18] utilized mobility prediction technologies to aid and prepare for handover in advance. The prediction is based on statistical data gained from the observation of movement across multiple cells. However, as a BSN is a small-scale network (in terms of both its network size and its mobility area), the mobility prediction in [18] is inaccurate and thus inapplicable in BSNs.

BSNs have some specific characteristics which provide potentials to improve the mobility prediction and aid the handover decision accordingly. In particular, BSNs typically move within a relatively constrained area, e.g., an inpatient or emergency department in hospital, and the movement trend of a BSN highly depends on the spatial deployment of the BSN application area as well as the personal habits of the BSN user. With this movement trend, the handover decision can be made more intelligently in a relatively long term. In this thesis, we proposed an improved handover scheme with movement trend awareness for BSNs.

1.2.2 Inter-user interference

Inter-user interference is incurred by simultaneous transmissions of BSNs in the same vicinity [19–21]. Natarajan et al. [22] highlighted the existence of inter-user interference, and found that such interference reduces packet delivery rate by 35% in the presence of eight or more interfering BSNs. Such a situation is aggravated when more BSN applications are deployed. The existing interference mitigation methods designed for other networks are not well suited to BSNs due to the following reasons:

First, the BSN communication has stringent requirements (as aforementioned) such as reliability and energy efficiency in healthcare applications. The commonly used contention-based carrier sense multiple access with collision avoidance (CSMA/CA) method [23] may not be able to satisfy the communication requirement of BSNs due to its unreliable clear channel assessment, traffic correlation, and severe collisions [24].

Second, exchange of messages exists only within the cluster of sensor nodes in a BSN and there is no message exchanges among BSNs. Without inter-BSN communication, it is challenging for BSNs to collect the surrounding information and take actions in a coordinated manner to reduce interference. For example, the mesh election algorithm effectively avoids collisions in the IEEE 802.16 wireless mesh network [25, 26] by using the neighborhood information obtained by inter-device coordination. However, such coordination is inapplicable in BSNs.

Third, BSNs are usually mobile which differentiates them from most other wireless sensor networks (WSNs) [27–29]. In WSNs, inter-cluster interference can be minimized by a self-organizing medium access control (MAC) allocation scheme based on the feedback derived from collisions experienced by the local nodes within a cluster [30]. This method is difficult to apply in BSNs, as the delay for the

feedback becomes intolerable when mobility is involved. Another similar example is the cluster scheduling and collision avoidance problem in IEEE 802.15.4 beacon-enabled cluster-tree WSNs [31], in which beacons from different clusters are assigned to transmit in their dedicated time slots using a time division method. However, a static and predefined deployment of wireless nodes is assumed, making it inapplicable in dynamic mobile BSN scenarios.

The above mentioned challenges motivate us to design a lightweight and distributed inter-user interference mitigation (IIM) scheme explicitly for BSNs. Towards this goal, first we study the prevalence and severity of the inter-user interference in a realistic BSN deployment scenario. Then we propose an IIM scheme, which takes into consideration the generic property of low channel utilization in BSNs and enables BSNs to adaptively reschedule their transmission time or channel if interference occurs. Finally, we present a stochastic geometry analysis of the inter-user interference to evaluate the performance of BSNs and optimize the general parameter such as interference detection range. This interference analysis is necessary and of significance, because the IEEE 802.15.6 MAC is a hybrid MAC protocol where BSNs may be at either contention-based or contention-free state at a given time in the absence of global synchronization, such MAC operations will incur more complex geometry distribution of the interferers compared to usual wireless networks with a single MAC operation [32–36].

1.3 The main contributions of the thesis

The main contributions of this thesis are as follows.

First, we propose an improved handover scheme with movement trend awareness for BSNs. The proposed scheme predicts the future position of a BSN user

using the movement trend extracted from its historical position, and adjusts the handover decision accordingly. Handover initiation time is optimized when the unnecessary handover rate is estimated to meet the requirement and the outage probability is minimized. Simulation results show that the proposed scheme reduces the outage probability by 21% as compared with the existing hysteresis-based handover scheme under the constraint of acceptable handover rate.

Second, we evaluate the performance of BSNs in the presence of inter-user interference in a realistic moderate-scale deployment case in hospital. Our study considers multiple factors that affect the BSN performance, including BSN density, traffic load, and transmission power. Simulation results show that with 20% duty cycle, only 68.5% of data transmission can achieve the targeted reliability requirement even in the off-peak period.

Third, we design a lightweight and distributed IIM scheme explicitly for BSNs. We take into consideration the generic property of low channel utilization in BSNs and enable BSNs to adaptively reschedule their transmission time or channel if interference occurs. It includes dynamic detection of inter-user interference, collection of neighboring information, and rescheduling of transmission accordingly. The proposed scheme is reservation-based, while the benefits of reservation-based and contention-based schemes are combined to reduce the rescheduling cost. Then, we conduct extensive performance evaluation through simulations and prove that the proposed scheme significantly improves throughput and energy consumption, as spectrum utilization is improved by rescheduling the transmissions of multiple BSNs on the same channel for the low loading BSN scenarios.

Fourth, we present a stochastic geometry analysis of the inter-user interference in IEEE 802.15.6 BSNs. The analysis evaluates the performance of BSNs in terms of outage probability and spatial throughput by averaging over all po-

tential geometrical realizations for the BSN interferers. Compared to the existing stochastic geometry analysis [37–39], we relax the assumptions that each node in the network follows the same MAC protocol at a given time. In our study, although all the BSNs employ the hybrid MAC structure defined in IEEE 802.15.6, BSNs may be at either contention-based or contention-free state at a given time in the absence of global synchronization. Based on the analysis, the interference detection range is optimized to achieve the maximum spatial throughput while the reliable transmission requirement is met. Moreover, implications are provided on the design of MAC for BSNs depending on the specific BSN applications. Finally, we conduct extensive simulations to validate the analysis.

1.4 Organization of the thesis

The remainder of the thesis is organized as follows. Chapter 2 summarizes the works related to this thesis. In Chapter 3, we propose an optimized handover scheme with movement trend awareness for BSNs. Chapter 4 studies the prevalence and severity of inter-user interference in a realistic BSN deployment scenario. In Chapter 5, we propose a lightweight and distributed mitigation scheme for inter-user interference in BSNs, with simulation verifications. In Chapter 6, we develop a stochastic geometry analysis of inter-user interference in BSNs. Chapter 7 contains a summary and suggestions for future research in this direction.

Chapter 2

Related Works

In this chapter, we first give a brief overview of the communication technologies in BSNs, then review the related works on handover schemes, and finally classify the related works on inter-user interference in BSNs into two categories, namely interference mitigation and interference analysis.

2.1 Communication technologies

In BSNs, a communication technology needs to meet the stringent requirement of BSNs (QoS, energy efficiency, scalability for heterogeneous data rate) considering the specific characteristics of BSNs. The applicable technologies include Bluetooth, IEEE 802.15.4 and IEEE 802.15.6 [40–42].

Bluetooth is a wireless technology standard for exchanging data over short distances between mobile devices. It works in the industrial, scientific and medical (ISM) radio bands from 2.4 to 2.485 GHz. In order to alleviate interference from other technologies which also work in this band such as Wi-Fi and ZigBee, Bluetooth uses frequency-hopping spread spectrum. Frequency hopping is to transmit

each packet on one of the 79 channels, and change channel after each transmission. Bluetooth adopts master-slave topology, supporting up to seven slaves. The number of slaves can be expanded by scatternets. However, very few actual implementations of scatternets have been done due to limitations of Bluetooth and the MAC address protocol. Moreover, Bluetooth does not support various traffic priorities, such as on-demand traffic, normal traffic, and emergency traffic in healthcare applications [43–45].

IEEE 802.15.4 is currently the most widely used radio standard in BSNs for its very low power consumption and cost [46–49]. ZigBee is based on IEEE 802.15.4. Compared with other short range communication technologies (e.g. Bluetooth, Wi-Fi), ZigBee has the least protocol complexity and wake-from-sleep time. Moreover, it provides several power options depending on the specific applications (from -25 dBm to 0 dBm), and it supports mesh network configurations. The only drawback is that ZigBee supports a data rate of up to 250 kbps, which may be insufficient for some BSN applications.

IEEE 802.15.6 working group has been formed to develop a standard for short-range, wireless communication in body area network (referred to as body sensor network in this thesis) [50, 51]. It supports QoS, low power, and data rates up to 10 Mbps. This standard considers effects on antennas in the presence of a human body (varying with male, female, thin, fat, etc.), radiation pattern shaping to minimize specific absorption of the human body, and changes in characteristics due to the BSN user motions. It defines a MAC layer that supports several physical layers, such as 2.4 GHz ISM Narrowband, ultra-wideband (UWB), and human body communications layers. Compared with IEEE 802.15.4, IEEE 802.15.6 requires a shorter communication range, and larger data rate, in order to safe more power cost, and enables support various applications.

Note that in this subsection we refer to the communication technology in intra-BSN communication, i.e., the communication between the sensor nodes and the corresponding coordinator in a BSN. For inter-BSN communication, i.e., the communication between the coordinator and the network interface, we consider WLAN in this thesis for low cost.

2.2 Handover scheme

Handover is the process of transferring an ongoing data transmission from one attachment point to another. There are two parameters associated with a handover decision: handover rate and outage probability. The higher the handover rate, the more network resources would be consumed to reroute the communication from one interface to another. However, when the handover rate is low, handover may not be performed promptly, causing signal to interference noise ratio (SINR) fall below a threshold (referred to as outage) [52, 53]. Finding the optimum handover initiation time means finding the optimum trade-off between outage probability and handover rate. BSNs have stringent requirements on outage probability and unnecessary handover rate.

RSSI is the most widely used metric in handover schemes because it is easy to measure and closely relates to the service quality [52, 53]. The RSSI from the serving network interface is compared with that from a target base station, and decisions are made using a constant margin. However, fluctuations of RSSI associated with shadow fading and multipath fading incur unnecessary handover, consuming additional energy [54, 55]. To suppress the unnecessary handover in RSSI-based handover, several location-based handover algorithms have been proposed [56–58]. Most studies assume that the location of the mobile can be determined using the

global positioning system (GPS), but GPS does not fit well in indoor environments where BSNs are commonly deployed [56]. Non-GPS-based solutions for indoor localization have been developed using RSSI-based WLAN localization or sensor-based tracking. The WLAN RSSI-based tracking schemes [59–62] estimate the distance between the target and reference points using the path loss function between RSSI and distance. Unfortunately, in indoor environments, the wireless channel is very noisy and the radio frequency signal may suffer from reflection, diffraction and multipath fading, and thus the RSSI is a complex function of distance. To overcome this problem, WLAN fingerprinting schemes use a priori radio map to capture the RSSI of each AP in the area of interest and live RSSI values are then compared to the radio map to find the closest match [57]. The major drawback is the need for dense training coverage and poor extrapolation to areas not covered during training. Another alternative indoor localization is inertial sensor-based kinematic tracking, which adopts kinematic relationship to estimate pedestrian localization [63]. But kinematic tracking is subject to accumulated measurement errors and calibration error. When the inertial sensor is used in a position tracking system, it becomes the source of unbounded error of position. There are methods on dealing with the growth in acceleration uncertainty, such as zero-velocity updates (ZVUs) [63]. Jin et al. [64, 65] proposed a robust dead-reckoning pedestrian tracking system with low cost sensors. The proposed method exploits the fact that, multiple dead-reckoning systems, carried by the same pedestrian, have stable relative displacements with respect to each other. Radio frequency identification (RFID) based tracking is another method proposed to track the tag on the object using RFID readers pre-deployed in the application area [66]. Cooperative and fuzzy localization schemes have been developed recently to combine the benefits of the RSSI-based scheme, inertial sensor

based scheme and RFID-based scheme [67–69]. In our work, we compensate the differences of the kinematic tracking and the WLAN RSSI-based tracking to get relatively accurate position estimation of a BSN user. Note that the objective of our research is to exploits the indoor localization provides historical trajectory to aid handover decision instead of developing novel localization system.

Note that handover performance is not only related with the current location of a mobile station but also with the movement trend (movement pattern, direction, and velocity) of the mobile station [70]. Almulla et al. [62] proposed a fast location-based handover scheme for IEEE 802.11 networks. With the position and movement direction of a mobile station and the location information of the surrounding APs, the most possible visiting APs are predicted and prioritized so that time can be saved for scanning channels. Mechaelis et al. [18] utilized mobility prediction technologies to aid and prepare for handover in advance. The prediction is based on statistical data gained from the observation of movement across multiple cells. In small-scale BSNs (in terms of both its network size and its mobility area), more accurate movement trend prediction is required to aid handover decision. BSNs have some specific characteristics which provide potentials to improve mobility prediction and aid handover decision accordingly. In particular, BSNs typically move within a relatively constraint area, e.g., inpatient or emergency department of a hospital, and thus the movement trend of a BSN highly depends on the spatial deployment of the BSN application area as well as the personal habits of the BSN user [71]. For example, a patient may always turn right at the corridor to the consultation room in a specific scenario. With this movement trend, the handover decision can be made more intelligently in a relatively long term. In this thesis, we proposed an improved handover scheme with movement trend awareness for BSNs.

2.3 Inter-user interference

2.3.1 Interference mitigation

The existing interference mitigation schemes for BSNs mainly fall into several categories: channel hopping, power control, and beacon shifting.

In IEEE 802.15.6, one of the mechanisms for mitigating inter-user interference in BSNs is channel hopping [50]. The coordinator of a BSN changes its operating channel in the operating frequency band periodically by including the current channel hopping state and next channel hop fields in its beacons. A BSN should choose a channel hopping sequence different from that of its neighboring BSNs. The drawback of channel hopping is that collisions cannot be effectively alleviated within a limited hopping bandwidth regardless of the delay and the energy consumption. Sergio et al. [72] proposed a channel hopping approach, where each BSN is assigned a different frequency channel at the network initialization phase. This approach allows monitoring as many patients as available channels, but radio channels are hard to be reused in a dynamic way. To increase the number of monitored BSNs and enable them to move freely, an alternative approach is to allocate channels dynamically in small-scale deployments of BSNs. Silva et al. [73] developed an infrastructure-based scheme, where BSNs are reallocated channels by a fixed infrastructure when they move into the radio range of each other. This scheme reduces interference effectively if the number of congregated BSNs within the interference range is fewer than the number of available channels. However, besides the infrastructure cost, this approach leads to frequent channel switching, which incurs much overhead and is thus unsuitable for occasional and short-term interference.

Power control is another approach to reduce the interference in multi-user

environments [74–78]. Kim et al. [76] proposed a decentralized power control algorithm based on the received signal interference. The transmit power is so determined that the transmitter can sustain a high data rate, while keeping the adverse interference effect on the other neighboring concurrent transmissions minimal. Wu et al. [75] proposed a power control approach for interference mitigation, where each BSN measures the interference from other BSNs and then selects a suitable channel and transmission power by utilizing non-cooperative game theory and a no regret learning algorithm. A major drawback of this method is the long iteration period (more than 20 iterations) to reach the optimal point. As such, the utilized channels and transmission powers may be changed frequently during the long computing period which makes the system unstable. Moreover, considering the specific characteristics of BSNs, Zhang et al. [77] developed a power control game based on the social interaction information to maximize the system's utility while minimize the energy consumption of BSNs. Power control improves spatial utilization of channels, but it may compromise transmission performance with a reduced transmission power [78]. Because of the simple structure of a BSN and the concern for energy conservation, power control is infeasible for BSNs.

In healthcare applications, the channel utilization of a BSN is usually low for energy conservation [9, 10]. In IEEE 802.15.6 [79], the coordinator of a BSN may transmit its beacons at different time offsets relative to the start of the beacon periods by including a beacon shifting sequence field in its beacons [80, 81]. However, it is challenging to keep a beacon shifting sequence mechanism in the mobile BSN scenario. Kim et al. [82] proposed a distributed flexible beacon schedule scheme to reduce the interference. By employing carrier sensing before each beacon transmission, collisions can be avoided if other BSNs attempt to access the channel at the same time. This scheme consumes additional energy in the channel access

as multiple carrier sensing iterations are possibly conducted before each beacon transmission. Considering the periodic data characteristics in most BSN applications, a reservation-based scheme outperforms a contention-based scheme in terms of energy conservation and throughput enhancement, because overhead and collisions are significantly reduced in the reservation-based approach. As such, our proposed IIM scheme utilizes the reservation-based approach, where reservations are made dynamically based on the information acquired from channel listening. Incorporated with channel switching, IIM can be used in many application scenarios with both light and heavy loads.

2.3.2 Interference analysis

Interference analysis is beneficial for interference mitigation and network management. The interference at the intended receiver is determined by a number of stochastic processes including the random spatial distribution of interferers, shadowing, and fading [83]. In a wireless network with many concurrent transmissions, characterizing the geometry and relevant placement of the interferers is of significance for the interference analysis. Typically, multiple topologies of interferers are assumed for the interference analysis, e.g. hexagonal lattice, regular lattice etc. [76, 84–86]. Wang et al. [87] investigated the inter-user interference by characterizing the distance between any two sensor nodes from different BSNs using the advanced geometrical probability approach. A hexagonal lattice is assumed to model the spatial locations of BSNs for the densest packing scenario [87]. However, for BSNs, it is impractical to assume typical topologies nor the densest packing topology, as BSN users move around without constraints.

Stochastic geometry provides a natural way of describing the interferer placement, by averaging over all potential geometrical realizations for the interferers.

It assumes interferers are placed according to some probability distribution, e.g. a Poisson point process[88–91]. Using the notions from point process theory, percolation theory, and probabilistic combinatory, wireless networks are analyzed in terms of the connectivity, the capacity, the outage probability and other fundamental limits. The reader is referred to [92] for a comprehensive survey. The MAC protocol affects the stochastic geometry analysis by determining which nodes transmit at a given time. In [37], an Aloha-type MAC mechanism for large mobile, multihop, wireless networks was defined and analyzed to find a compromise between the spatial density of communications and the range of each transmission. Andrew et al. [93] proposed a tractable approach to determine the coverage and rate for Aloha-based downlink transmissions in cellular networks and considered an additional dimension of randomness by assuming the base stations are distributed as a Poisson point process and a node always transmits to the nearest base station. Nguyen et al. [39] modeled the interferences under CSMA/CA in dense 802.11 networks using a Matern point process [94, 95] such that the distance between any two selected nodes is larger than a carrier sense range. Gong et al. [38] studied the effects of mobility on the interference statistics in random networks by incorporating the distance variations of mobile nodes to the channel gain fluctuations. According to [38], for a uniform mobility model (e.g. random walk, discrete-time Brownian motion), the mobile network can be treated as a correlated realization of a static network. Hence the existing results of the interference in static networks also apply to the uniformly mobile networks [96, 97].

The existing stochastic geometry analysis cannot be applied in BSNs directly due to the following reasons. (1) In IEEE 802.15.6, where a hybrid MAC protocol consisting of both contention-based and contention-free MAC mechanisms is employed, the geometry distribution of the interferers is more complex (when

compared to a traditional wireless network with a single MAC protocol). In particular, a contention-based BSN would block the transmissions of its neighboring BSNs within a carrier sense range, while the contention-free BSNs may transmit simultaneously in the same vicinity. (2) Due to the presence of the human body, the transmissions within a BSN follows a different channel model from that of the transmission between interfering BSNs. These challenges motivate us to perform a stochastic geometry analysis of the inter-user interference in IEEE 802.15.6 BSNs.

Chapter 3

An Improved Handover Scheme with Movement Trend Awareness for BSNs

---

This chapter presents an optimized handover scheme with movement trend awareness for BSNs. The proposed scheme predicts the future position of a BSN user using the movement trend extracted from its historical position, and adjusts the handover decision accordingly. Handover initiation time is optimized to minimize the outage probability while the handover rate is estimated to meet the requirement. Simulation results show that the proposed scheme reduces the outage probability by 21% as compared with the existing hysteresis-based handover scheme under the constraint of acceptable handover rate.

3.1 Network model

In a BSN, there is a single coordinator and multiple sensor nodes. The physiological sensor information collected by sensor nodes is first delivered to a coordinator worn on the body, which then forwards the information to the concerned agents via a WLAN AP (see Fig. 1.1).

Each BSN is typically equipped with inertial sensors such as accelerator, gyroscope, and magnetometer for healthcare applications. Based on the data accumulated by inertial sensors[1], the position of the BSN user can be estimated using its last know kinematic state (position, velocity, acceleration) following kinematic relationships [59]. In a moderate-scale BSN deployment scenario, multiple WLAN APs are commonly deployed with overlapping coverage within the area of interest. A BSN measures the RSSI from these APs, and calculates the distances by the path loss model. A typical example of WLAN based tracking includes the Horus WLAN location determination system [60].

In this study, we compensate for the differences of the two tracking schemes (i.e., kinematic tracking and WLAN RSSI-based tracking) and fuse them to get a more accurate position prediction.

3.2 Proposed handover scheme

The proposed handover scheme has the following modules: (1) position tracking, (2) position prediction, and (3) handover decision accordingly. In this section, we first give an overview of the proposed handover scheme and then provide details of the three component modules.

[1]The raw data from the accelerators is first filtered with a low-pass filter, and then decoupled with the gravity obtained from the readings of gyroscopes and magnetometers. For details please refer to [98, 99].

3.2.1 Overview of the proposed handover scheme

The proposed handover scheme comprises the following steps:

Step 1 (Position tracking): Position tracking (see subsection 3.2.2) is initiated when RSSI from the current AP decreases significantly (falls below a certain threshold).

Step 2 (Position prediction): When the BSN crosses the AP boundary (RSSI from the current AP equals to that from the target AP), position prediction (see subsection 3.2.3) is performed.

Step 3 (Handover decision): Based on the position prediction, the coordinator of the BSN executes the handover decision (see subsection 3.2.4) to determine the handover initiation time.

Step 4 (Handover initiation): Handover is performed at the handover initiation time when the actual position of the BSN is within an acceptable deviation range from the predicted position. Otherwise, handover is performed immediately.

AP boundary is defined as the line whose points have the same distance to the current AP and to the target AP. The overall flow chart of our proposed approach is shown as Fig. 3.1.

3.2.2 Position tracking

In Step 1 of the workflow described in subsection 3.2.1, the position tracking is executed when the RSSI from the current AP decreases significantly. The position of the BSN user is obtained by fusion of the inertial sensor-based kinematic tracking scheme and the WLAN RSSI-based tracking scheme. A Kalman filter [100] is used as the fusion tool to compensate for the differences of the two tracking schemes and improve the positioning accuracy.

The state vector of the Kalman filter is expressed as $X_k = [s_k, v_k, a_k]^T$,

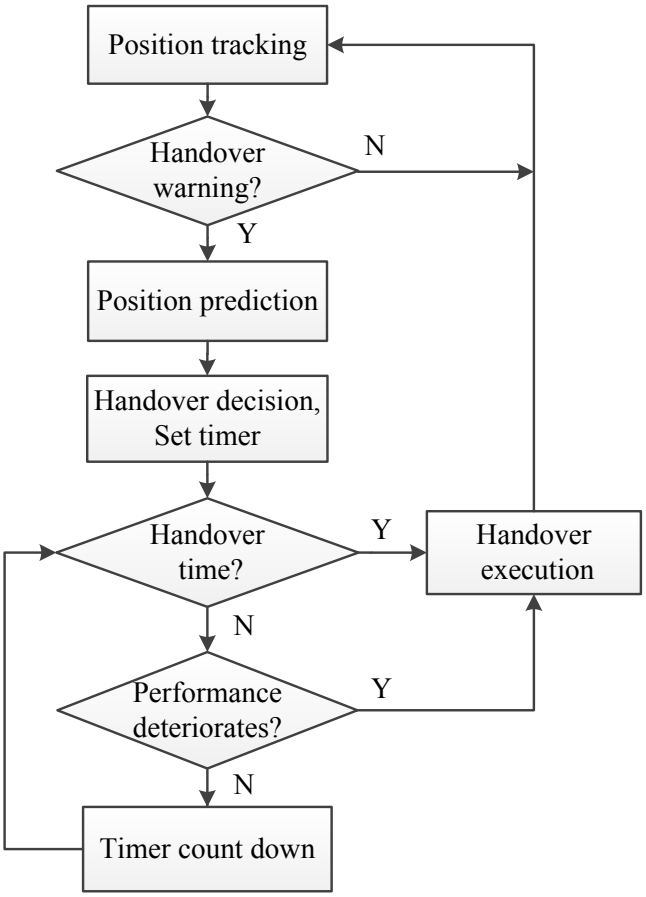

Fig. 3.1: Flow chart of the proposed handover scheme.

where s_k, v_k, a_k are the target position, velocity, and acceleration at time k respectively. Each of them is a two-dimensional vector along x-axis and y-axis, i.e. $s_k = [s_k^x, s_k^y]^T$, $v_k = [v_k^x, v_k^y]^T$, $a_k = [a_k^x, a_k^y]^T$. The system state transition function of the Kalman filter can be expressed as

$$X_k = F_k X_{k-1} + w_k, \tag{3.1}$$

where F_k is the state transition matrix and w_k is the process noise. In the Wiener-process acceleration model (WPAM) [101], where the acceleration is a Wiener

process, $F_k = [1, T, T^2/2; 0, 1, T; 0, 0, 1]$. This system state transition function performs the kinematic tracking.

In the measurement vector $z_k = [s_k, a_k]^T$, s_k is obtained by WLAN RSSI-based Horus system [60], while a_k is calculated based on readings from the inertial sensors [98]. The observation equation is

$$z_k = H_k X_k + n_k, \tag{3.2}$$

where H_k is the observation matrix and n_k is the measurement noise that is determined empirically.

From the output of the Kalman filter, a relatively accurate trajectory of the BSN user s_k and the real-time velocity information v_k are obtained, which are to be utilized in position prediction.

3.2.3 Position prediction

In Step 2 of the workflow described in subsection 3.2.1, the position prediction is performed when the BSN crosses the AP boundary. Note that the future trajectory of a BSN would possibly follow a similar movement trend with its historical trajectory. In this study, we utilize the average velocity $\overline{v}$ over the last N time slots of the historical trajectory as the movement trend.

To model the future positions, we make the following assumptions:

- The future trajectory of a BSN follows the WPAN model [101];
- The future trajectory starts with the velocity of $\overline{v}$;
- The future acceleration a_i follows a white Gaussian distribution, i.e., $a_i \sim N(0, \sigma_a^2)$, where σ_a^2 is extracted from the historical trajectory by taking their variances, i.e., $\sigma_a^2 = \text{var}[a_{k-1}, a_{k-2}, ..., a_{k-N}]$.

Assume k is the current time index. The movement trend $\overline{v}$ is obtained by averaging over the historical velocities $[v_{k-1}, v_{k-2}, ..., v_{k-N}]$,

$$\overline{v} = \frac{v_{k-1} + v_{k-2} + ... + v_{k-N}}{N}, k > N. \tag{3.3}$$

We predict the future position s_i, $k < i \leq k + \tau$, where τ is the tolerable prediction period, as follows:

$$v_i = \begin{cases} \bar{v}, & i = k \\ v_{i-1} + a_i T, & k < i \leq k + \tau \end{cases} \tag{3.4}$$

$$s_i = s_k + \sum_{j=k}^{i} \left(\frac{v_{j-1} + v_j}{2} \right) T = s_k + (i-k) T \bar{v} + \sum_{j=k}^{i} T \left[(i-j) + \frac{1}{2} \right] a_j \tag{3.5}$$

$$\hat{s}_i = E[s_i] = s_k + (i-k) T \bar{v}. \tag{3.6}$$

In Eqn. (3.4), the future velocity v_i is predicted based on $\bar{v}$ and the historical acceleration a_i. In Eqn. (3.5), the future position s_i is obtained based on the current position s_k, movement trend $\bar{v}$, and trajectory-based acceleration a_j. As can be seen from Eqn. (3.5), s_i also follows a Gaussian distribution with a mean of $\hat{s}_i$ and an accumulated variance (as a_i is assumed to follow Gaussian distribution). Note that the prediction position $\hat{s}_i$ is proportional to the movement trend $\overline{v}$ (see Eqn. (3.6). This makes sense as $\overline{v}$ carries the prediction information by indicating both the movement trend and average speed in our scheme.

Fig. 3.2 depicts the procedure of the position prediction. As can be seen, curve AB is the historical trajectory of the BSN. When the BSN crosses the AP boundary at point B (also denoted as s_k), the position prediction is performed,

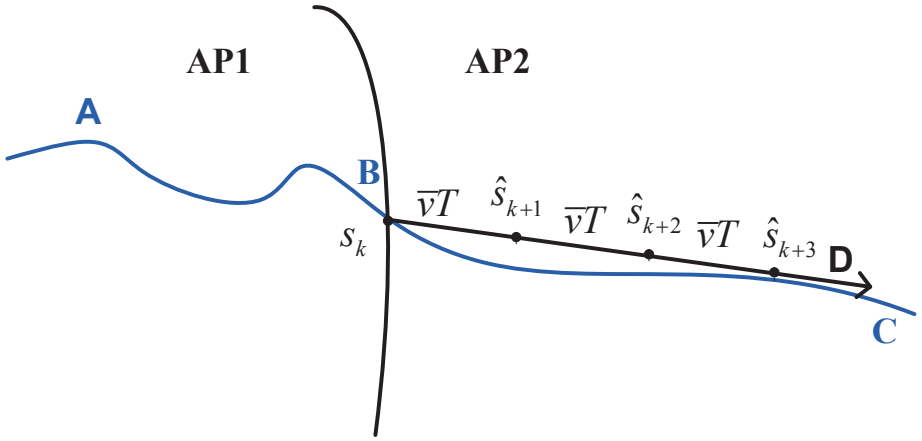

Fig. 3.2: Position prediction.

and $\hat{s}_k$, $\hat{s}_{k+1}$, and $\hat{s}_{k+2}$ are the predicted positions in the time index k, $(k+1)$, and $(k+2)$ respectively.

3.2.4 Handover decision

Confidence probability

The confidence probability $\Pr_{con}(i)$ is defined as the probability that a BSN actually enters the coverage of the target AP at time index i, given that the BSN being predicted to be within the coverage of the target AP. As such, the unnecessary handover probability, which is the probability that the BSN would be back to the previous AP at the time index i, can be expressed as $(1 - \Pr_{con}(i))$.

To calculate $\Pr_{con}(i)$, we map the predicted position s_i along the orthogonal direction of the AP boundary (as only the orthogonal factors contribute to the handover decision). Denote the orthogonal mean and standard deviation of s_i as $\Delta\tilde{s}_i$ and $\tilde{\sigma}_i$ respectively. The confidence probability is expressed as

$$Pr_{con}(i) = 1 - Q\left(\frac{\Delta\tilde{s}_i}{\tilde{\sigma}_i}\right), \tag{3.7}$$

where $Q(\cdot)$ is the complementary distribution function of the standard Gaussian [102].

Let P be the mapping vector that is orthogonal to the AP boundary. $\Delta\tilde{s}_i$ and $\tilde{\sigma}_i$ are calculated as follows:

$$\Delta\tilde{s}_i = (\hat{s}_i - s_k)\, P = (i-k)T\bar{v}P, \tag{3.8}$$

$$\tilde{\sigma}_i^2 = E[P^T(s_i - E[s_i])^2 P] = P^T\sigma_{s_k}^2 P + \frac{(i-k)^2T^2}{4}P^T\sigma_a^2 P, \tag{3.9}$$

where $\sigma_{s_k}^2$ is the uncertainty of the current point s_k.

As can be observed in Eqn. (3.7), $\Delta\tilde{s}_i/\tilde{\sigma}_i$ increases with i, thus $\mathrm{Pr}_{con}(i)$ also increases with i. It means that the farther the user's predicted position is from the boundary of the serving AP, the higher the probability that the user is actually within the coverage of the target AP.

In Fig. 3.3, $\mathrm{Pr}_{con}(i)$ is the shadow part under the probability density function (PDF) of s_i at the target AP (AP2 in this case) side. $\mathrm{Pr}_{con}(k+1)$, $\mathrm{Pr}_{con}(k+2)$, $\mathrm{Pr}_{con}(k+3)$ are the confidence probabilities at the time index k, $(k+1)$, and $(k+2)$ respectively.

Handover initiation

Based on the confidence probability, we determine the optimized handover initiation time. The higher the handover rate, the more network resources would be consumed to reroute the communication. However, when the handover rate is low, handover may not be performed promptly resulting in outage. Thus the determination of handover time should meet the unnecessary handover probability requirement and the outage probability requirement concurrently.

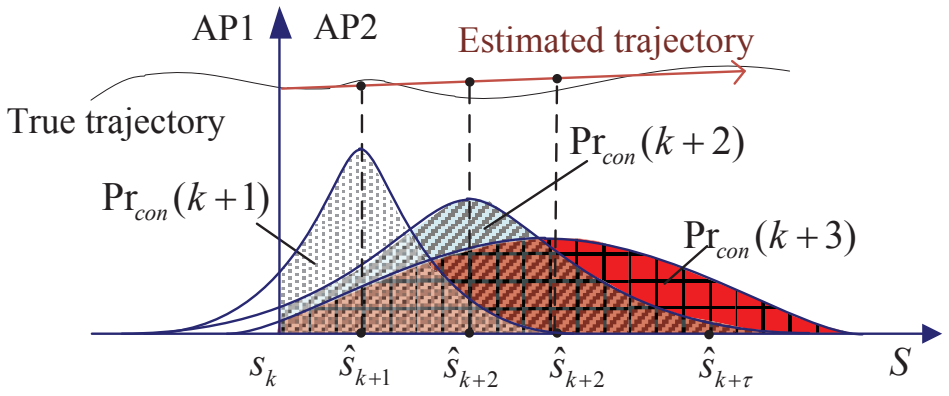

Fig. 3.3: Confidence probability prediction.

A handover from AP1 to AP2 occurs at time index i when the following two criteria are satisfied,

$$\text{Criterion 1:} \quad 1 - Pr_{con}(i) \leq \xi \tag{3.10}$$

$$\text{Criterion 2:} \quad Pr_{out}(i) \leq \theta \tag{3.11}$$

where ξ is the required unnecessary handover rate, $\Pr_{out}$ is the outage probability, and θ is the target outage probability. Outage occurs when SINR falls below a certain threshold, and $\Pr_{out}$ can be calculated by the RSSI of the current AP given the noise power is known and the interference is negligible. Criterion 1 is to ensure the unnecessary handover rate requirement, while Criterion 2 is to ensure the outage probability requirement.

Fig. 3.4 depicts the performance gain achieved by the proposed handover scheme along the orthogonal direction to the AP boundary. $\hat{s}_{i,\min}$ is the point where criterion 1 is met, $\hat{s}_{i,\max}$ is the point where criterion 2 is met. Thus any $i_{opt} \in [i_{\min}, i_{\max}]$ satisfies the two criteria concurrently. If i_{opt} is chosen closer to

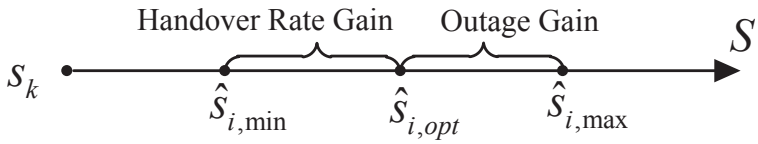

Fig. 3.4: Performance gain.

$i_{\min}$, the outage probability could be further reduced, which is shown as outage gain. Conversely, if i_{opt} is closer to $i_{\max}$, the handover rate could be further reduced, which is shown as handover rate gain. As outage is crucial for BSNs, we choose the point $i_{opt} = i_{\min}$ as the optimal handover initiation time. At i_{opt}, the unnecessary handover rate is estimated to meet the requirement and the outage probability is minimized.

3.3 Simulation results

We implemented the proposed handover scheme in the Matlab 7.0 simulator [103]. The performance of the proposed handover is compared with the basic scheme and the hysteresis-based handover. The basic scheme [53] performs handover once the BSN crosses the AP boundary, while the hysteresis-based handover performs handover when the hysteresis requirement being met.

3.3.1 Simulation settings

The BSN deployment area is covered by a WLAN, commonly based on an IEEE 802.11a/b/g/n network. We assume that APs of the WLAN follow a traditional hexagonal layout, and the coverage radius of each AP is 50 meters. BSNs move inside the BSN deployment area following a Gauss-Markov mobility model [104]. The pedestrian characteristics of each BSN user are set according to [105].

The sensor radio of a BSN has a 250 Kbps data rate and outage SINR of -10 dB. To remove the effect of differing initial conditions on the performance, we run the simulation fifty times with different initial BSN positions and then calculate the average results. In the simulation, the position of a BSN is predicted through the experimental results from the WLAN RSSI-based Horus system [60] and inertial sensor-based kinematic tracking [63]. In the simulation, we incorporate the acceleration with measurement noise to represent the inertial sensor-based kinematic tracking, ignoring the pre-processing from the readings of accelerometer and magnetometer. When utilize the acceleration information, the drift error of inertial sensors is compromised at run-time with the fingerprint-based RSSI-based localization using a Kalman filter.

We first study the effects of the localization accuracy on the handover performance. Then the proposed handover scheme is considered in two scenarios: a BSN deployment scenario without constructive constraints and a realistic BSN deployment scenario with constructive constraints.

3.3.2 Simulation results

The effects of the localization accuracy

Fig. 3.5 compares the CDF of location errors using the proposed tracking scheme and that using the WLAN RSSI-based tracking. As expected, the positioning accuracy achieves significant improvement by fusion of the kinematic tracking and WLAN RSSI-based tracking. In particular, 90% of the location errors are within 2.5 meters, while that of RSSI-based tracking stays within 3.5 meters.

Table 3.1 investigates the the performance of the proposed handover scheme over various localization errors. The number of drop calls is recorded among the 50

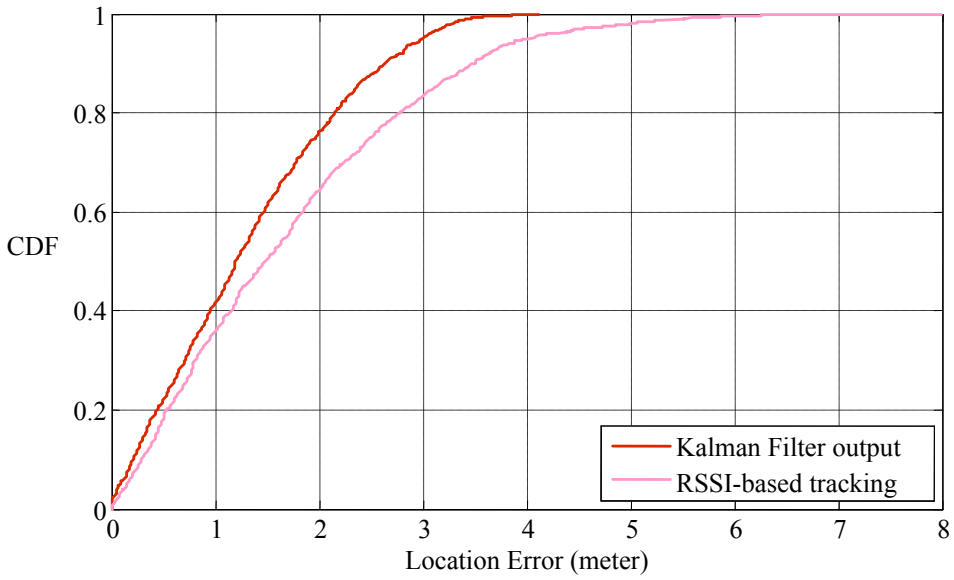

Fig. 3.5: CDF of location errors using Kalman filter tracking and RSSI-based tracking

Table 3.1: Handover rate and outage times over various localization errors.

Location Error (m)	Handover Rate	Drop Call Times
0.82	0.7532	15
1.21	0.7845	16
1.62	0.7947	15
2.01	0.8062	17

trials. It can be seen that within the tolerable error range the proposed handover performance changes slightly with location errors. This is because the proposed scheme is mainly based on the movement trend and user profile, which is extracted from a large volume of historical data.

Simulation results in the case without constructive constraint

In this part, we consider the BSN deployment scenario without constructive constraints, where BSNs move inside an area of 100X100 square meters. The

handover performance is investigated under different hysteresis margins. For the proposed handover method, the hysteresis margin refers to the distance between the APs boundary and the position where the outage requirement is met. By changing the hysteresis margin, the outage requirement is also changed. The results are shown in Figs. 3.6 and 3.7.

Fig. 3.6 presents the handover rate, i.e., the actual number of handovers performed using the three schemes normalized by the number of handovers using the basic scheme. As expected, the handover rate of the hysteresis-based scheme decreases when the hysteresis margin gets larger, as it is harder to meet the handover requirement. For the proposed scheme, the handover rate also decreases and remains similar to that of the hysteresis-based scheme when the hysteresis margin is relatively small. It can be explained by the increasing chance to meet the confidence requirement (Criterion 1) when the hysteresis margin increases, and thus there is a trend of decreasing the handover rate by avoiding unnecessary handover. When the hysteresis margin gets larger, there is enough space for the

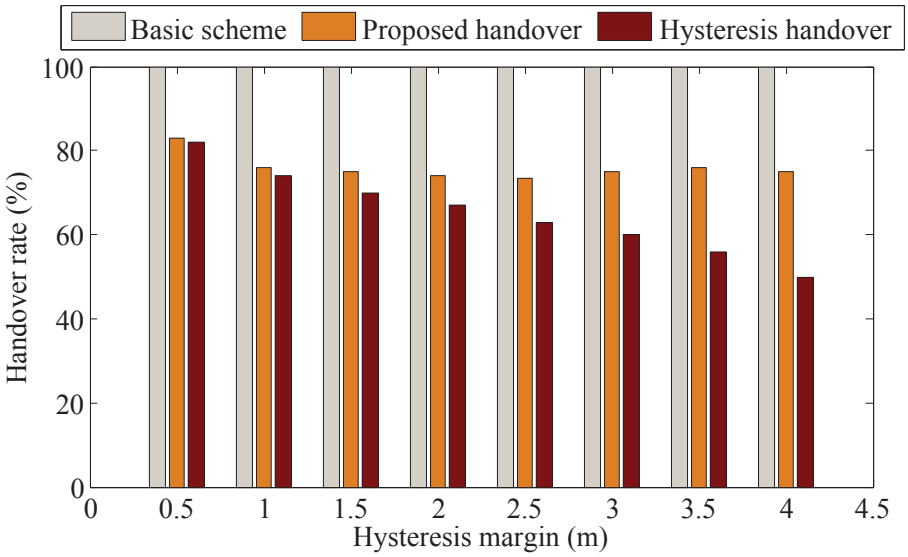

Fig. 3.6: Handover rate in the BSN deployment scenario without constructive constraints.

confidence requirement (Criterion 1) to be met and the handover rate remains stable as shown in Fig. 3.6 since most of the unnecessary handovers have been alleviated.

Fig. 3.7 shows the comparison of the outage times versus the hysteresis margin. Outage times are counted for the 1000 iterations. It is observed that the outage times of the basic scheme are lower than the other two approaches. However, it is at the expense of much higher handover rate as shown in Fig. 3.6. The outage times of the proposed scheme significantly outperforms that of hysteresis-based handover (about 21% on average), especially when the hysteresis gets larger. This is because as long as the BSN user is predicted to enter another AP with high confidence probability, the handover is performed immediately to reduce outage.

Simulation results in the case with constructive constraint

In this part, we consider the BSN deployment scenario with constructive constraints, where BSNs move inside a realistic BSN deployment area in hospi-

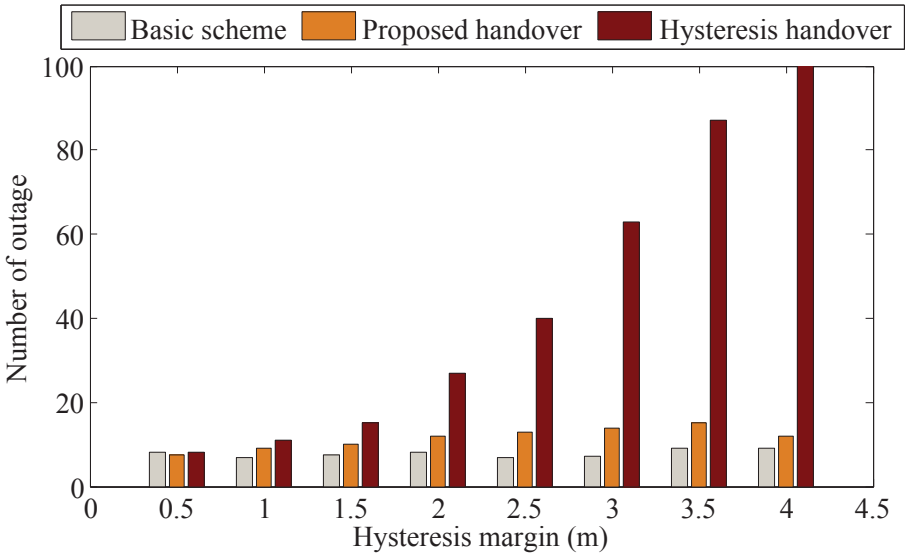

Fig. 3.7: Outage times in the BSN deployment scenario without constructive constraints.

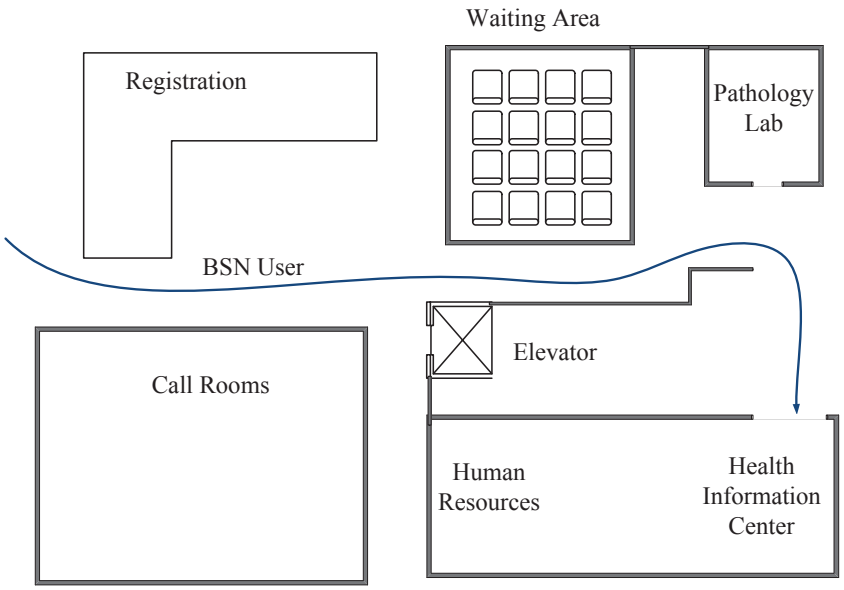

Fig. 3.8: Floor map of Emergency Department in UK Good Samaritan Hospital.

tal. Fig. 3.8 shows the floormap of UK Good Samaritan Hospital. The standard operational process of emergency is as follows: the patient first registers at the registration counter, then waits for triage at the waiting area, and later goes to the Health Information Center to get preliminary consultations and later checked in the Pathology Lab by doctors. In the simulation, a BSN user follows certain predefined routes, leaving only the movement velocity to be predicted. One possible route of BSN user is shown in Fig. 3.8.

Fig. 3.9 shows the handover rate in the BSN deployment scenario with constructive constraints. As can be seen from Fig. 3.9, the handover rate of the proposed scheme is lower than that of the case without constructive constraints (see Fig. 3.6). This is because when the route of the BSN users is known, the only predicted parameter is movement velocity, resulting in more accurate position prediction. Fig. 3.10 shows the outage times in the case with constructive constraints. For our proposed scheme, the outage times in Fig. 3.10 is lower than that of the

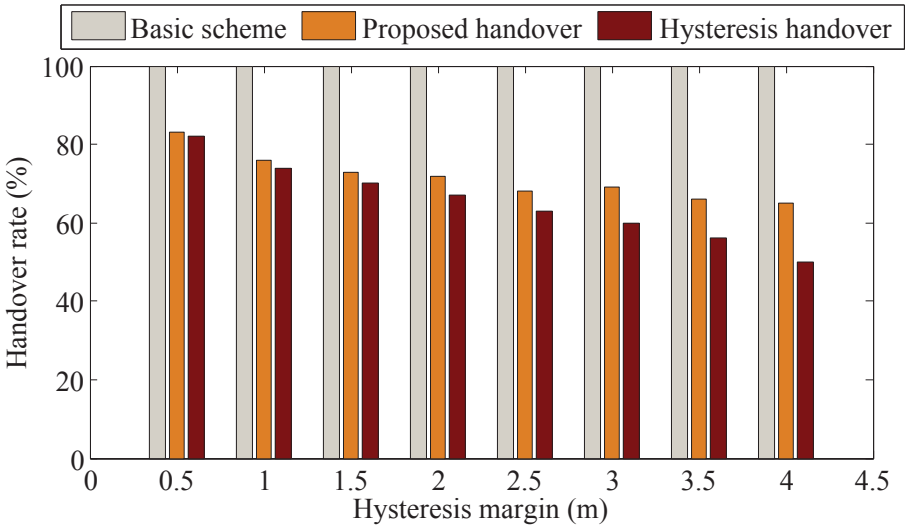

Fig. 3.9: Handover rate in the BSN deployment scenario with constructive constraints.

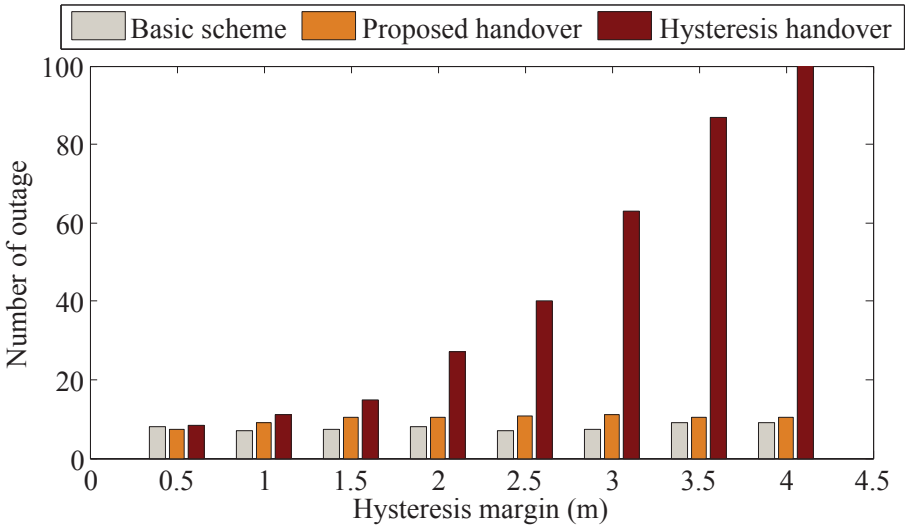

Fig. 3.10: Outage times in the BSN deployment scenario with constructive constraints.

case without constructive constraints (see Fig. 3.7). Similarly, this is because with more accurate position prediction, handover can be performed promptly to avoid outage.

3.4 Summary

In this chapter, we have proposed an optimized handover scheme with movement trend awareness for BSNs. The proposed scheme predicts the future position of a BSN user using the movement trend extracted from historical position, and adjusts the handover decision accordingly. Confidence probability is introduced to measure the accuracy of position prediction, and estimate the unnecessary handover rate as well. Handover initiation time is optimized when the outage probability is minimized and the estimated handover rate meets the requirement. The coordinator of a BSN is responsible for position tracking, confidence probability calculation, and handover decision. There is no handshaking between the coordinator and APs nor the coordinator and the sensor nodes in the BSN. The simulation results showed that the proposed handover scheme reduces the outage probability by 21% as compared with the existing hysteresis-based handover scheme under the constraint of acceptable handover rate. Moreover, when the geometric information of the BSN deployment area is known, the performance of the proposed handover scheme is further improved. The proposed handover scheme could incorporate any of the existing localization schemes as long as the movement trend of the BSN user could be obtained. In the case where the localization information is known beforehand, the overhead of our proposed handover scheme is further reduced.

Chapter 4

A Case Study in Moderate-scale BSN Deployment Scenario

In this chapter, we investigate the severity and prevalence of inter-user interference in a realistic BSN deployment scenario in hospital. We consider multiple factors that affect the BSN performance, including BSN density, traffic load, and transmission power. Simulation results show that with 20% duty cycle, only 68.5% of data transmission can achieve the target reliability requirement even in the off-peak period. Interference mitigation schemes are then suggested based on the specific BSN deployment scenario.

We first introduce the interference model, and then investigate the inter-user interference in the case study.

4.1 Interference characterization

4.1.1 Network model

The signal attenuates as it propagates over space in BSNs. The attenuation may either be due to propagation losses caused by the natural expansion of the radio wave in the environment, referred to as path-loss, or multipath propagation, referred to as multipath induced fading, or due to shadowing from obstacles affecting the wave propagation, sometimes referred to as shadow fading [102, 106]. In this study, we consider the path-loss and shadow fading for simplicity. The path-loss function is given by $l(d) = G \cdot d^{-\alpha}(d > d_0)$, where d is the distance between the transmitter and receiver, G is a constant accounting for system loss, α is the path-loss exponent with $\alpha > 2$, and d_0 is the reference distance. Denote the shadow fading factor as γ. At a given time t, the received signal strength is expressed as

$$\Omega\left(d\right) = \Omega_0 \cdot \gamma \cdot l\left(d\right), \tag{4.1}$$

where Ω_0 is the transmission power.

In BSNs, there are two different channel models, i.e. the wireless channel between the sensor nodes and the coordinator in a BSN (referred to as on-body channel model) and that between two BSNs (referred to inter-body channel model). Due to the blockage and disruption of the radio signal by the human body, the on-body channel model experiences more severe attenuation (with a path-loss exponent α_O) than the inter-body channel model (with a lower path-loss exponent α_I and $2 < \alpha_I < \alpha_O$) [107, 108].

4.1.2 PER of BSNs

Data transmissions of a BSN incur interference to its neighboring BSNs, referred to as inter-user interference. Packet error rate (PER) is utilized to characterize the level of service degradation of BSNs due to inter-user interference. PER is defined as the ratio of the number of incorrectly received data packets to the total number of transmitted packets.

PER can be derived from the signal to interference noise ratio (SINR) of a BSN. Note that not all the neighboring BSNs transmit at time t. We denote $\mathbb{1}_j(t)$ as the transmission status of BSN j at t. $\mathbb{1}_j(t) = 1$ when BSN j transmits at time t, and $\mathbb{1}_j(t) = 0$ when BSN j does not transmit at t. It is noted that the probability of $\mathbb{1}_j(t) = 1$ also represents the duty cycle of BSN j.

The SINR of BSN i at time t is expressed as,

$$P_{SINRi}(t) = \frac{\Omega(r_i(t))}{\sum_{j \neq i} \mathbb{1}_j(t) \cdot \Omega(u_{i,j}(t)) + \Omega_n}, \tag{4.2}$$

where $r_i(t)$ is the distance between the transmitting sensor and the coordinator for the BSN i at time t, $u_{i,j}(t)$ is the distance between the transmitting node of BSN j and the coordinator of BSN i at t, and Ω_n is the background noise power [109].

When offset quadrature phase shift keying (OQPSK)[2] is utilized as the modulation scheme, the average bit error rate (BER) and PER for BSN i can be expressed as,

$$P_{BER} = \frac{1}{2} erfc\left(\sqrt{2E_b/N_0}\right) = \int_{t_{min}}^{t_{max}} \int_{\gamma_{min}}^{\gamma_{max}} \frac{1}{2} erfc\left(\sqrt{P_{SINRi}(t)}\right) \cdot P(\gamma) d\gamma dt \tag{4.3}$$

[2]Adopted by the PHY in IEEE 802.15.4 standard at 2.4 GHz [110].

$$P_{PER} = \sum_{a=1}^{m+k-m/2} C_{m+k}^{a+m/2} \cdot {P_{BER}}^{(a+m/2)} \cdot (1 - P_{PER})^{(m+k-(a+m/2))} \tag{4.4}$$

where E_b/N_0 is SINR per bit, $erfc(\cdot)$ is the complementary error function [111], m is the number of information bit, k is the number of additional coding bit, and $C_{m+k}^{a+m/2}$ is the set of all $(a+m/2)$ combinations out of a set $(m+k)$, t_{min} and t_{max} are the lower and upper integral limits of time factor, γ_{min} and γ_{max} are the lower and upper integral limits of shadow fading factor [112]. Eqns. (4.3) and (4.4) can be applied to other modulation schemes as well with little modification [113].

As can be seen from Eqn. (4.4), multiple factors affect the PER performance, including neighboring BSN number, traffic load, and transmission power. The effects of those factors are investigated in the case study.

4.2 Case study

In order to study the severity and prevalence of inter-user interference, a case study has been performed in the waiting area of Emergency Department of the National University Hospital (NUH) of Singapore.

4.2.1 Deployment scenario

Fig. 4.1 shows the floormap of NUH Emergency Department waiting area. The standard operational process of NUH emergency is as follows: (1) the patient first registers at the registration counter, (2) the patient then waits for triage at the triage waiting area, (3) after the triage, the patient waits at the consultation waiting area to get preliminary consultations at the consultation counter and later treated in one of the consultation rooms by doctors. When BSNs are deployed in the Emergency Department of a hospital, BSNs will be operational during

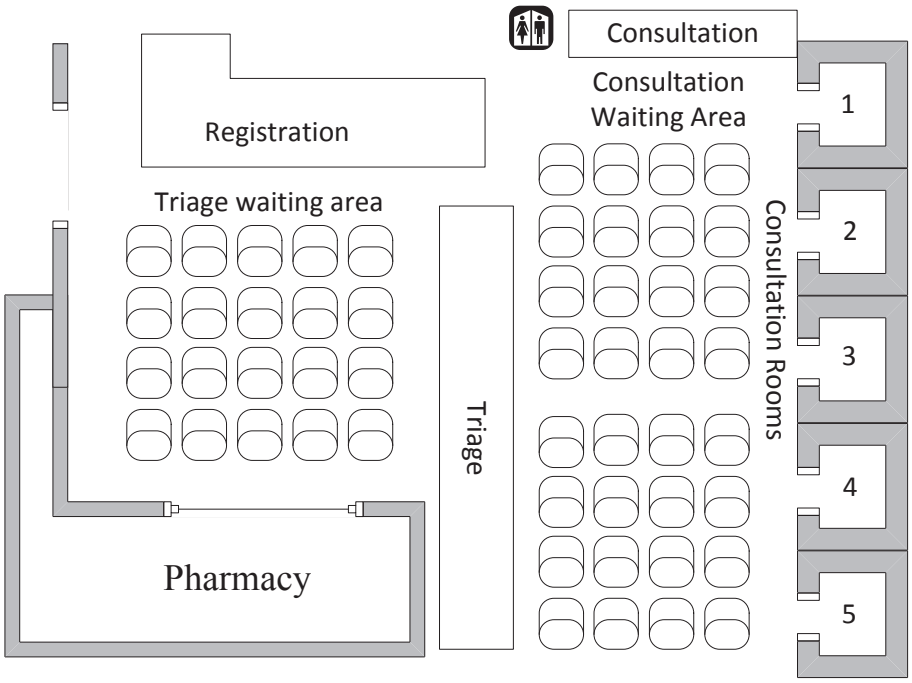

Fig. 4.1: Floor map of waiting area in NUH Emergency Department.

processes (2) and (3).

From the statistics of the NUH Emergency Department, the total waiting time a patient spends at the waiting area of Emergency Department of NUH is one to two hours on average for different visiting periods, i.e. peak or off-peak time. Because a patient's status may deteriorate during the waiting time, it is necessary to monitor critical physiological data of an unattended patient through a BSN in the waiting areas. Once any emergency situation is detected, the patient should be given priority to be treated [114–116].

4.2.2 Experimental settings

We observe the distribution of the patients in the NUH Emergency Department waiting area for three days. The observation period is 15 hours per day

from 8:00 hr to 23:00 hr. It is found that the observation periods of a day can be divided into three categories:

- Peak time (8:00 to 10:30): 58 BSNs are in the waiting area on average, thus the average area per BSN is 2 square meters per person;
- Moderate time (10:30 to 21:00): 40 BSNs are in the waiting area on average, thus the average area per BSN is 3 square meters per person;
- Off-peak time (21:00 to 23:00): 16 BSNs are in the waiting area on average, thus the average area per BSN is 6 square meters per person.

In the analysis, we consider all BSNs transmitting at the same power $\Omega_s \in [-25\text{dBm}, 0\text{dBm}]$. The signal transmitted in the same BSN attenuates according to the on-body path loss model [107, 117], while the interference signal reaches the BSN of interest according to the inter-body path loss model [108], as listed in Table 4.1. For simplicity, the duty cycles of all BSNs are set the same as well. In addition, we assume all the BSNs operate on the same channel. The performance of multiple available channel scenario can be easily obtained from that of the single channel scenario with the same number of BSNs per channel.

Table 4.1: The parameter settings of the simulation in case study.

m	12	k	52
d_0 (cm)	10	# of channels	1
σ (dB)	6.2	Ω_0 (dBm)	0
Ω_n (dBm)	-80	$\Omega_l(d_0)$ (dB)	35.7
α_O	3.38	α_I	2.6

4.2.3 Simulation results

This section investigates the effects of BSN density, traffic load, and transmission power on the BSN performance. PER of BSNs are calculated using Matlab 7.0 [103] according to Eqn. (4.4).

Effect of BSN density

Fig. 4.2 shows the CDF of PERs in the peak time scenario, moderate time scenario, and off-peak time scenario respectively. Each curve shows the CDF of PERs with a specified duty cycle. The PER increases with the duty cycle. This is reasonable because when the duty cycle gets higher more BSNs transmit simultaneously resulting in higher PER. When comparing the three graphs in Fig. 4.2, the PER decreases as the BSN density decreases from 2 square meters per person in peak period (see Fig. 4.2(a)) to 6 square meters per person in off-peak period (see Fig. 4.2(c)). This is caused by less severe interference due to lower density BSNs.

From Fig. 4.2, we obtain the reliability level of data transmission in BSNs. The reliability level is defined as the ratio of the number of successfully received data packets (with PER less than a certain target PER requirement $PER_{required}$) to the number of transmitted data packets. The reliability level can be calculated as $\Pr(PER < PER_{required})$. Assuming that reliability requires PER being less than 0.05 ($PER_{required} = 0.05$), the reliability level is listed in Table 4.2. For instance, in the case of *Duty cycle=0.2*, under the scenario of peak time, the reliability level is only 21.9%. At the off-peak time, the reliability level is 68.5%.

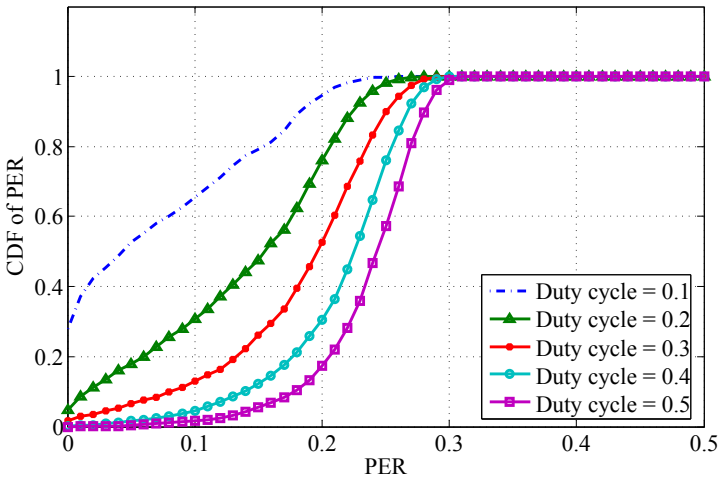

(a) Peak time scenario.

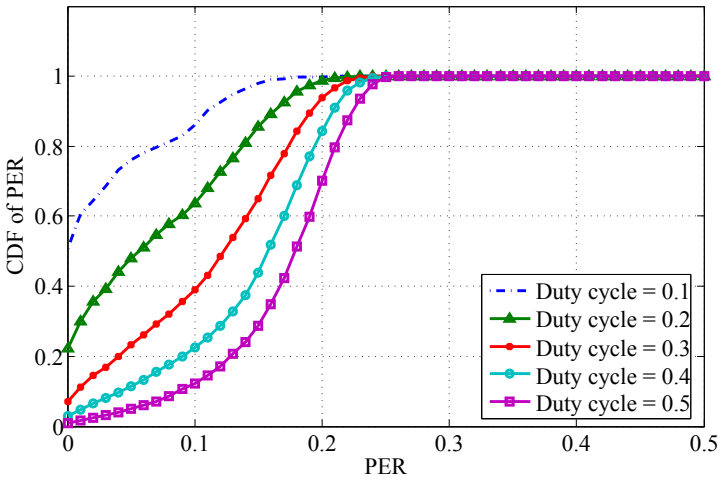

(b) Moderate time scenario.

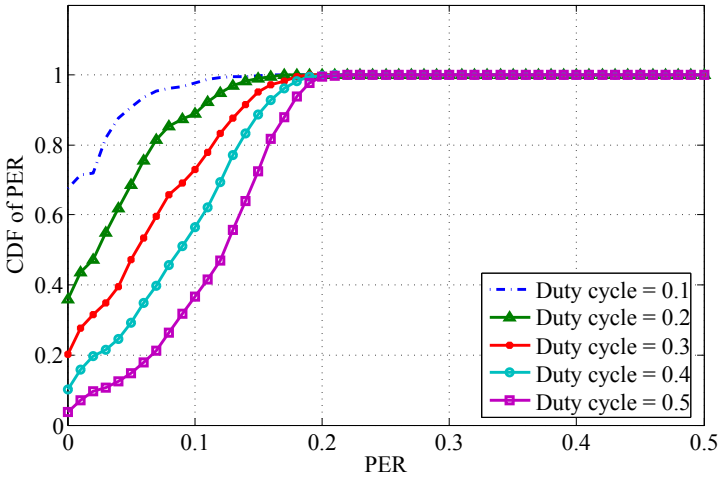

(c) Off-peak time scenario.

Fig. 4.2: The CDF of PER for three scenarios.

Table 4.2: Reliability level (%) with PER lower than 0.05.

Duty Cycle (%)	10	20	30	40	50
Peak time scenario (58 BSNs)	57.3	21.9	7.7	2.5	0.7
Moderate scenario (40 BSNs)	81	49.9	23.3	11.5	5
Off-peak scenario (16 BSNs)	90.8	68.5	47.3	29.1	14.8

Effect of transmission power

Fig. 4.3 shows the PER of BSNs under different transmission power settings. The PER is obtained by averaging over all the BSNs in the moderate time period at the respective transmission power. As can be seen in Fig. 4.3, the average PER increases when the transmission power gets lower. In particular, when the transmission power is -25 dBm, the average PER is 54% higher than that of 0 dBm. It is also found that the PER difference caused by duty cycles becomes less obvious when the transmission power gets lower. This is because when the transmission power is low, the main reason for erroneous or loss of packets is the radio signal blockage by the human body rather than inter-user interference. In comparison, when the transmission power is sufficiently high, the packets loss is mainly due to inter-user interference.

4.3 Discussion

This interference investigation provides insights and guidelines for BSN deployment configurations, such as the maximum traffic load of a BSN and the

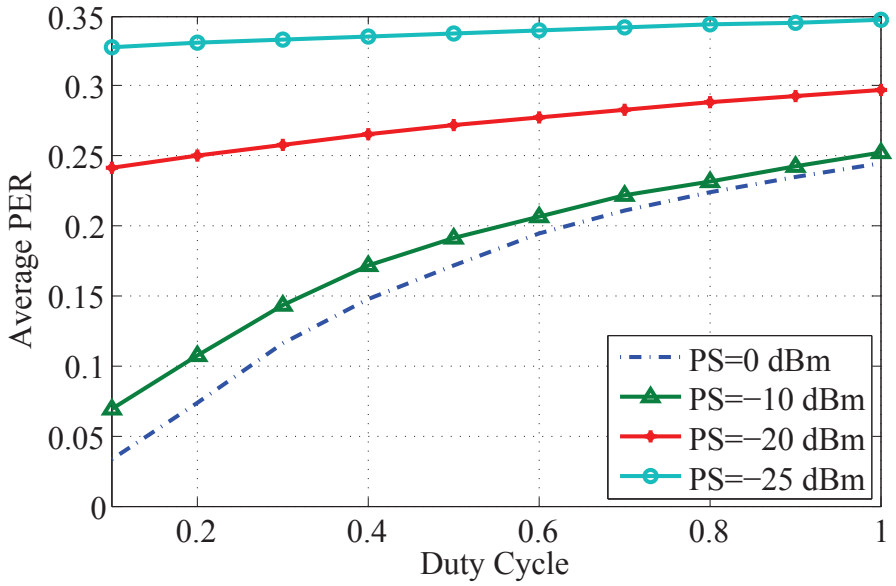

Fig. 4.3: Average PER for different transmission power (PS).

maximum BSN density, to meet the reliable communication requirements. For instance, in the moderate scenario, given the reliability requirement (PER is less than 0.05) and the reliability level (at least 90% of the data packets are transmitted reliably), the duty cycle of a BSN should be less than 10% (obtained from Table 4.2). Conversely, given that the duty cycle of a BSN is 10% and the reliability level is 90%, the maximum number of BSNs that can be accommodated on one channel is around 16 in the off-peak scenario (also obtained from Table 4.2). In addition, given the BSN density and transmission power, there is a maximum traffic load (duty cycle) for each BSN. For example, from Fig. 4.3, given the reliability requirement (PER is less than 0.1), the maximum duty cycle of a BSN is around 30% with a transmission power of 0 dBm, while the maximum duty cycle of a BSN is around 20% with a transmission power of -10 dBm. Also from Fig. 4.3, we know that when the transmission power is low, the main reason for erroneous or lost packet reception is the radio signal blockage by the human body

rather than inter-user interference. Thus a minimum transmission power has to be ensured to avoid packet loss by blockage of human body.

In addition, the investigation gives implications on mitigation schemes for inter-user interference in BSNs when the multitude of operating scenarios is predetermined. For instance, we may reduce the probability of overlapping transmission to improve the SINR. To achieve this goal, transmissions of neighboring BSNs can be rescheduled to avoid overlapping transmissions when the BSN density is low. Moreover, when the BSN density is high, exceeding the maximum number of BSNs that can be accommodated, a channel switching scheme can be incorporated to reduce the congestion level of the current channel. In addition, each BSN is able to select its transmission power adaptively according to its surrounding environment and performance requirement. The BSN with higher priority use higher transmission power to ensure its reliable transmission.

4.4 Summary

In this chapter, we have investigated the significance of the inter-user interference in a realistic moderate-scale BSN deployment scenario in hospital. Simulation results showed that with the target PER requirement (e.g. 0.05), the reliability level of BSN transmission is only 21.9% at the peak time. Even at the off-peak time, the reliability level is only 68.5%. Thus inter-user interference exists widely and severely in the BSN deployment scenario. Based on the investigation, the BSN deployment configurations such as maximum BSN number and the maximum traffic load are implicated. In addition, inter-user interference mitigation schemes are suggested based on the specified scenario.

Chapter 5

A Lightweight Distributed Mitigation Scheme for Inter-User Interference in BSNs

---

In this chapter, we present a lightweight and distributed inter-user interference mitigation (IIM) scheme, that can be easily integrated with the IEEE 802.15.4 protocol stack. The proposed scheme takes into consideration the generic property of low channel utilization in BSNs and enables affected BSNs to adaptively reschedule their transmission time or switch channels. Based on the detected information from neighboring BSNs, BSNs reschedule their transmissions in a distributed and coordinated manner, so that wireless channels can be effectively utilized by multiple BSNs. Moreover, the IIM scheme is performed only when the performance of the BSN is degraded to an unacceptable level due to severe interference to reduce the rescheduling cost. Simulation results show that the proposed scheme improves the network throughput by 18% and reduces the energy consumption by 22% as

compared with the existing beacon schedule scheme.

5.1 Network model and problem description

5.1.1 Network model and assumptions

Currently the most widely used radio standard for BSN communication is the IEEE 802.15.4 (ZigBee) standard[3] [120]. The IEEE 802.15.4 protocol usually operates in a star topology in a BSN, i.e., the sensor node either transfers data to the coordinator, or polls the coordinator to receive data. There are two modes designed for the IEEE 802.15.4 multiple access scheme: non-beacon enabled and beacon enabled, depending on whether the network supports the transmission of beacons. In a non-beacon enabled scheme, a sensor node simply transmits data using unslotted CSMA/CA. In a beacon enabled mode, beacons are utilized to synchronize the transmission of sensor nodes in a superframe.

In this study, we consider the IEEE 802.15.4 wireless technology with the beacon-enabled mode [121] for the BSN communication. Fig. 5.1 shows the superframe structure of the beacon-enabled mode, which contains an active period and an inactive period. The active period is further divided into a contention access period (CAP) and an optional contention free period (CFP). At the beginning of the active period, the coordinator of a BSN synchronizes its sensor nodes by broadcasting a beacon packet. The beacon packet contains schedule information of the BSN. According to the beacon information, a sensor node that wishes to communicate during the CAP competes with other nodes using a slotted CSMA/CA mechanism. In the CFP, nodes transmit in a TDMA mode in their allocated slots without

[3]While IEEE 802.15.6 is the standard developed for BSNs, IEEE 802.15.4 is widely used in BSNs for its low cost and energy efficiency [118, 119].

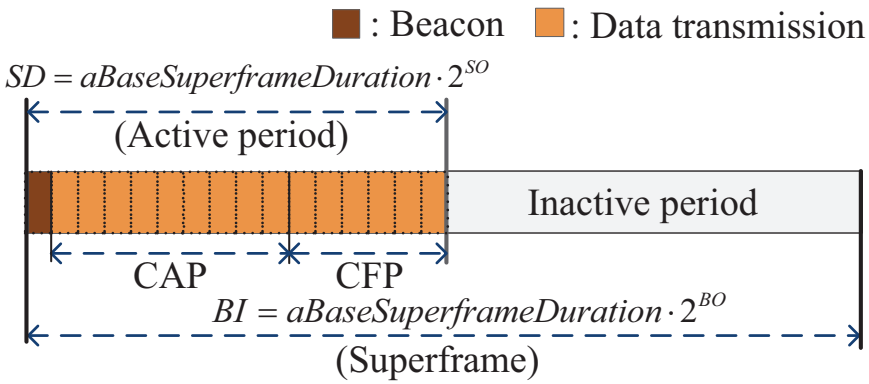

Fig. 5.1: An example of the IEEE 802.15.4 MAC superframe structure ($SO = 0$, $BO = 1$).

competition. Sensor nodes are in sleep mode in the inactive period to save energy. The length of a superframe is equal to a beacon interval (BI), and the length of the active period is equal to a superframe duration (SD). BI and SD are set by the beacon order (BO) and the superframe order (SO) ($0 \leq SO \leq BO \leq 14$) respectively. As shown in Fig. 5.1, $aBaseSuperframeDuration$ denotes the minimum duration of the superframe, which is 15.36 ms assuming 250 kbps transmission rate in 2.4 GHz frequency band.

BSN communication remains within the cluster of sensor nodes worn on a human body. Inter-user interference is significantly affected by BSN mobility when the BSNs move into the interference range of each other and transmit simultaneously. Mobility models of the mobile users are considered in the IIM design and performance evaluation. The pedestrian characteristics of the mobility pattern of BSNs are set according to [105].

In this study, we make the following assumptions:

(1) All the BSNs have the same priority for their data transmission.

(2) The length of the superframe (BI) is the same for all BSNs, while the starting time of the superframes may be different.

(3) Periodic and low duty cycle data transmissions are assumed in BSNs, which is the case in most healthcare applications.

5.1.2 Problem description

In this subsection, we first formulate the inter-user interference problem, and then propose our solution.

The schedule information of BSN i is expressed as (SD^i, BI^i, c^i, b^i), where SD^i and BI^i are the SD and BI of BSN i, c^i is the channel index and t^i is the next transmission time of BSN i. As shown in Fig. 5.2, BSN i starts transmission at t^i, the transmission lasts for SD^i and repeats every period of BI^i on channel c^i if no collision occurs. Collision happens when a neighboring BSN j has overlapping transmission with BSN i on the same channel, i.e., $\|t^i - t^j\| \leq SD^i$. Such overlapping transmission is referred to as inter-user interference. The interference lasts until the departure of the interferer BSN j.

As shown in Fig. 5.2, our proposed IIM scheme reschedules BSN i's transmission from t_0^i to t^i in order to avoid collisions. Each rescheduling operation incurs a delay T_{delay} from the original transmission time t_0^i to the rescheduled transmission

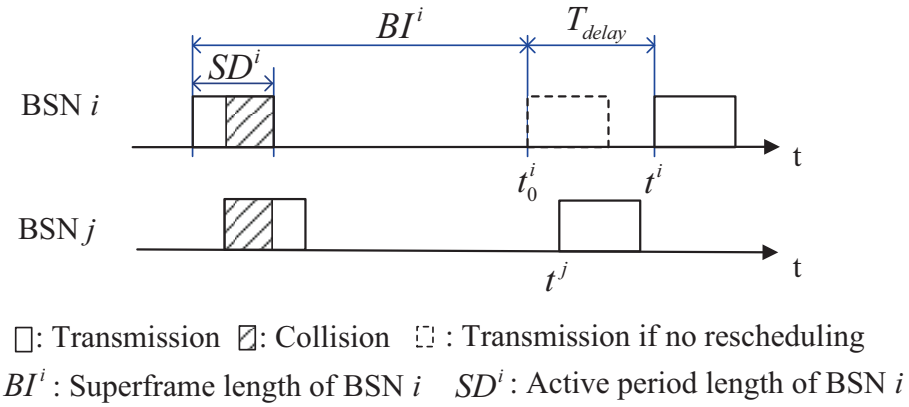

Fig. 5.2: The inter-user interference between BSN i *and BSN* j.

time t^i. The minimum delay T_{delay} is desirable for achieving optimal throughput. In the case that N BSNs congregate together, denoting the neighbor set of BSN i as $\{\Omega^i : (SD^j, BI^j, c^j, t^j) | 1 \leq j \leq N, j \neq i\}$, BSN i needs to avoid collisions with all the BSNs in its neighbor set Ω^i in rescheduling. Moreover, when multiple channels can be utilized, the transmission can be rescheduled in two dimensions (c^i, t^i). Fig. 5.3 shows the transmission status of neighboring BSNs around BSN i in a multiple-channel scenario, which depicts whether it is collision or collision-free for BSN i to start transmission at (c^i, t^i). Similar to the scenario in Fig. 5.2, each reschedule decision (c^i, t^i) has a delay $T_{delay}(c^i, t^i)$ from the original transmission time to the rescheduled transmission time. In general, the objective of our IIM scheme is to select a collision-free duration, starts with t^i on channel c^i and lasts for SD^i, with minimum latency T_{delay},

$$(c^i, t^i) = \arg\min_{(c_l, b_k)} (T_{delay}(c_l, b_k)), \tag{5.1}$$

where c_l is the channel index in the available channel set, b_k is the time slot index in the rescheduled superframe. Because of the slotted access in the IEEE 802.15.4 beacon-enabled mode, t^i needs to be selected from one of the time slots b_k. After selecting (c^i, t^i), BSN i reserves the successive SD^i for transmission by announcing the schedule in the next beacon.

It is challenging to obtain such a transmission status table in the absence of global synchronization. Note that the beacon contains the schedule information (SD^i, BI^i, c^i, t^i). The transmission status table of BSN i can be obtained by overhearing the beacon packets of its neighboring BSNs. In the next section, we will describe the IIM scheme in detail.

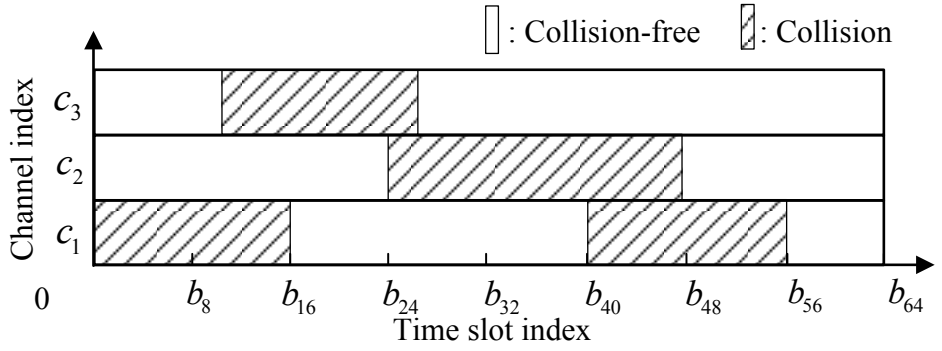

Fig. 5.3: Transmission status of neighboring BSNs around BSN i *in a multiple channel scenario.*

5.2 IIM scheme

5.2.1 IIM procedure

The IIM scheme has the following modules: (1) inter-user interference detection, (2) transmission status collection from other BSNs, in this module, beacons are collected from other BSNs, and (3) rescheduled time and channel selection module, as shown in Fig. 5.4. In particular, four steps are followed:

Step 1 (Initiation): The IIM scheme is initiated when a BSN (e.g. BSN i) experiences significant performance degradation. That is the coordinator identifies significant decrease in throughput or packet reception ratio, while the received signal strength does not obviously drop. In this case, the performance degradation is probably due to BSN congestion instead of bad channel. Upon initiation, sensor nodes of BSN i fall asleep as usual during the inactive period, and wake up at

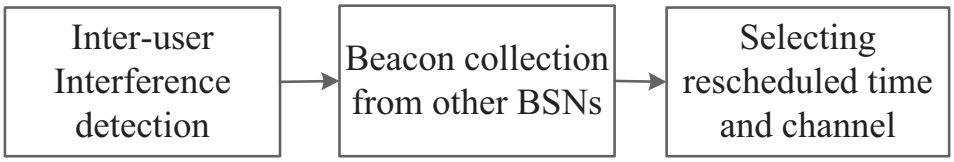

Fig. 5.4: Modules of the IIM scheme.

the next active period to await the beacon packet from the coordinator. The coordinator enters the listening period instead of falling asleep after this active period.

Step 2 (Listening): The coordinator of BSN i listens for a superframe length (BI) to collect its neighbors' information by overhearing their beacon packets. BSN i can then decode the overheard beacons and get the schedule information from them. Based on the overheard beacon information, BSN i establishes its neighbour list with their schedule information. The problem of incomplete neighbour list problem will be addressed in Step 4.

Step 3 (Rescheduling): After the listening period, the coordinator of BSN i executes the ***rescheduling algorithm*** (described in subsection 5.2.2) to determine the possible rescheduled transmission time t^i_{temp}. This step ensures that overlapping transmissions can be alleviated, while the existing transmissions of other BSNs are not affected.

Step 4 (Collision avoidance in case of incomplete neighbor information): To avoid collisions caused by an incomplete neighbor list, the BSN transmits at the rescheduled transmission time t^i_{temp} with carrier sensing and backoff (see subsection 5.2.3). The coordinator informs its sensor nodes of the new schedule through its beacon. After that, the sensor nodes of BSN i transmit periodically in the assigned time slots until the next IIM initiation.

In Step 3, when the ***rescheduling algorithm*** fails to obtain t^i_{temp} on the current channel, the channel is deemed fully-occupied. Accordingly, the coordinator switches to another channel and executes from Step 2 again. The flow chart of the IIM scheme is shown in Fig. 5.5. Fig. 5.6 gives an example of the IIM procedure where four co-located BSNs are transmitting on the same channel. In Fig. 5.6, BSN *1* maintains its regular transmission in the absence of collisions,

while BSN *2*, BSN *3*, and BSN *4* are initiated sequentially to reschedule their transmissions due to collisions. After a listening period, they are rescheduled to avoid collisions without interrupting the transmission of BSN *1*. The schedule is

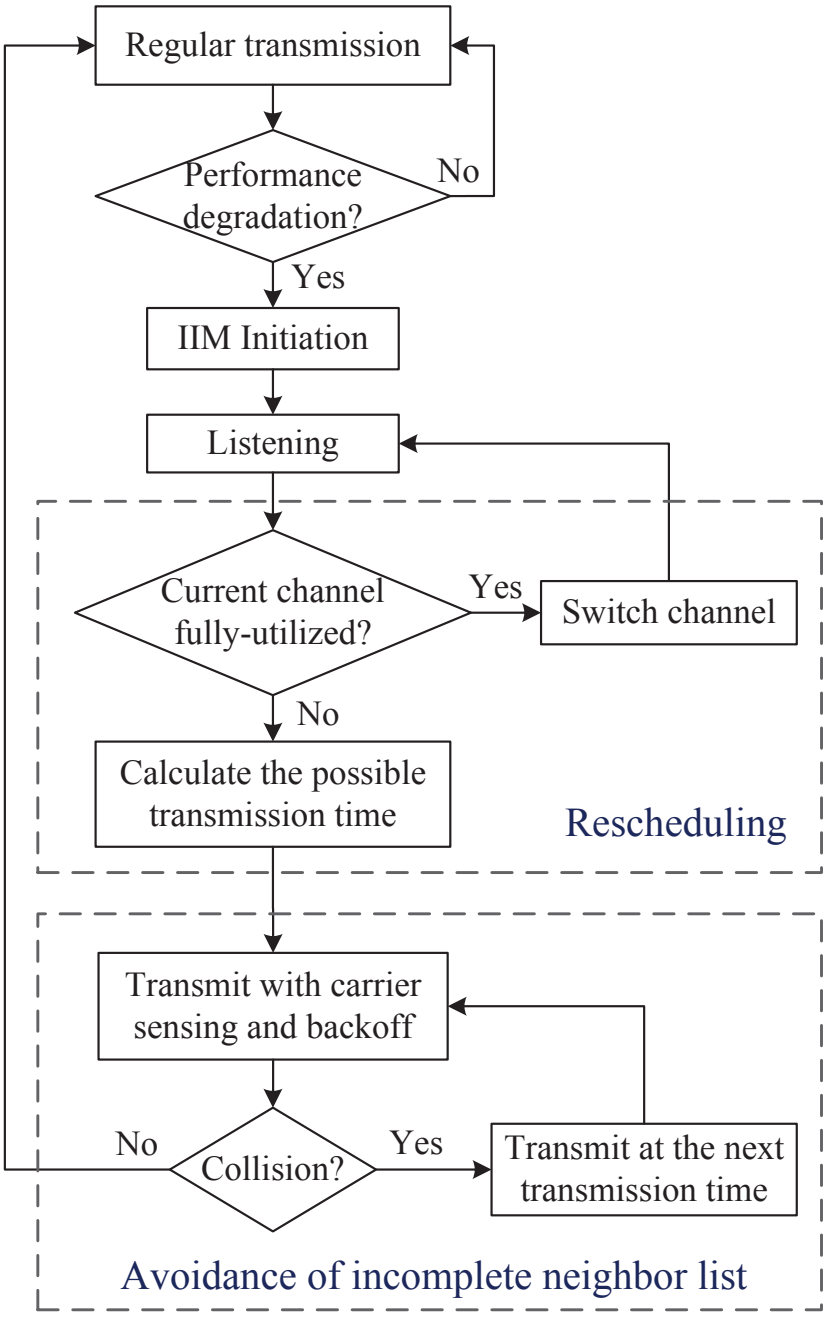

Fig. 5.5: Flow chart of the IIM scheme.

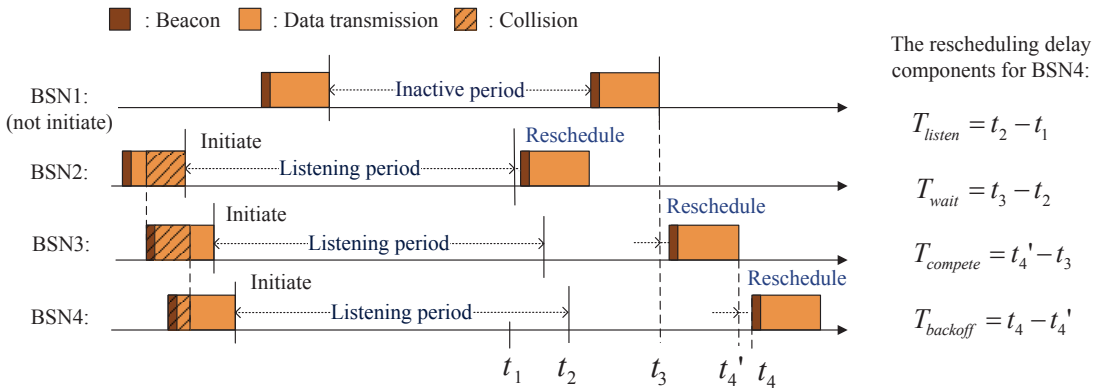

Fig. 5.6: Example of the IIM scheme.

maintained periodically thereafter until the next initiation.

There are a few design considerations in IIM:

- Carrier sensing and backoff are performed only before the rescheduled beacon transmission.
- Rescheduling transmission time is preferred for interference mitigation as compared with switching channels for spectrum efficiency when the channel utilization is low.
- If switching channel is desirable, the coordinator of BSN i first informs its sensor nodes of the schedule using the original channel. Then the coordinator and sensor nodes switch to the new channel to start transmissions.

5.2.2 Rescheduling algorithm

In Step 3 of the workflow described in Section 5.2.1, the rescheduling algorithm is executed to determine the possible transmission time t^i_{temp} for BSN i. It consists of establishing the transmission status table and selecting t^i_{temp} accordingly.

We define two superframes in the IIM scheme: (1) **listening superframe**, where BSN i listens to the beacon packets from other BSNs; and (2) **rescheduling superframe**, where BSN i establishes its transmission status table and reschedules its transmission. The transmission status table indicates whether transmission on time slot b_k of the rescheduling superframe will be interfered or not. Fig. 5.7 shows BSN i establishes its transmission status table in the presence of an interferer BSN j. In Fig. 5.7, the listening superframe of BSN i is from $(t_0 - BI)$ to t_0, and the rescheduling superframe is from t_0 to $(t_0 + BI)$. During the listening superframe, BSN i receives BSN j's beacon packet at t^j_{-1}. From the information obtained from the beacon (SD^j, BI^j, c^j, t^j), it is known that the current transmission of BSN j lasts for a period of SD^j, and the next transmission of BSN j will start at t^j. The transmission status table of BSN i is established in the rescheduling superframe of BSN i by marking the time slots that has overlapping transmission with BSN j as collision.

When multiple BSNs congregate together, within the interference range of one another, their transmission status tables are established similarly, except that all the BSNs in the neighbor set $\{\Omega^i : (SD^j, BI^j, c^j, t^j) | 1 \leq j \leq N, j \neq i\}$ are considered. In general, two principles are followed:

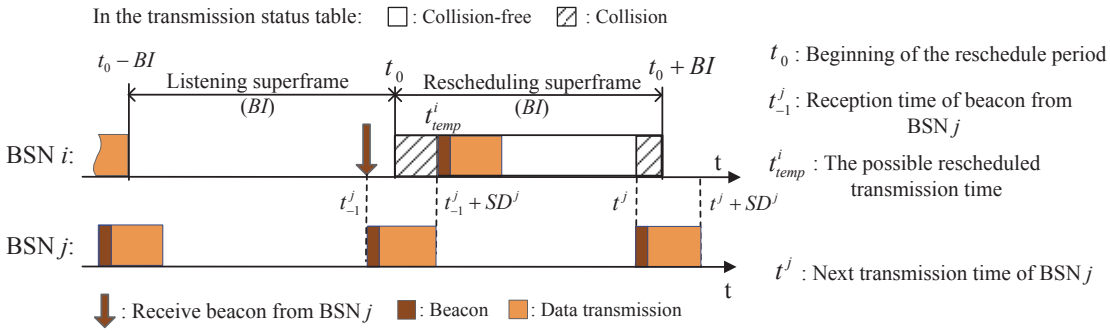

Fig. 5.7: The procedure of establishing the transmission status table of BSN i *in the presence of an interferer BSN* j.

(1) If the current transmission of BSN j falls in the rescheduling superframe of BSN i, i.e., $t^j_{-1} \leq t_0 \leq t^j_{-1}+SD^j$, mark the corresponding time slots $b_k \in (t_0, t^j_{-1}+SD^j)$ as collision.

(2) If the next transmission of BSN j is in the rescheduling superframe of BSN i, i.e., $t_0 \leq t^j \leq t_0 + BI$, mark the corresponding time slots $b_k \in (t^j, \min[t_0 + BI, t^j+SD^j])$ as collision.

The algorithm is implemented over all the members in the neighbor list Ω^i. The other time slots in the rescheduling superframe are set to be collision-free in the transmission status table.

From the transmission status table, the next possible transmission time t^i_{temp} of BSN i is determined as the time slot whose subsequent collision-free time slots are sufficiently long for BSN i's transmission. We record all the possible transmission time slots, and sort them by their corresponding rescheduling delays $T_{delay}(q) = t^i_{temp}(q) - t_0$. It is always preferred to transmit at the earliest possible transmission time ($q = 1$). For example, in Fig. 5.7, BSN i selects t^i_{temp} as its earliest possible transmission time to avoid collision with BSN j. However, if the transmission fails at the first trial ($q = 1$) due to an incomplete neighbor list (see subsection 5.2.3), the transmission is attempted at the next possible transmission time $t^i_{temp}(q + 1)$. The procedure of the rescheduling algorithm is shown in Algorithm 1.

5.2.3 Collision avoidance in case of incomplete neighboring information

In Step 4 of the workflow, to avoid the collision caused by an incomplete neighbor list, carrier sensing and backoff are performed before the rescheduled

Algorithm 1 Rescheduling algorithm

Input: Neighbor list of BSN i $\{\Omega^i : (SD^j, BI^j, c^j, t^j) | 1 \leq j \leq N, j \neq i\}$.
Output: Collision-free transmission opportunity t^i_{temp}.

At the end of the listening period, BSN i performs the following:
$(b_1, ..., b_n) \leftarrow$ collision $-$ free;
for BSN j in the neighbor list Ω^i **do**
  if there is a transmission going on, $t^j_{-1} \leq t_0 \leq t^j_{-1} + SD^j$ **then**
    $b_k \in \left(t_0, t^j_{-1} + SD^j\right) \leftarrow$ collision;
  end if
  if the next transmission of BSN j is in the reschedule superframe of BSN i, i.e., $t_0 \leq t^j \leq t_0 + BI$ **then**
    $b_k \in (t^j, \min[t_0 + BI, t^j + SD^j]) \leftarrow$ collision;
  end if
end for
for b_k in the rescheduling superframe **do**
  if there is a collision-free time duration starting with b_k for the transmission of BSN i **then**
    $t^i_{temp}(q) \leftarrow b_k$;
    $q \leftarrow q + 1$;
    $k \leftarrow k + 1$;
  end if
end for
if collision-free duration is not found, $q = 0$ **then**
  Switch channel;
end if

beacon transmission. As the neighbor list is obtained from the received beacons, the derived neighbor list may be incomplete due to collision of beacons or hidden terminals. When a BSN with an incomplete neighbor list transmits according to t^i_{temp}, it may collide with the undetected BSNs, whose information is not updated in the neighbor list as expected. For instance, in Fig. 5.6, BSN *3* decides its t^i_{temp} as t_3 and postpones its transmission until t_3. Because of the deferment, BSN *4*, which is initiated after it, misses BSN *3*'s beacon and also decides on t_3. As a result, both BSN *3* and BSN *4* would transmit at t_3 causing packet collisions.

To avoid collisions caused by an incomplete neighbor list, before t^i_{temp}, the coordinator of BSN i senses the channel to check if there is an on-going transmission of the undetected BSNs. If the channel is idle for a certain period, called *holding time*, the coordinator transmits after a backoff period as planned. Otherwise, if the channel is sensed busy (either immediately or during the holding time), the coordinator monitors the channel at the next possible transmission time until it is sensed to be idle for one holding time, and then transmits after a backoff period. The holding time is configured to be a two-slot duration. Fig. 5.8 shows the case when the channel is idle and the affected BSN transmits after a holding time and backoff time. Therefore, the final rescheduled transmission time is the time that BSN i successfully accesses the channel after channel sensing and backoff, while t^i_{temp} obtained in the ***rescheduling algorithm*** is just the time that BSN i tries to access the channel and starts channel sensing.

Because most collisions have been alleviated by the rescheduling algorithm (subsection 5.2.2), the exponential backoff mechanism is not necessary and a short fixed backoff window is sufficient to avoid collisions.

In the presence of interference from other networks (e.g. WLAN), IIM explores the utilization of the current channel and schedules transmissions adap-

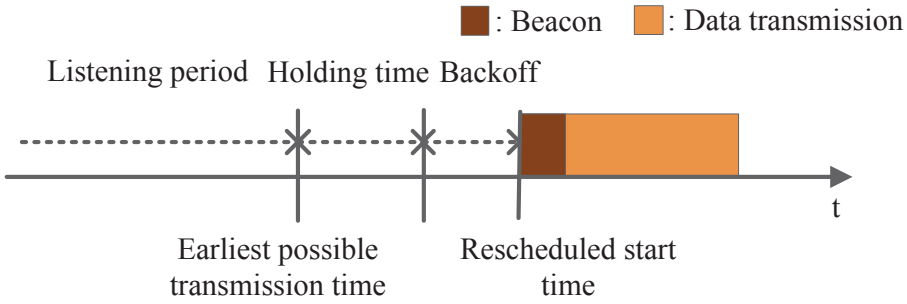

Fig. 5.8: Carrier sensing and backoff before the rescheduled beacon transmission.

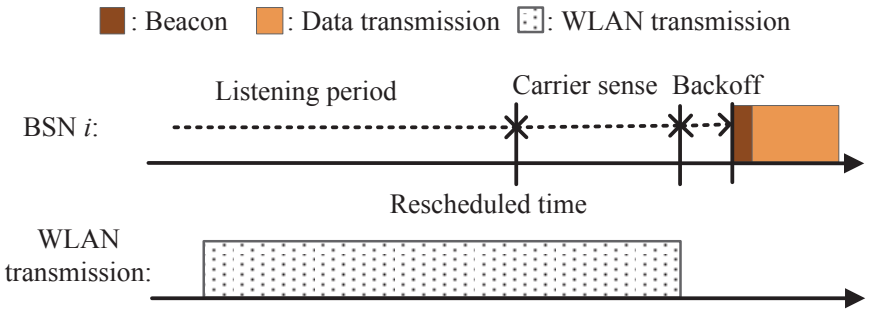

Fig. 5.9: Example of IIM scheme in the presence of WLAN.

tively. As an example, Fig. 5.9 depicts the transmission scheme of BSN i in the presence of WLAN. As shown in Fig. 5.9, BSN i reschedules its transmission through carrier sensing after the WLAN transmission to avoid collisions, although it is unable to collect the transmission status of the WLAN during the listening period in the absence of beacon packets. In the case of severe interference from other networks, IIM detects significant performance degradation while identifies very few neighboring BSNs and cannot obtain the transmission status of other networks during listening period. In such a case, the channel utilization is high so that rescheduling transmission in the same channel does not make much sense, and only channel switching can improve the system performance.

5.3 Performance analysis and discussion

In this section, we first calculate the maximum number of BSNs that can be supported by IIM $N_{\max}$. Then we analyze the rescheduling delay T_{delay}, throughput, and convergence of IIM.

If the number of neighboring BSNs is below $N_{\max}(c_l)$ on channel c_l, BSN i can find a suitable schedule. Otherwise, switching channel is desirable.

Assume all the BSNs have the same superframe length (BI) and active period length (SD). When BSNs transmit exactly after each other, the upper bound of $N_{\max}(c_l)$ on channel c_l is achieved as

$$N_{\max}^{UB}(c_l) = \left\lfloor \frac{BI}{SD} \right\rfloor, \tag{5.2}$$

where $\lfloor \bullet \rfloor$ is the integer floor function. This equation indicates that $N_{\max}^{UB}(c_l)$ is the multiplicative inverse of the duty cycle (SD/BI). For example, if the duty cycle of a BSN is 1/5, the theoretical maximum BSN number that can be supported in a channel is 5.

However, $N_{\max}(c_l)$ is reduced when BSNs do not transmit exactly after one another. With carrier sensing and backoff, the channel utilizing period of a BSN is slightly longer than the actual transmission time. The worst case happens when the interval between two transmissions is slightly less than the transmission period of a BSN. In this case, the lower bound of $N_{\max}(c_l)$ is expressed as

$$N_{\max}^{LB}(c_l) = \left\lfloor \frac{BI}{2SD + W} \right\rfloor, \tag{5.3}$$

where W is the fixed backoff window size and $(SD + 0.5W)$ is the transmission period of a BSN. In general, the $N_{\max}(c_l)$ is between the upper bound and lower bound. Thus we have

$$N_{\max}(c_l) \in [N_{\max}^{LB}(c_l), N_{\max}^{UB}(c_l)]. \tag{5.4}$$

In practice, $N_{\max}(c_l)$ is decided dynamically according to the neighbor list (see subsection 5.2.2). In particular, if BSN i is unable to find a possible transmission time t_{temp}^{i} after searching its transmission status table, the number of congregated BSNs is deemed to exceed $N_{\max}(c_l)$ on channel c_l. In this case, switching channel is desirable, as shown in the last section of Algorithm 1. When multiple channels are available, the maximum number of BSNs that can be supported by IIM is

$$N_{\max} = \sum_{c_l=1}^{m} N_{\max}(c_l), \tag{5.5}$$

where m is the channel number. If the number of congregated BSNs exceeds $N_{\max}$, IIM decides that some of the BSNs have to change channels for effective transmissions. Alternatively, each BSN has to reduce its duty cycle to support more BSNs operating in the common space.

The rescheduling delay T_{delay} of IIM is defined from the original transmission time to the rescheduled transmission time. It has four components:

- Listening delay (T_{listen}): it is introduced by channel listening. While the length of the listening period is a superframe length (BI), the length of T_{listen} is only an active period (SD) because the other part of the listening period falls in the inactive period.

- Waiting delay (T_{wait}): it is introduced to avoid overlapping transmissions with the neighboring BSNs. Its value is determined by the specific interference situation of BSN i.

- Competition delay ($T_{compete}$): it happens when BSN i fails to transmit at

the first trial $t^i_{temp}(q)$ and waits until the next transmission opportunity $t^i_{temp}(q+1)$ to access the channel.

- Backoff delay ($T_{backoff}$): this delay is for the carrier sensing and backoff before the rescheduled beacon transmission.

Hence T_{delay} is expressed as

$$T_{delay} = T_{listen} + T_{wait} + T_{compete} + T_{backoff}. \tag{5.6}$$

In Eqn. (5.6), when T_{delay} is less than (SD+BI), the BSN is able to find a suitable schedule on the current channel. (SD+BI) is the summation of the listening delay and the rescheduling superframe length. The four components of rescheduling delay T_{delay} are indicated in Fig. 5.6.

Assume a BSN scans n channels before choosing a suitable schedule, T_{delay} is expressed as

$$T_{delay} = (n-1)BI + T_{listen} + T_{wait} + T_{compete} + T_{backoff}.$$

The first term of the right-hand side of the above equation represents the time for scanning $(n-1)$ channels (Eqn. (5.6) is the special case when $n = 1$).

In summary, each BSN has three states, namely the interfered transmission state, the IIM execution state, and the regular transmission state. The above three states may transit to one another, as shown in Fig. 5.10. When the interference occurs, the BSN transmission is adversely affected. The average length of the interfered transmission is half of the active period ($0.5SD$), because the interferers arrive during the active period with equal probability and IIM is always initiated at the end of the active period. Upon initiation, IIM is executed to find a suitable

schedule. The length of the execution period is $T_{delay}(k)$, where k indicates the kth initiation. After interference mitigation, the regular transmission is maintained for a length of $T_{reg}(k)$ until the the next interference occurrence. [4]Let the throughput of the regular transmission after the kth initiation be $\varphi(k)$, the overall throughput φ is expressed as

$$\varphi = \sum_{k=1}^{K} \frac{T_{reg}(k)}{T_{reg}(k) + T_{delay}(k) + 0.5 \cdot SD} \cdot \varphi(k), \tag{5.7}$$

where K is the total initiation times during the BSN operating duration.

The inter-user interference occurs for two reasons in contention-based rescheduling schemes: (1) a BSN moves into the interference range of BSN i; (2) an existing neighboring BSN reschedules to transmit simultaneously with BSN i. In IIM, interference occurs only due to the first reason, because a BSN always reserves time slots with the awareness of the transmissions of others when it gets rescheduled. As a result, K in Eqn. (5.7) is minimized. When the total operating duration is fixed, the interference duration $T_{reg}(k)$ is maximized as K is minimized. Moreover, T_{delay} is chosen as the shortest delay to find a collision-free time slot. Therefore throughput can be maximized by the proposed IIM scheme.

As long as the number of the congregated BSNs is less than $N_{\max}$, the BSN state will finally converge to the regular transmission state. The regular transmission state is maintained until the next occurrence of inter-user interference.

5.4 Simulation results

We implement the proposed IIM scheme in the QualNet 5.0.2 simulator [122]. The performance of IIM is compared with the basic scheme of IEEE 802.15.4 [111]

[4]The throughput of the interfered transmission state is negligible due to its short duration.

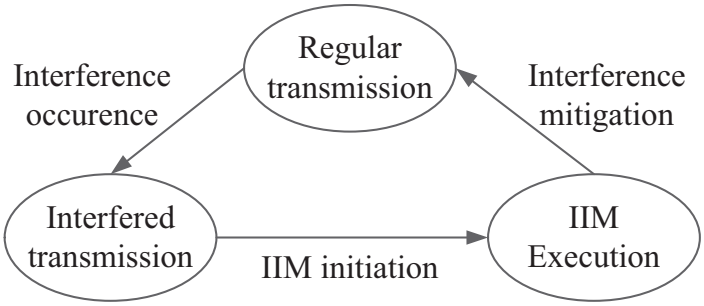

Fig. 5.10: System states of the IIM scheme.

and the flexible beacon scheduling scheme [82] where beacons are scheduled using the contention-based scheme.

5.4.1 Simulation settings

In the simulations, a coordinator and a sensor node form a BSN. The radio settings are configured according to the IEEE 802.15.4 standard and the profiles of TelosB motes [123]. As we focus on the investigation of inter-user interference, we consider an inter-body path loss model with a path loss exponent of 2.4 and a shadowing standard deviation of 6.2 dB [110]. We choose a radio data rate of 250 kbps and a superframe length (BI) of 0.1 s. For healthcare applications, the data rate requirements of commonly used sensor nodes are 5 kbps for ECG and EEG, and 1 kbps for temperature sensor, respiratory sensor, and pulse sensor [11]. Consider the combined usage of those sensors in a BSN, the traffic load per BSN varies from 5 to 25 kbps in the simulations. For simplicity, the traffic load for all the BSNs are set the same in a specific scenario.

We consider the typical BSN deployment in a hospital scenario[5], where the average area occupied by each patient is from 5 to 10 square meters. Considering

[5]The configuration settings of Changi General Hospital and Tan Tock Seng Hospital in Singapore.

Table 5.1: The parameter settings of the simulation in IIM.

Mobile speed interval (m/s)	[0.2, 2.2]
BSN walk interval (s)	[2, 6]
BSN pause interval (s)	[0, 6]
Direction interval (degree)	[-180, 180]
Simulation time (s)	[1000]

the general case where only partial patients utilize BSNs, we start with 5 BSN wearers moving randomly and freely within the space $30m \times 30m$. Later the results are compared with other two scenarios with 10 BSNs and 20 BSNs, respectively. Each BSN moves according to the random waypoint model[6] [101, 104]. The pedestrian characteristics of each BSN wearer are listed in the Table 5.1 according to [105]. Initially, all BSNs are uniformly deployed and then they move independently. To remove the effect of differing initial conditions on performance, we run the simulation fifty times with different initial conditions and then calculate the average results.

5.4.2 Simulation results

In this section, we investigate the performance of the IIM scheme in terms of the ratio of the undetected BSNs, rescheduling delay, collision probability, throughput, and energy consumption.

Ratio of the undetected BSNs

Fig. 5.11 shows the ratio of the undetected BSNs to the actual neighboring BSNs over various traffic loads. Each curve represents a scenario with a certain

[6]We also implemented IIM using the Gauss-Markov mobility model with similar pedestrian settings. The obtained results are similar to that of random waypoint model, and thus not shown in the thesis.

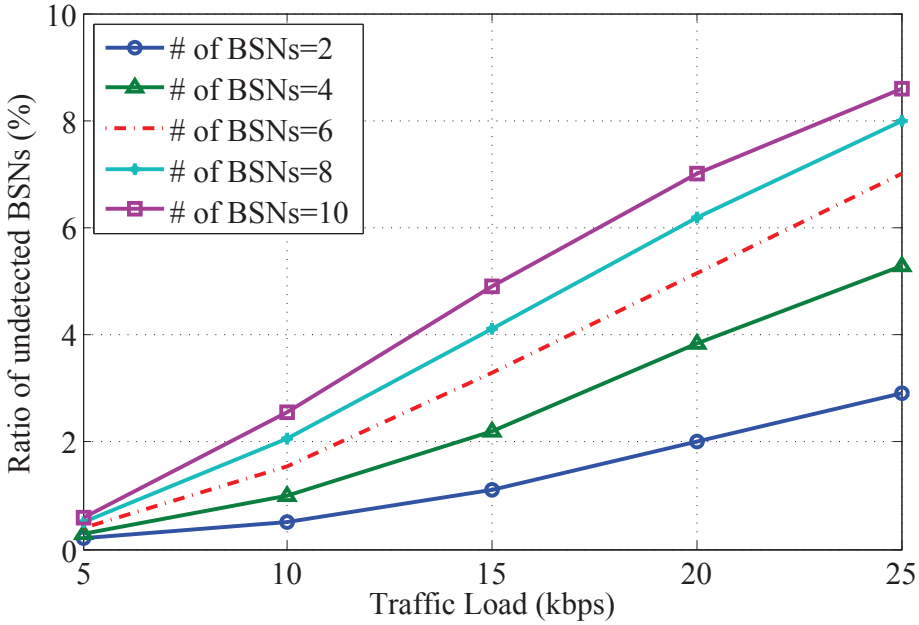

Fig. 5.11: The ratio of the undetected BSNs to the actual neighboring BSNs.

number of BSNs. It can be seen that the undetected ratio increases when either the traffic load of each BSN or the number of neighboring BSNs increases. The reason is that when interference becomes more severe, more beacons are lost. It is noticed that even in the worst case (10 BSNs with the traffic load of 25 kbps each), the neighbor list contains more than 91% of the information of all neighboring BSNs. Hence, the neighbor list can provide sufficient information for rescheduling.

Rescheduling delay

Fig. 5.12 displays the average rescheduling delay T_{delay} in three scenarios: (1) 5 BSNs in a single channel scenario, (2) 10 BSNs in a single channel scenario, (3) 20 BSNs in a double channel scenario. The result converges well with the analysis in Section 5.3. In particular, T_{delay} in the single channel scenario is less than 0.11s, which is $(SD + BI)$ in Eqn. (5.6). In the double channel scenario, BSNs suffer longer delays (less than $(2BI + SD)$). It is also noticed that T_{delay} increases when

the traffic load increases, as it is more challenging for a BSN to find rescheduled time in the channel with a higher load. However, even the highest delay of 0.134 s in the third scenario is tolerable to most applications [124].

Fig. 5.13 shows the ratio of the average delay per superframe to the superframe length in the scenario of 10 BSNs operating in a single channel. For IIM, it is obtained by averaging T_{delay} into superframes over the relatively long interference duration. The result of IIM is compared with that of the basic scheme and beacon schedule scheme. As shown in Fig. 5.13, the delay of IIM is quite low (lower than 2% of superframe length), because rescheduling is performed only when the interference situation changes. For the beacon schedule scheme, the delay is longer because multiple carrier sensing iterations are possibly conducted before each beacon transmission. Regular transmission of a BSN can be interrupted by its neighboring BSN operations, resulting in more rescheduling times. For the ba-

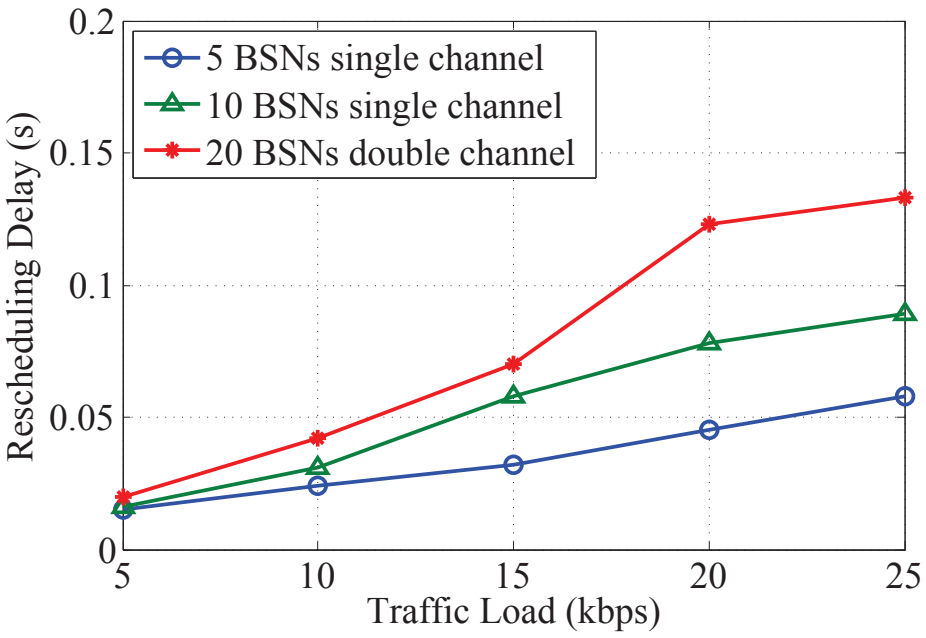

Fig. 5.12: The rescheduling delay of IIM for three scenarios.

sic scheme, the delay is near zero because packets are transmitted directly at the cost of much higher energy consumption and lower throughput. When the number of the congregated BSNs increases, the delay of the beacon schedule method obviously increases, because the BSNs experience long backoff time on the current fully-occupied channel in the absence of an effective channel switching approach.

Collision probability

Fig. 5.14 shows the collision probability of beacons in the scenario of 10 BSNs operating in a single channel. It can be seen that the collision probability of IIM is the lowest, because collisions are effectively eliminated through rescheduling. For the basic scheme, BSNs transmit independently according to fixed schedules, resulting in severe collisions. For the beacon schedule method, a BSN has to compete with all its neighboring BSNs to access the channel, thus collision is more

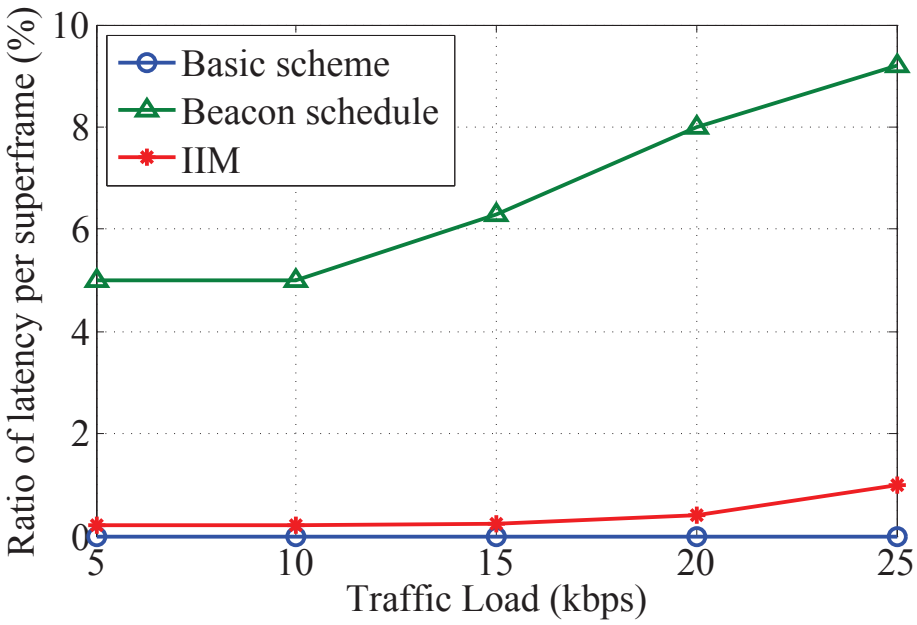

Fig. 5.13: The ratio of average delay per superframe to the superframe length.

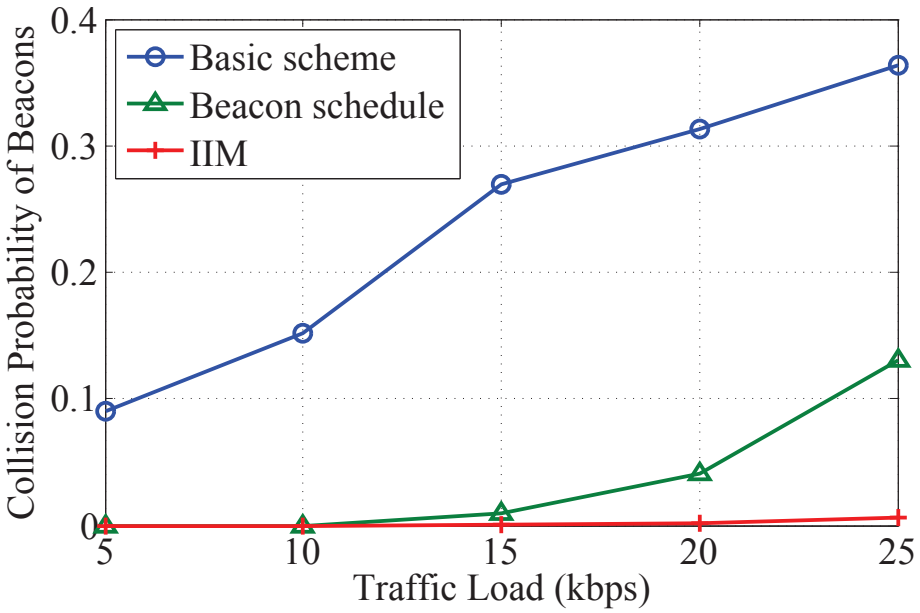

Fig. 5.14: The collision probability of beacons.

severe than that of IIM. In addition, once collision happens, there will be collisions every superframe for the whole interference duration because of the periodic data characteristic of BSNs.

Throughput

Fig. 5.15 depicts the throughput of various traffic loads in three scenarios. As discussed in Section 5.3, IIM achieves the highest throughput among the three schemes. The average throughput improvement is around 30% compared to the basic scheme and 18% compared to the beacon schedule method with all traffic loads. This is because collisions are effectively eliminated by IIM with minimum rescheduling delay, shown in Eqn. (5.7). For the basic scheme, the fixed schedule leads to severe collisions. For the beacon schedule scheme, the throughput is lower than IIM, because collisions are more severe and the delay is longer.

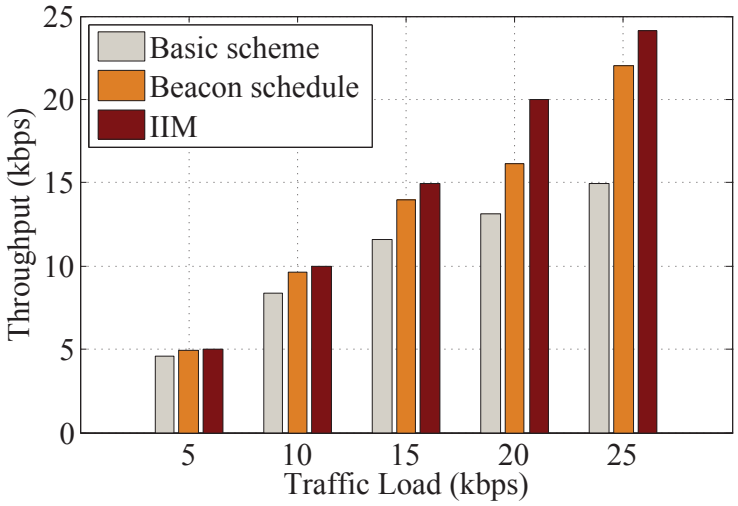

(a) 5 BSNs in single channel scenario.

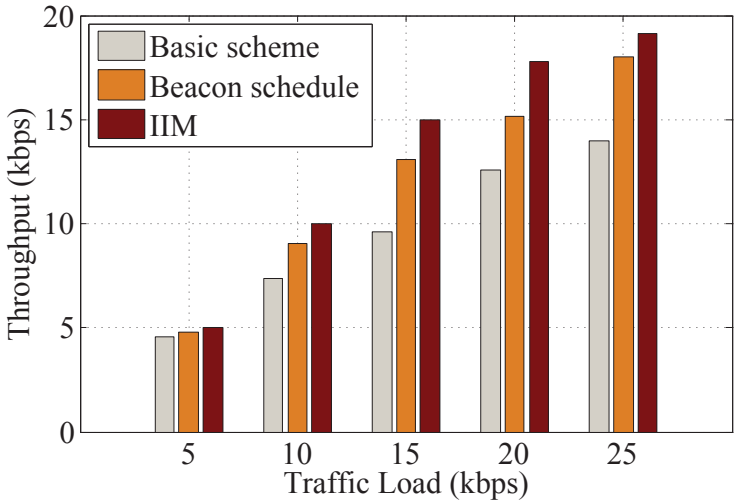

(b) 10 BSNs in single channel scenario.

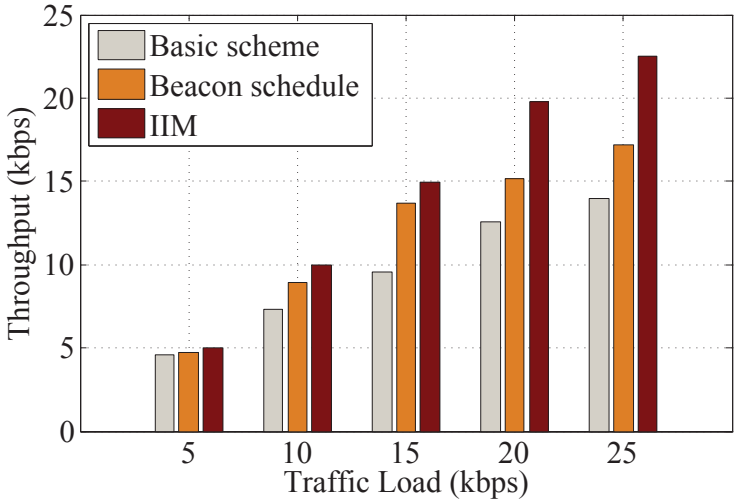

(c) 20 BSNs in double channel scenario.

Fig. 5.15: Throughput versus the traffic load for three scenarios with a random waypoint mobility model.

When the density of BSNs increases from 5 BSNs to 10 BSNs, the performance of the basic scheme decreases significantly because there is higher possibility that a BSN interferes with one another (see Figs. 5.15(a) and 5.15(b)). The comparative performance of IIM and the beacon schedule method are still acceptable. When the traffic load of BSNs increases to a certain level, channel switching should be incorporated to ensure the network throughput.

Fig. 5.15(c) shows the throughput in the scenario of 20 BSNs with two available channels. It can be seen that with channel switching the throughput of IIM improves even when the average number of BSNs per channel is the same as that in Fig. 5.15(b). The reason is that channels can be effectively utilized in two dimensions by IIM. For the beacon schedule scheme, without the effective channel switching method, the BSNs continuously compete on the current channel resulting in low throughput.

Fig. 5.16 shows the throughput in the scenario of 10 BSNs in a single channel, where the BSNs move following a Gauss-Markov mobility model with similar pedestrian settings with the random waypoint model. As can be seen from Fig. 5.16, the throughput obtained by Gauss-Markov mobility model is 4% less than that of random waypoint model (see Fig. 5.15(b)). This is because BSNs have less paused time following a Gaussian-Markov mobility model (increasing the rescheduled times due to the frequently changing interference situation). This also shows that our proposed scheme achieves performance improvement despite the employed mobility model.

Energy consumption

Fig. 5.17 shows the energy consumption per successfully delivered packet in the single channel scenario of 10 BSNs. It is calculated from the power consump-

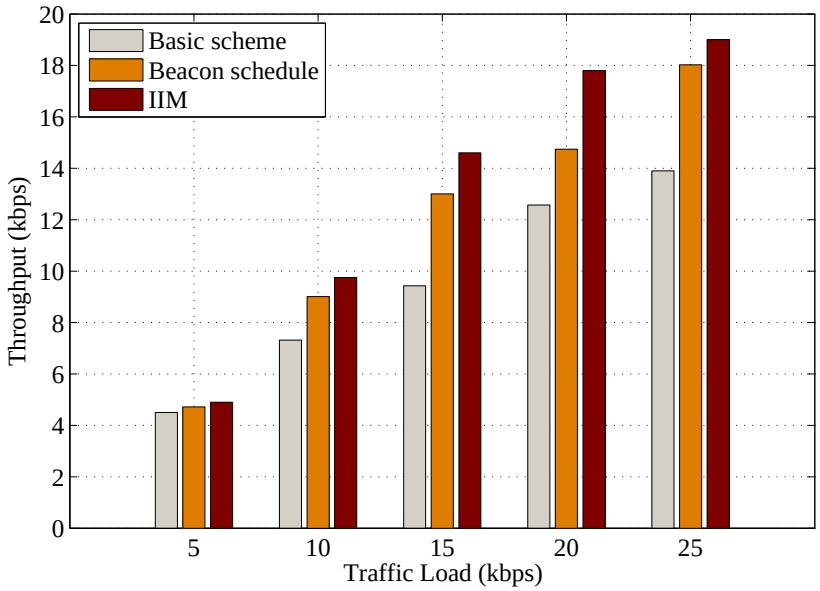

Fig. 5.16: Throughput in 10 BSNs in single channel scenario with a Gauss-Markov mobility model.

tion of TelosB mote, shown in Table 5.2. As expected, the energy cost of delivering a packet using IIM is much lower than that of the other two methods, i.e. around 16% lower than the basic scheme and 22% lower than the beacon schedule method. This is because IIM effectively avoids collision, and hence reduces the number of retransmissions. For the basic scheme, much energy is wasted by collisions and retransmissions. For the beacon schedule method, much energy is consumed for carrier sensing before each beacon transmission. When the traffic load increases, the energy cost gets higher. Especially for beacon schedule method, much energy is consumed as multiple carrier sensing iterations are possibly conducted before each beacon transmission.

Table 5.2: The power consumptions of TelosB radio.

Idle mode	0.8 mW
CCA mode	40 mW
Receive mode	40 mW
Transmit mode	30 mW

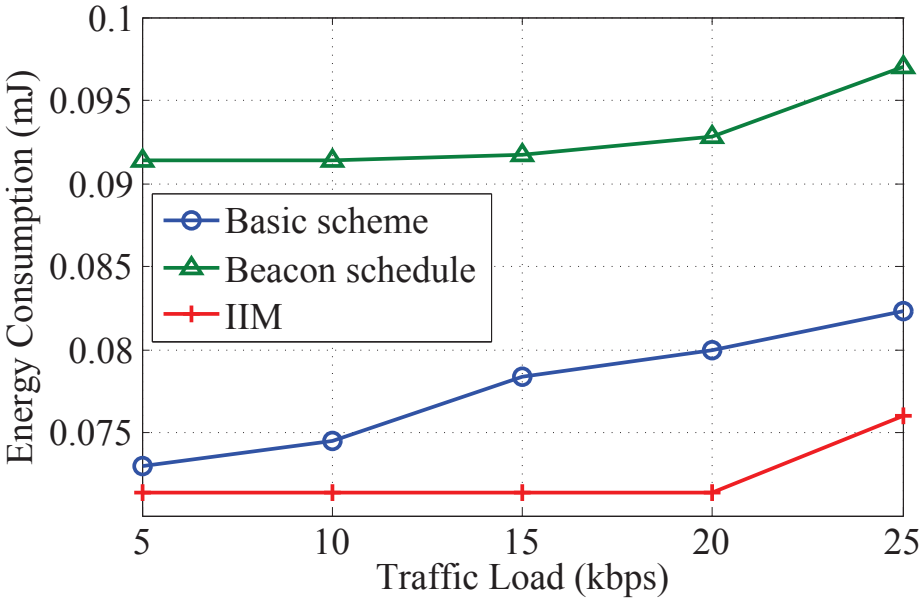

Fig. 5.17: Energy consumption per successfully delivered packet for the 10 BSNs in single channel scenario.

5.5 Summary

In this chapter, we have proposed a lightweight and distributed scheme for mitigating inter-user interference in BSNs. The proposed scheme considers the generic property of low channel utilization of BSNs and enables BSNs to adaptively reschedule their transmission time or channel when the interference occurs. Based on the neighboring information, two actions are conducted: 1) BSNs reschedule their transmissions in a coordinated manner to reduce the rescheduling cost when

the channel utilization is low. 2) When the channel is fully-occupied, channel switching decision can be made promptly so that wireless channels can be effectively utilized. The simulation results showed that the proposed IIM scheme outperforms the basic scheme and the beacon schedule scheme in terms of throughput and energy efficiency. The results confirm that when the density of BSNs becomes higher, the performance improvement of the IIM scheme are more significant.

Chapter 6

A Stochastic Geometry Analysis of Inter-User Interference

In this chapter, we present a stochastic geometry analysis of the inter-user interference in BSNs. The framework considers BSN interferers which are spatially scattered according to a Poisson point process and transmit using either contention-free or contention-based MAC mechanism according to the IEEE 802.15.6 standard. Outage probability and spatial throughput are derived in traceable expressions. Based on the analysis, the interference detection range is optimized to achieve the maximum spatial throughput while the reliable transmission requirement is met. Moreover, implications are provided on the design of MAC for BSNs depending on the specific BSN applications.

6.1 Network model

6.1.1 MAC mechanism in IEEE 802.15.6

The IEEE 802.15.6 standard is specified to coordinate the intra-BSN communication [50]. There are three standardized modes: beacon mode with beacon periods, non-beacon mode with beacon periods, and non-beacon mode without beacon periods, depending on whether the network supports the transmission of beacons and the boundaries of beacon periods.

We consider the beacon mode with beacon periods in this study. The coordinator transmits a beacon frame in each beacon period, except in inactive superframes. Fig. 6.1 shows the superframe structure, which is divided into exclusive access phase 1 (EAP1), random access phase 1 (RAP1), managed access phase (MAP), exclusive access phase 2 (EAP2), random access phase 2 (RAP 2), managed access phase (MAP), and a contention access phase (CAP). In EAP, RAP and CAP periods, nodes contend for the resource allocation using either CSMA/CA. The EAP 1 and EAP 2 are used for highest priority traffic such as reporting emergency events. The RAP1, RAP2, and CAP are used for regular traffic only. Only in a MAP, may the coordinator arrange scheduled uplink allocation intervals, scheduled downlink allocation intervals, and scheduled bi-link allocation intervals; provide unscheduled bi-link allocation intervals, and improvise type-I, but not type-II, immediate polled allocation intervals and posted allocation intervals starting in this MAP.

Typically, the hybrid MAC defined in the IEEE 802.15.6 standard comprises two categories of MAC protocols:

- Contention-free access mechanism: e.g. unscheduled access, or scheduled access and variants, where a BSN transmits whenever there is a packet to

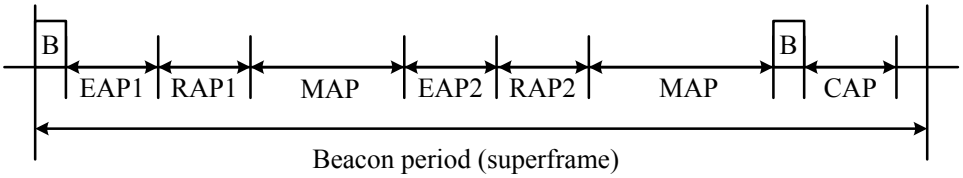

Fig. 6.1: IEEE 802.15.6 superframe structure.

be transmitted.

- Contention-based access mechanism: e.g. CSMA/CA, where a BSN transmits only if other BSNs within the detection range are detected silent.

In short we say a BSN transmits using contention-based or contention-free scheme instead of its sensor nodes.

6.1.2 Channel model

In a wireless channel, signal attenuates (e.g. path-loss, shadow, multi-path fading) before it arrives at the intended recipient. In this study, we consider path-loss and multipath fading for simplicity and leave the shadow fading modeling for future work. The path-loss function is given by $l(d) = G \cdot d^{-\alpha}(d > d_0)$, where G is a constant which accounts for system loss, d is the distance between the transmitter and receiver, d_0 is the reference distance, and α is the path-loss exponent and $\alpha > 2$. We consider Rayleigh fading for multipath fading. Rayleigh fading is a reasonable model when there are many objects in the environment that scatter the radio signal before it arrives at the receiver, which is the case in the BSN application area. The envelope of the channel response will be Rayleigh distributed with the parameter of $1/\mu$.[7]

[7]Combined with the constant transmit power, the received signal h follows exponential distribution with the mean $1/\mu$ [37].

At a given time t, the received signal strength $\Omega(d)$ is expressed as

$$\Omega(d) = \Omega_0 \cdot h \cdot l(d), \tag{6.1}$$

where Ω_0 is the transmission power and h accounts for multipath fading.

The wireless channel between the sensor node and the coordinator in a BSN (referred to as on-body channel model) and that between two BSNs (referred to inter-body channel model) are assumed to follow different channel models. Due to the blockage of the radio signal and its disruption by the human body, on-body channel model experiences more severe attenuation (with a path-loss exponent α_O) than the inter-body channel model (with a lower path-loss exponent α_I and $2 < \alpha_I < \alpha_O$) [107, 108, 125]. In addition, as on-body channel is subject to a number of factors such as gender, body shape of the BSN user and the application environment [126, 127], we utilize a factor K to represent the effects of individual characteristics on the on-body channel model.

6.1.3 Deployment topology of BSNs

We assume that BSNs are distributed uniformly and independently in the BSN deployment area according to a homogeneous Poisson point process [128] with the intensity of λ_0. Denote the set of BSN locations as $\Phi_0 = \{Y_1, Y_2, ..., Y_k, ...\}$. Considering BSNs have active and inactive periods, with the duty cycle of a BSN η, the BSNs which intend to transmit at a given time can be divided into two categories:

- The BSNs which intend to transmit under contention-free scheme Φ_1. Φ_1 is an independent thinning of Φ_0 and also follows a Poisson point process with

the intensity of

$$\lambda_1 = w_1 \eta \lambda_0, \tag{6.2}$$

where w_1 is the ratio of contention-free traffic to the total traffic in a superframe;

- The BSNs which intend to transmit under contention-based scheme Φ_2. Similarly, Φ_2 follows a Poisson point process as well with the intensity of

$$\lambda_2 = w_2 \eta \lambda_0, \tag{6.3}$$

where $w_2 = 1 - w_1$.

The interfering BSNs Φ is defined as the set of BSNs which are transmitting effectively and simultaneously at a given time in the same channel. We are concerned with the interfering BSNs as they actually contribute to the inter-user interference. For the contention-free BSNs, the set of interfering BSNs is exactly Φ_1 as BSNs transmit whenever they intend to. For the contention-based BSNs, however, a BSN may hold-on or back-off due to the busy medium, and transmit only when other BSNs, either contention-based or contention-free based, are detected silent within a carrier sense range R. We have $\Phi = \Phi_1 \cup \Phi_m$ and $\Phi_1 \cap \Phi_m = \phi$. To model this case, we propose a modified Matern point process Φ_m which will be detailed in Section 6.2.

Fig. 6.2 shows an example of the BSN application area (e.g. in hospital) where BSNs that intend to transmit are depicted. As can be seen, BSN1 and BSN3 may hold-on or back-off due to the transmission of BSN2 and BSN4 respectively, while contention-free BSNs, e.g., BSN4 and BSN5, are able to transmit directly although they are quite close to each other. In the BSN application area, the

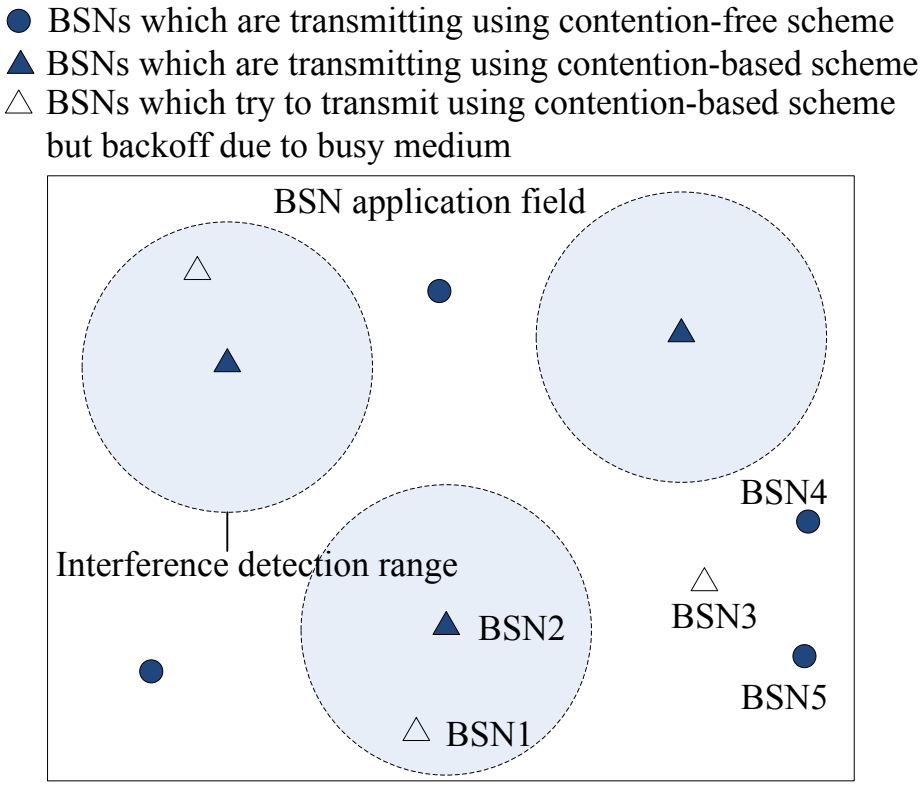

Fig. 6.2: Example of a BSN application area.

coordinator and sensor nodes in a BSN share the same coordination, as sensor nodes in a BSN are vertically deployed and the distance between sensors in the horizontal direction is relatively small. Thus sensor nodes in a BSN are at the same interference situation.

In addition, BSNs move without constraints in the BSN deployment area. According to [38], the interference analysis in static networks also applies to the mobile networks with certain transformation. Thus in this study, we focus on the static case of BSNs.

6.2 Interference analysis

In this section, we propose a modified Matern point process to characterize the inter-user interference. We calculate the intensity and the outage probability of the interfering BSNs, and then derive the spatial throughput.

6.2.1 The intensity of the interfering BSNs

As aforementioned, the *Matern point process* models the spatial distribution of nodes under CSMA/CA. It is a non-independent thinning of the Poisson point process such that the distance between any two nodes in the Matern thinning is larger than a carrier sense range R. It is typically used to describe the spatial distribution of nodes which are effectively transmitting using CSMA/CA at a given time, while the original Poisson point process represents the potential node distribution.

In this study, we propose a *modified Matern point process* to represent the spatial distribution of the interfering BSNs under contention-based scheme. Let $\Phi_m = \{Y_1, Y_2, ..., Y_M\}$ be the set of BSNs which are chosen for the modified Matern point process. Φ_m is also an non-independent thinning of the original Poisson point process Φ_2. It differs from the classic Matern process as the selection of points in Φ_m does not only depend on the contention-based set Φ_2 but also depends on the contention-free set Φ_1. This captures the fact that BSN i under contention-based scheme is allowed to transmit when BSNs from both Φ_1 and Φ_2 are detected silent within the open disc $B(Y_i, R)$ centered in Y_i and of radius R. In particular, each point of Φ_2 is attributed an independent mark uniformly distributed in the interval [0,1]. A tagged BSN i of Φ_2 is selected in Φ_m when the hardcore assigned to BSN i is smaller than that of any other points of $B(Y_i, R)$ in Φ_2 and there is

no point of Φ_1 within $B(Y_i, R)$. This node selection method simulates the back-off mechanism in CSMA/CA where only the node with the smallest back-off time within $B(Y_i, R)$ is allowed to transmit.

To analyze the modified Matern point process, we use the following terms:

- *Intensity* is the spatial average of the number of BSNs within a unit area. In this study, this term is the same as the BSN density.
- *Interference detection range* (also referred to as carrier sense range) is the range within which a BSN under contention-based scheme is not allowed to transmit if other BSNs transmit.
- *Outage probability*: Outage occurs when SINR of a BSN is less than a threshold. In this study, outage probability is used to measure the performance of an individual BSN.
- *Spatial throughput* measures the number of BSNs that transmit simultaneously and successfully within a unit area. It measures the overall performance of BSNs.

Proposition 1. The intensity of the interfering BSNs using contention-based scheme, i.e. modified Matern point process, is given by

$$\lambda_m = \frac{e^{-\lambda_1 \pi R^2} \cdot \left(1 - e^{-\lambda_2 \pi R^2}\right)}{\pi R^2}, R > 0, \tag{6.4}$$

where λ_1 and λ_2 are obtained from Eqns. (6.2) and (6.3), R is the interference detection range.

Proof: Assume the Matern hardcore assigned to a tagged BSN i in the contention-based set Φ_2 is $m(Y_i) = t$. From the modeling of the modified Matern

point process, we know that BSN i is allowed to transmit when the Matern hard-core of other BSN j ($j \neq i$) within $B(Y_i, R)$ from Φ_2 is larger than t and there is no BSN from Φ_1 in $B(Y_i, R)$. The integration is taken over all possible $m(Y_i) = t$ (from 0 to 1) and all possible number of BSNs in $B(Y_i, R)$. We get the spatial probability that BSN i transmits by

$$\begin{aligned} p &= \int_0^1 \sum_{n\in\mathrm{N}} \Pr\left\{ \prod_{j=1,j\neq i}^{n} m(Y_j) > t | \phi_2(B(Y_i,R)) = n, m(y) = t \right\} \\ &\cdot \Pr\left\{\phi(B(Y_i,R)) = n\right\} \cdot \Pr\left\{m(Y_i) = t\right\} \cdot \Pr\left\{\phi_1(B(Y_i,R)) = 0\right\} dt \\ &= \int_0^1 \sum_{n\in\mathrm{N}} \frac{(\lambda_2\pi R^2)^n}{n!} \cdot e^{-\lambda_2\pi R^2} \cdot e^{-\lambda_1\pi R^2} \cdot (1-t)^n dt \\ &= \frac{e^{-\lambda_1\pi R^2} \cdot \left(1 - e^{-\lambda_2\pi R^2}\right)}{\lambda_2\pi R^2}. \end{aligned}$$

Thus we get the intensity of Φ_m (as shown in Proposition 1) by multiplying the spatial probability with the number of contention-based BSNs within R.

As can be seen from Proposition 1, the modified Matern point process Φ_m depends on the contention-free set Φ_1, while Φ_1 is independent from Φ_m. The intensity of the interfering BSNs ($\Phi = \Phi_1 \cup \Phi_m$) is the addition of BSNs under both contention-based and contention-free schemes.

Corollary 2. The intensity of interfering BSNs is given by

$$\lambda = \lambda_1 + \lambda_m. \tag{6.5}$$

6.2.2 Outage probability

In the presence of inter-user interference, outage occurs when the SINR of a BSN is below an acceptable threshold β, i.e.,

$$SINR = \frac{h r^{-\alpha_o}}{\Omega_I + \Omega_n} < \beta, \tag{6.6}$$

where r is the distance between the coordinator and sensor nodes in a BSN, Ω_I is the interference power normalized with transmission power Ω_0, and Ω_n is the average noise power also normalized with Ω_0. We assume the noise is white noise, i.e., constant with frequency.

Proposition 2. The outage probability of a BSN under contention-based scheme is expressed as

$$P_o^{(2)} = 1 - \exp\left(-\pi\lambda A \int_{R^2 A^{-1}}^{\infty} \frac{1}{1 + x^{\alpha_I/2}} dx - \mu\beta\Omega_n r^{\alpha_o}\right), \tag{6.7}$$

where $A = r^{2\alpha_o/\alpha_I}\beta^{2/\alpha_I}$. This is under the assumption that all the interfering BSNs around the tagged BSN i are outside $B(Y_i, R)$ and the dependence between interfering BSNs is ignored.

Proof:

As h in Eqn. (6.6) is exponentially distributed with the mean of $1/\mu$, the outage probability can be written as

$$\Pr\left\{h < \frac{\beta\left(\Omega_I + \Omega_n\right)}{r^{-\alpha_o}}\right\} = 1 - \exp\left(-\mu\beta\Omega_n r^{\alpha_o}\right) \cdot \exp\left(-\mu\beta\Omega_I r^{\alpha_o}\right). \tag{6.8}$$

As can be observed, the last term $\exp\left(-\mu\beta\Omega_I r^{\alpha_o}\right)$ is the Laplace transformation of Ω_I with parameter $s = \mu\beta r^{\alpha_o}$.

Note that for a tagged BSN under contention-based scheme, other BSNs within the detection range R have to be detected silent. Thus the interfering BSNs around the tagged BSN can be approximated as a Poisson point process by ignoring the dependence between points in modified Matern point process outside $B(Y_i, R)$. Let $\phi_u = \{u_i = \|y - Y_i\|\}$ $(u \geq R)$ be the set of distances of the interfering BSNs to the tagged BSN. ϕ_u is an inhomogeneous Poisson point process

with the intensity of $\lambda(u) = \lambda_m u$ $(u \geq R)$. Note that the transmissions between sensor nodes in a BSN and between BSNs follow different channel models, i.e., on-body and inter-body channel model. We get the Laplace transform of inter-user interference Ω_n

$$\begin{aligned} L_I(s) &= \mathrm{E}[e^{-sI}] = \mathrm{E}\left\{\exp\left[\sum_{u\in\Phi_u} \exp\left(-shu^{-\alpha_I}\right)\right]\right\} \\ &= E_\Phi\left[\prod\nolimits_{u\in\Phi\setminus B} E_h\left[\exp\left(-shu^{-\alpha_I}\right)\right]\right] \\ &= E_\Phi\left[\prod\nolimits_{u\in\Phi\setminus B} \tfrac{\mu}{\mu+su^{-\alpha_I}}\right] = \exp\left(-2\pi\lambda \int_R^\infty \left(1-\tfrac{\mu}{\mu+su^{-\alpha_I}}\right) u du\right) \end{aligned}$$

Substitute $s = \mu\beta r^{\alpha_o}$ and change the parameter $x = u^2 A^{-1}$, which concludes Proposition 2.[8]

Moreover, when the effects of individual characteristics on on-body channel model is considered (denote as K), the outage probability of a BSN under contention-based scheme is expressed as

$$P_o^{(2)} = 1 - \exp\left(-\pi\lambda A \int_{K_{\min}}^{K_{\max}} \left(\int_{R^2 A^{-1} K^{-2/\alpha_I}}^{\infty} \frac{1}{1+x^{\alpha_I/2}} dx - \mu\beta\Omega_n K^{-1} r^{\alpha_o} \right) f(K)\, dK \right),$$

where $f(K)$ is the PDF of K, $K_{\min}$ and $K_{\max}$ are the lower and upper integral limits of the factor K.

Corollary 4. The outage probability of a BSN using the contention-free scheme is approximated as

$$P_o^{(1)} = 1 - \exp\left(-\pi\lambda A \int_0^\infty \frac{1}{1+x^{\alpha_I/2}} dx - \mu\beta\Omega_n r^{\alpha_o}\right). \tag{6.9}$$

[8]The proof of Proposition 3 differs from that of Ref. [93] as R is fixed as the interference detection range in this study instead of an integration valuable in [93]. In addition, we leverage on different channel models for on-body and inter-body transmission.

6.2.3 Spatial throughput

A specific metric in stochastic geometry is spatial throughput which characterizes the number of successfully transmitting nodes (i.e. BSNs in the context of this study) within a unit area [37, 129]. It considers the successful transmission probability of a node as well as the spatial reuse. In the case of Aloha and half-duplex transceivers [37], the spatial throughput is expressed as $p\,(1-p)\,(1-P_o)$, where p is spatial transmission probability, $(1-p)$ is the probability that the intended receiver is listening (not transmitting) when the transmitter transmits, and $(1-P_o)$ is the transmission successful probability. In BSNs, the receiver is coordinated to be listening when the transmitter transmits by intra-BSN MAC, thus the term $(1-p)$ is negligible. Moreover, we use the intensity of interfering BSNs, e.g. λ_1 and λ_m, instead of spatial probability p to take into account the ratio of contention-based traffic and contention-free traffic in the context of IEEE 802.15.6 BSNs.

Corollary 5. The spatial throughput is given by

$$\psi = \lambda_1 \left(1 - P_o^{(1)}\right) + \lambda_m \left(1 - P_o^{(2)}\right). \tag{6.10}$$

Eqn. (6.10) is evaluated from Eqns. (6.4), (6.5), (6.7), and (6.9). The first term accounts for the interfering BSNs under contention-free scheme while the second term for that of the contention-based scheme. As can be seen from Eqn. (6.10), the spatial throughput is determined by a number of factors, including the interference detection range, the traffic allocation w_1, and BSN intensity. We will investigate the effects of these factors in the next section.

6.3 Numerical results

In this section, we optimize the interference detection range to achieve the best tradeoff between the successful transmission probability and spatial throughput. In addition, implications are given on the MAC design of a BSN.

6.3.1 Optimized interference detection range

The interference detection range R (also referred to as carrier sense range) determines the distance between two simultaneous transmitting BSNs under contention-based scheme. It is beneficial to schedule a number of short detection range R transmissions for spatial reuse. On the other hand, when R is short, a BSN is likely to experience severe outage due to inter-user interference.

The interference detection range R is optimized to achieve the maximum spatial throughput while the reliable transmission requirement of a BSN is met. That is

$$\max \quad \psi = \lambda_1 \left(1 - P_o^{(1)}\right) + \lambda_m \left(1 - P_o^{(2)}\right) \tag{6.11}$$

$$\text{s.t.} \qquad P_o^{(2)} \leq \kappa \tag{6.12}$$

where κ is the acceptable outage probability requirement.[9]

The above optimization is a complex non-linear problem. To get the trend of Eqn. (6.11), we show the spatial throughput as a function of R in Fig. 6.3. As can be seen, spatial throughput increases when R is small, after arriving at an optimal threshold (when R=2), it decreases. To consider the outage probability constraint (6.12), Figs. 6.4 and 6.5 show the outage probability as a function of detection

[9]Note that Eqn. (6.12) only considers the outage probability of BSNs under contention-based scheme. Outage of contention-free BSNs is considered by the BSN deployment settings.

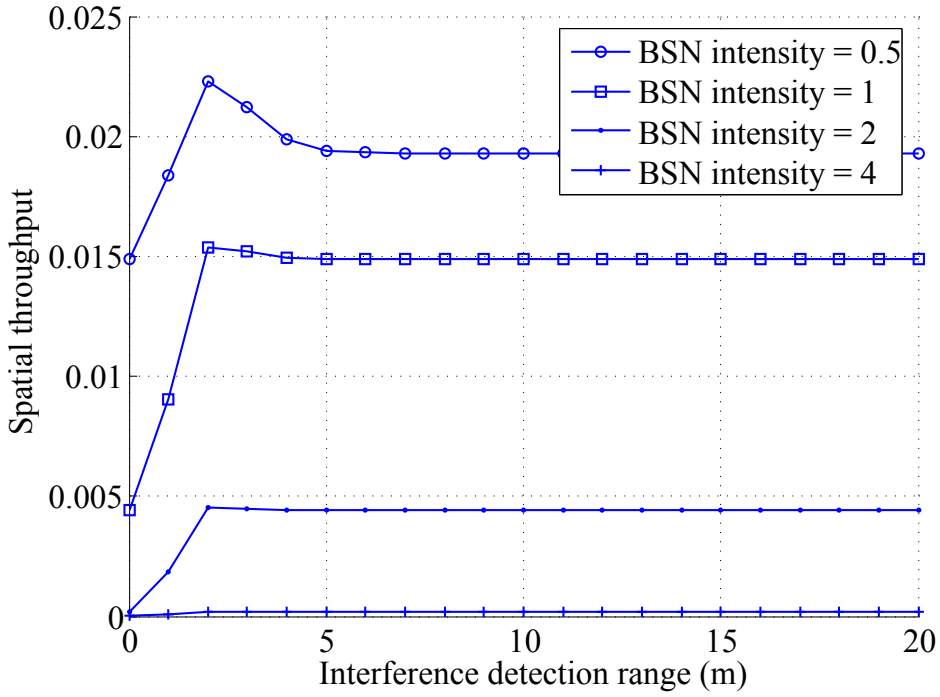

Fig. 6.3: Spatial throughput as a function of interference detection range under different BSN intensities.

range under difference SINR threshold and BSN intensity respectively. As can be seen from Figs. 6.4 and 6.5, the outage probability requirement cannot be met at R=2 for a typical reliability requirement, i.e., the target outage probability $\kappa = 90\%$. In fact, we investigate the typical BSN deployment scenarios (BSN intensity varies from 0.1 to 5), spatial throughput is a monotonically decreasing function over R within the acceptable detection range which defined by the outage constraint. Thus we get the following proposition:

Proposition 6. The optimum interference detection range, which maximize the spatial throughput while keeps the outage probability of a BSN meets the reliability requirement, is achieved when the equality holds for the outage probability requirement $P_o(R) = \kappa$.

6.3.2 Implications on the MAC design for BSN

In a BSN, the ratio of contention-free traffic w_1 is typically determined by the data type of a BSN, e.g. determined or random traffic. In this subsection, we show that w_1 affects the spatial throughput given the other settings fixed. Finding the optimum traffic allocation means finding the optimum trade-off between spatial reuse (more contention-free traffic results in a higher density of concurrent transmissions) and success probabilities (a high w_1 results in higher interference and thus a lower success probability).

Fig. 6.6 shows the spatial throughput as a function of w_1. As can be seen, for a specific BSN intensity, spatial throughput increases when w_1 is still low, after arriving at an optimal value, it decreases. This is because when w_1 is still low, the number of simultaneous transmissions increases with w_1, resulting in the improve-

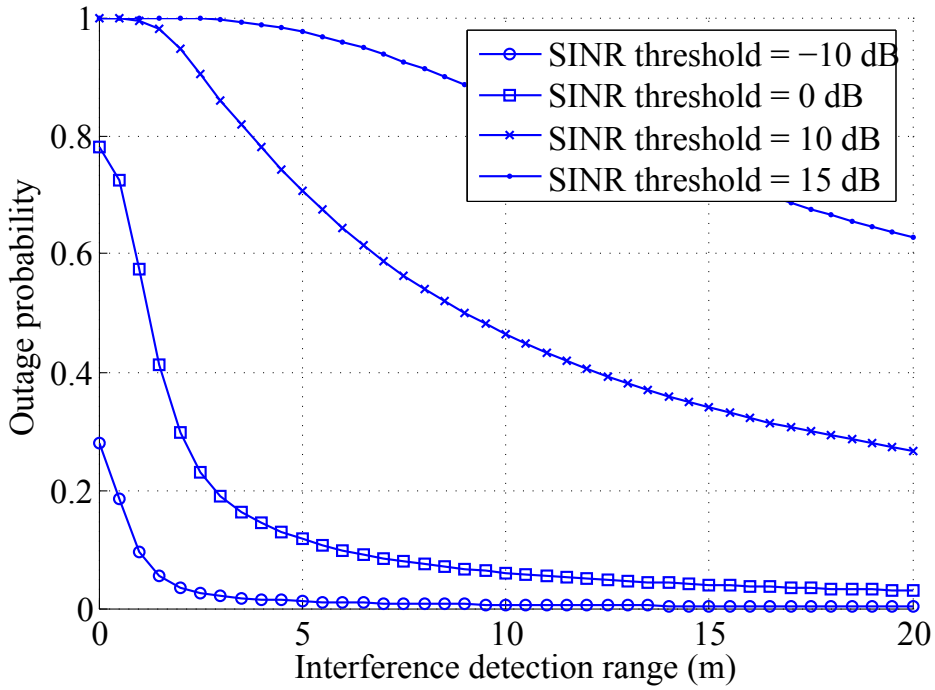

Fig. 6.4: Outage probability as a function of interference detection range when SINR threshold is -10, 0, 10, 15 dB and BSN intensity is 1.

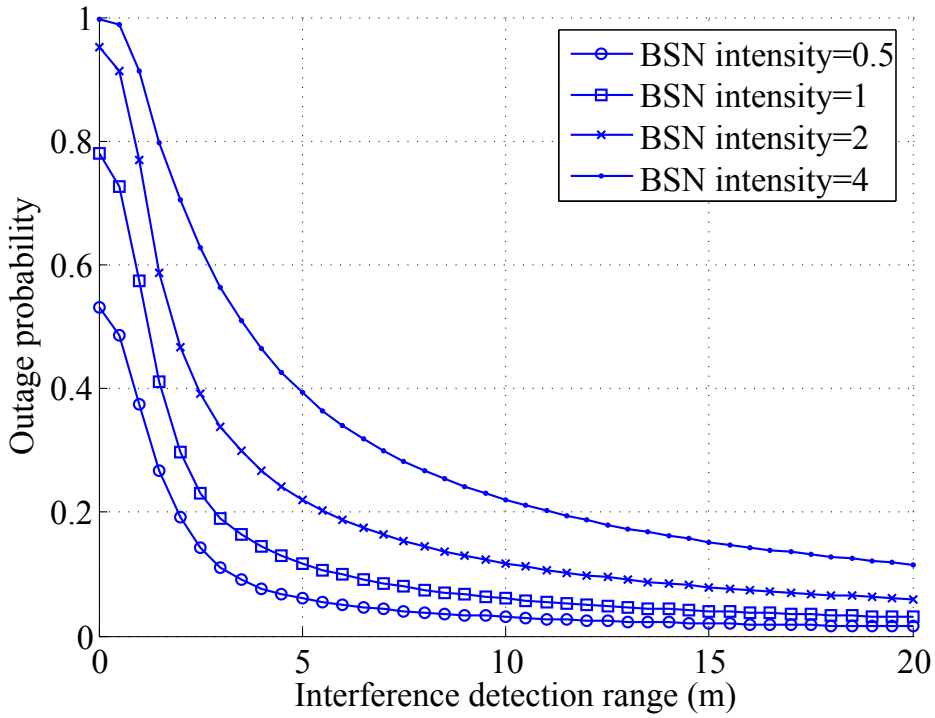

Fig. 6.5: Outage probability as a function of interference detection range when BSN intensity is 0.5, 1, 2, 4 and SINR threshold is 0 dB.

ment of spatial throughput. However, when w_1 increases to some extent (optimal point), the increment of contention-free traffic incurs severe outage, deteriorating spatial throughput. In addition, the optimal w_1 decreases when the BSN intensity increases. This is because when the BSN intensity is low, it is beneficial to use contention-free mechanism to improve the number of simultaneous transmissions. On the other hand, when the BSN intensity is high, contention-based mechanism is more suitable to alleviate collisions.

Based on the analysis, we are able to determine the optimal ratio of contention-based mechanism and contention-free mechanism w_1 not only depending on the data characteristics, i.e., determined or random traffic, but also on the specific BSN intensity.

Similarly, we are able to maximize the spatial throughput by adjusting the

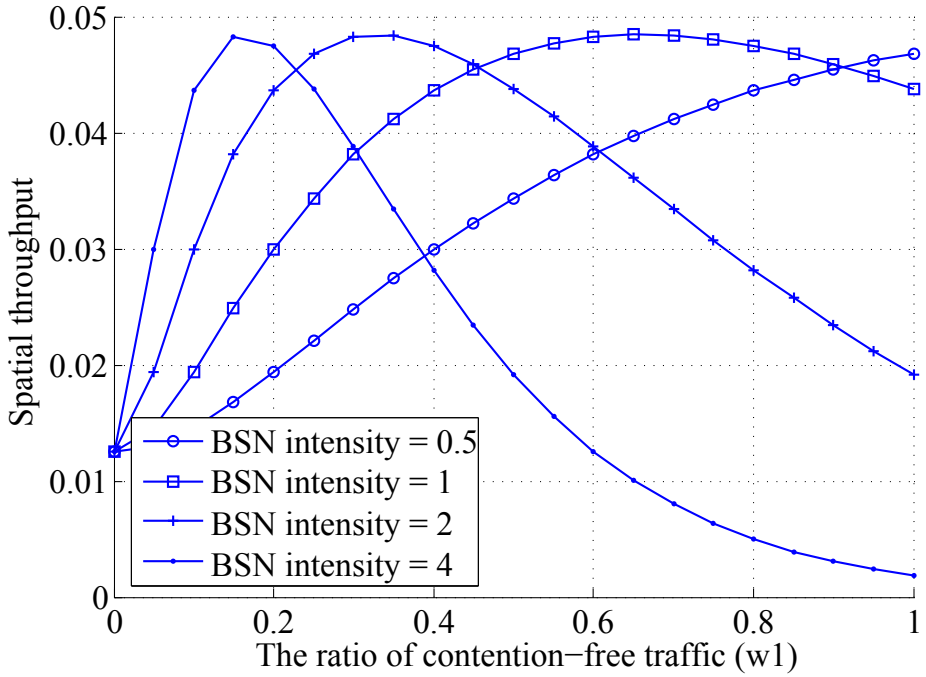

Fig. 6.6: The spatial throughput as a function of the ratio of contention-free traffic w_1.

BSN deployment, i.e. BSN intensity, given the MAC design of a BSN. Fig. 6.7 shows the spatial throughput as a function of BSN intensity given the traffic allocation w_1. As can be seen, for higher w_1, the maximum BSN intensity is lower. This is because when the number of BSNs under contention-free scheme is large, the BSN intensity should be kept low to ensure the reliable transmission. For a specific w_1, there exists an optimal BSN intensity to achieve the maximum spatial throughput. In practice, we choose to adjust the parameter, i.e. either the traffic allocation or the BSN intensity, which is more convenient, given other parameters fixed, to achieve maximum spatial throughput.

6.4 Validation by simulation

We investigate the performance of BSNs in the presence of inter-user interference using the network simulator QualNet 5.0.2. The simulation results are compared with the analytical results to validate the analysis.

6.4.1 Simulation settings

In the simulation, a coordinator and a sensor node form a BSN. The distance between the coordinator and sensor node in a BSN is 1 meter. The radio settings are configured according to the IEEE 802.15.6 standard [81]. In this study, we consider an on-body path-loss model with an exponent of α_O and an inter-body path-loss model with an exponent of α_I, shown in Table 6.1. The radio signal is

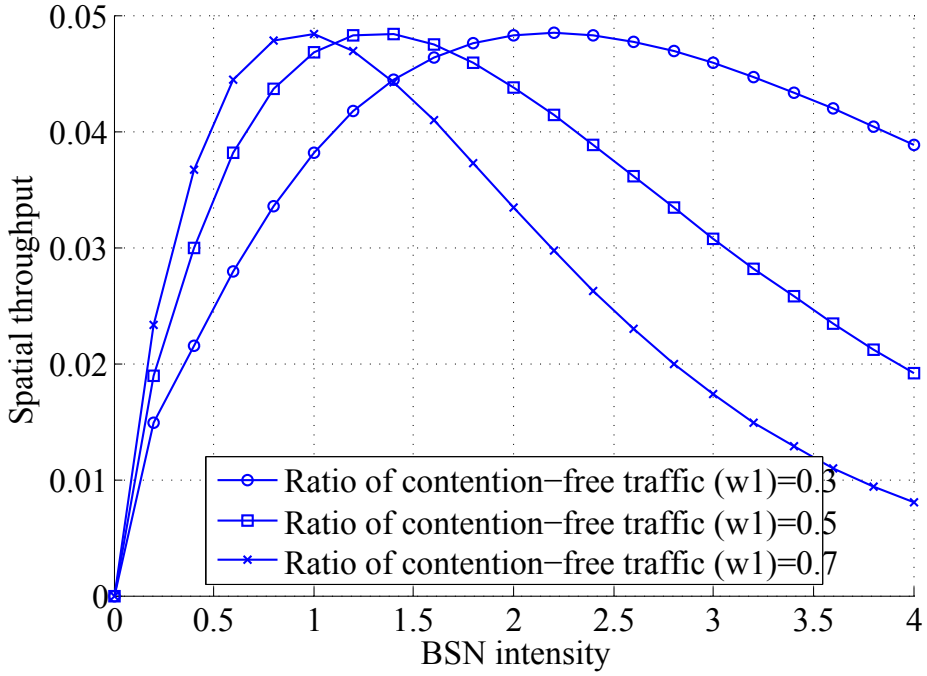

Fig. 6.7: Spatial throughput as a function of BSN intensity under different ratios of contention-free traffic (w1).

Table 6.1: The parameter settings of the simulation in interference analysis.

Transmission power Ω_0 (dBm)	-10
BSN density λ (# of BSNs per square meter)	1
Duty cycle of a BSN η (%)	20
Noise level Ω_n (dBm)	-30
Rate parameter of shadow fading μ (dB)	6.2
On-body path-loss exponent α_O	3.6
Inter-body path-loss exponent α_I	3
The distance between coordinator and sensor node r (m)	1
SINR threshold β (dB)	5~15

also deteriorated with Rayleigh fading with standard deviation of 6.2 dB [110]. The traffic load and traffic allocation for all the BSNs are set the same.

According to the comprehensive survey [4, 5], BSN intensity varies from 0.1 to 5 (BSNs per unit area) depending on the specific BSN application. Each BSN moves according to the random waypoint model [101]. Initially, all BSNs are uniformly deployed and then they move independently. To remove the effect of differing initial conditions on performance, we run the simulation fifty times with different initial conditions and then calculate the average results. The related parameters are listed in Table 6.1.

6.4.2 Simulation results

The intensity of the interfering BSNs

Fig. 6.8 compares the intensity of the interfering BSNs obtained through simulation with that obtained through analysis by Eqn. (6.5). As can be seen, the

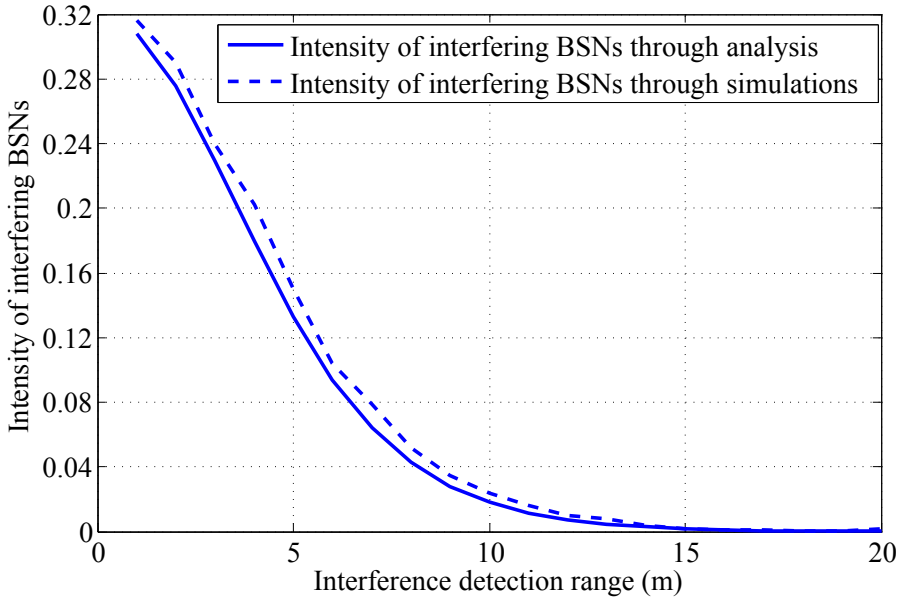

Fig. 6.8: Comparison of intensity of the interfering BSNs obtained through analysis and simulations.

analytical results are a bit lower than the actual results. This is because Matern point process is a conservative model as it underestimates the following case. Suppose that BSN1, BSN2, and BSN3 congregate together, BSN1 is silenced by its only neighbor BSN2, whereas BSN2 is in turn actually silenced by its neighbor BSN3. In the Matern model, BSN1 and BSN2 will not be retained, but if BSN1 and BSN3 are not neighbors and BSN3 has only BSN2 as neighbor, then CSMA/CA will allow BSN1 and BSN3 to transmit simultaneously. In [130], it is shown that only 78% of the transmitting nodes can be appropriately modeled. In our modified Matern point process, this underestimation still exists, and thus the modified Matern point process is conservative as well. It shows an improvement as compared with the classic Matern point process, because the intensity also comprises the BSNs under contention-free scheme which is comprehensive modeled in the analysis.

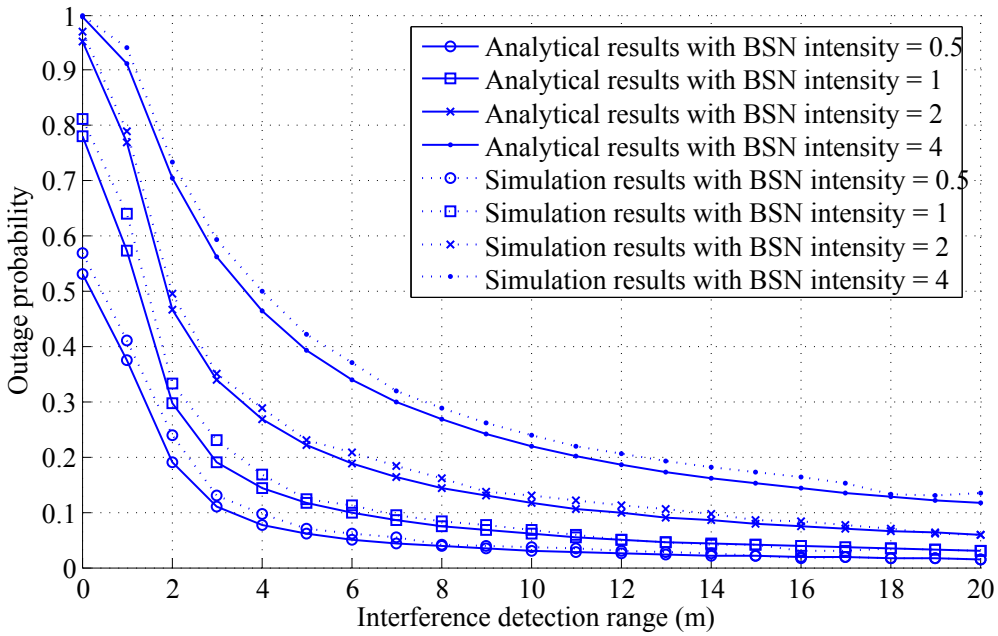

Fig. 6.9: Comparison of outage probability obtained through analysis and simulations.

Outage probability

Fig. 6.9 compares the outage probability of the interfering BSNs through simulations with that obtained through analysis. Each curve represents a scenario with a certain BSN intensity. As can be seen, the simulation results are close to the analytical results, which validates the approximation of ignoring the dependence between BSNs which are interference detection range away from the tagged BSN. This is because although all the interferers contribute to the interference, the nearest interfering BSNs dominates the inter-user interference. It is also noted that the actual outage probability is a bit higher than the analytical results due to the conservation of the modified Matern point process.

6.5 Summary

In this chapter, we have presented a stochastic geometry analysis of the inter-user interference in IEEE 802.15.6 BSNs. The framework considers BSN interferers which are spatially scattered according to a Poisson point process and transmit using either contention-free or contention-based MAC mechanism according to the IEEE 802.15.6 standard. Outage probability and spatial throughput are derived in traceable expressions. Based on the analysis, two implications are given: 1) The interference detection threshold is optimized to achieve the maximum spatial throughput while the reliable transmission requirement is met. 2) The design of MAC for BSNs is optimized depending on the specific BSN applications.

Chapter 7

Conclusion and Future Work

In this thesis, we have devoted our research efforts to improving performance of body sensor networks (BSNs) in moderate-scale deployment scenarios. Particularly, we first conduct a preliminary study on and propose a handover scheme to improve the inter-BSN communication (between the coordinator of a BSN and the network interface), and then perform an in-depth investigation on and mitigate the inter-user interference in BSNs to improve the intra-BSN communication (between sensor nodes and the coordinator in a BSN). In this final chapter, we summarize our work and suggest several areas that merit future research.

7.1 Handover scheme

We have proposed an improved handover scheme with movement trend awareness for BSNs. The proposed scheme predicts the future position of a BSN user using the movement trend extracted from its historical position, and adjusts the handover decision accordingly. Handover initiation time is optimized when the outage probability is minimized and the predicted unnecessary handover probability meets the requirement. As handover decision is made in advance, it is

beneficial for network management and channel reservation. The simulation results showed that the proposed handover scheme reduces the outage probability by 21% as compared with the existing hysteresis-based handover scheme under the constraint of acceptable handover rate. Moreover, when the geometric information of the BSN deployment area is known, the performance of the proposed handover scheme is further improved. The proposed handover scheme could incorporate any of the existing localization schemes as long as the movement trend of the BSN user could be obtained. In the case where the localization information is known beforehand, the overhead of our proposed handover scheme is further reduced.

In the future work, we will employ the proposed handover scheme in some existing localization system to improve the flexibility of the proposed handover scheme. In addition, we will develop more complex movement trend considering the spatial dependence of a BSN user in an constraint BSN application area to achieve further performance improvement.

7.2 A case study on inter-user interference

We have investigated the significance of the inter-user interference using a case study in a moderate-scale BSN deployment scenario in hospital. Simulation results show that, with 20% duty cycle, only 21.9% data packets can be transmit with a packet error rate (PER) lower than 0.05 at the peak time. Even at the off-peak time, only 68.5% can be transmit reliably. Thus inter-user interference exists widely and severely in such a deployment scenario. Based on the investigation, the BSN deployment configurations such as maximum BSN number that can be accommodated and the maximum tolerable traffic load can be easily determined. In addition, inter-user interference mitigation schemes are suggested based on the

specified scenario.

Besides the average PER of BSNs studied in this thesis, contact duration is another metric to characterize inter-user interference. Contact duration is defined as the duration that a BSN interferes with its neighboring BSNs, and its distribution over various number of interfering BSNs also concerns. It determines how frequently an interference mitigation scheme is initiated and the interference situation. Both PER of BSNs and contact duration determine the performance of the mitigation scheme for inter-user interference in BSNs, and thus give implications on the design of the interference mitigation scheme. In the current chapter, as mobility is not considered, we leave the investigation on contact duration to future work.

7.3 Interference mitigation

We have proposed a lightweight and distributed scheme (IIM) for mitigating inter-user interference in BSNs. The proposed scheme considers the generic property of low channel utilization of BSNs and enables BSNs to adaptively reschedule their transmission time or channels when the interference occurs. Based on the neighboring information, two actions are conducted: 1) BSNs reschedule their transmissions in a coordinated manner to reduce the rescheduling cost when the channel utilization is low. 2) When the channel is fully-occupied, channel switching decision can be made promptly so that wireless channels can be effectively utilized. The simulation results showed that the proposed IIM scheme outperforms the basic scheme and the beacon schedule scheme in terms of throughput and energy efficiency. The results confirm that when the density of BSNs becomes higher, the performance improvement of the IIM scheme are more significant. Although IIM

is designed for the beacon-enabled IEEE 802.15.4 protocol in this study, it can also be implemented in other BSN communication schemes (e.g., IEEE 802.15.6 MAC protocol) as long as a beacon packet is involved to synchronize the transmissions of the sensor nodes.

In future work, we will provide a profound performance analysis on the proposed IIM scheme by investigating the suitable models for arrivals of BSNs and their traffic patterns. It is challenging because the performance of a BSN highly relies on the arrival of its neighboring BSNs (number and timing of the arriving BSNs depending on the mobility of BSNs) and their traffic pattern, i.e., how they overlap with the BSN of interest. The widely used Poisson point process may not be appropriate because the number of BSN arrivals within the interference range of a BSN is not large enough. Thus in the performance analysis part of the IIM scheme, we only showed that our algorithm maximized the performance of a BSN given the interference situation in terms of minimizing the number of rescheduling times as well as the length of the rescheduling delays. Moreover, we will also implement IIM in an actual BSN system and evaluate the performance with extensive experiments.

7.4 Interference analysis

We have presented a stochastic geometry analysis of the inter-user interference in IEEE 802.15.6 BSNs. The framework considers BSN interferers which are spatially scattered according to a Poisson point process and transmit using either contention-free or contention-based media access control (MAC) mechanism according to the IEEE 802.15.6 standard. Outage probability and spatial throughput are derived in traceable expressions. Based on the analysis, two impli-

cations are given: 1) The interference detection threshold is optimized to achieve the maximum spatial throughput while the reliable transmission requirement is met. 2) The design of MAC for BSNs is optimized depending on the specific BSN applications. Although the stochastic geometry analysis is designed for inter-user interference in BSNs in this thesis, it can also be implemented in heterogeneous networks where various MAC mechanisms are employed.

We suggest two future directions based on this work. Firstly, we will employ realistic on-body and inter-body channel model in the interference analysis which are obtained from extensive experiments. In this thesis, we provide a general model with the on-body path-loss exponent. In the future work, we will study the variance between individuals and their effects on the performance of a BSN. For on-body channel model, it highly relies on the specific characteristics of the BSN user, e.g. male, female, fat, thin, etc. With different on-body channel model, the detection threshold to achieve the target outage probability differs from each BSN. Secondly, we will compare the spatial average performance of BSNs achieved in this analysis with that obtained through simulation in a certain specific BSN deployment scenario to capture the practical significance of the analysis.

Bibliography

[1] G. Z. Yang, *Body Sensor Networks*. Springer, 2006.

[2] Q. Fang, S. Lee, H. Permana, K. Ghorbani, and I. Cosic, "Developing a wireless implantable body sensor network in MICS band," *IEEE Transaction on Information Technology in Biomedicine*, vol. 15, no. 4, pp. 567–576, 2011.

[3] S. Movassaghi, M. Abolhasan, J. Lipman, and D. Smith, "Wireless body area networks: a survey," *IEEE Communications Surveys and Tutorials*, vol. 6, no. 99, pp. 1–29, 2014.

[4] B. Latre, B. Braem, I. Moerman, C. Blondia, and P. Demeester, "A survey on wireless body area networks," *Wireless Networks*, vol. 17, no. 1, pp. 1–18, 2011.

[5] O. Omeni, A. Wong, A. Burdett, and C. Toumazou, "Energy efficient medium access protocol for wireless medical body area sensor networks," *IEEE Transaction on Biomedical Circuits and Systems*, vol. 2, no. 4, pp. 251–259, 2008.

[6] G. Zhou, J. Lu, C. Wan, M. D. Yarvis, and J. A. Stankovic, "BodyQoS: Adaptive and radio-agnostic QoS for body sensor networks," in *Proc. IEEE INFOCOM*, (Phoenix, AZ, USA), Apr. 2008.

[7] A. Pantelopoulos and N. G. Bourbakis, "A survey on wearable sensor-based systems for health monitoring and prognosis," *IEEE Transaction on System, Man, and Cybernetics*, vol. 40, no. 1, pp. 1–12, 2010.

[8] M. Yuce, S. W. Ng, N. Myo, J. Khan, and W. Liu, "Wireless body sensor network using medical implant band," *Journal of Medical Systems*, vol. 31, no. 6, pp. 467–474, 2007.

[9] B. Otal, L. Alonso, and C. Verikoukis, "Highly reliable energy-saving MAC for wireless body sensor networks in healthcare systems," *IEEE Jounal on Selected Area in Communications*, vol. 27, no. 4, pp. 553–565, 2009.

[10] H. Li and J. Tan, "Heartbeat-driven medium-access control for body sensor networks," *IEEE Transactions on Information Technology in Biomedicine*, vol. 14, no. 1, pp. 44–51, 2010.

[11] S. Ullah, H. Higgins, B. Braem, B. Latre, C. Blondia, I. Moerman, *et al.*, "A comprehensive survey of wireless body area networks," *Journal of Medical Systems*, vol. 36, no. 3, p. 1065, 2012.

[12] J. Khan, M. Yuce, G. Bulger, and B. Harding, "Wireless body area network design techniques and performance evaluation," *Journal of Medical System*, vol. 36, no. 3, pp. 1441–1457, 2012.

[13] L. Wang, T. Gu, X. Tao, and J. Lu, "A hierarchical approach to real-time activity recognition in body sensor networks," *Pervasive and Mobile Computing*, vol. 8, no. 1, pp. 115–130, 2012.

[14] C. Wu and Y. Tseng, "Data compression by temporal and spatial correlations in body-area sensor network: A case study in pilates motion recognition," *IEEE Transactions on Mobile Computing*, vol. 10, no. 10, pp. 1459–1472, 2011.

[15] H. Lin, V. Jilkov, and D. Lin, "Validation of an improved location-based handover algorithm using gsm measurement data," *IEEE Transaction on Mobile Computing*, vol. 4, pp. 530–536, 2005.

[16] T. Inzerilli, A. Vegni, A. Neri, and R. A. Cusani, "A cross-layer location-based approach for mobile-controlled connectivity," in *Journal of Digital Multimedia Broadcasting*, pp. 1–13, 2011.

[17] W. Lee, E. Kim, J. Kim, I. Lee, and C. Lee, "Movement-aware vertical handoff of wlan and mobile wimax for seamless ubiquitous access," *IEEE Transaction on Consumer Electronics*, vol. 53, pp. 1268–1275, 2007.

[18] S. Michaelis and C. Wietfeld, "Comparison of user mobility pattern prediction algorithms to increase handover trigger accuracy," in *IEEE VTC*, pp. 952–956, 2006.

[19] A. Zhang, D. Smith, D. Miniutti, L. Hanlen, D. Rodda, and B. Gilbert, "Performance of piconet co-existence schemes in wireless body area networks," in *Proc. IEEE WCNC*, pp. 1–6, Apr. 2010.

[20] A. Natarajan, B. De Silva, K. Yap, and M. Motani, "To hop or not to hop: Network architecture for body sensor networks," in *Proc. IEEE SECON*, (Rome, Italy), Jun. 2009.

[21] B. Cao, Y. Ge, C. Kim, G. Feng, and H. Tan, "An experimental study for inter-user interference mitigation in wireless body sensor networks," *IEEE Sensors Journal*, vol. 13, pp. 3585–3595, 2013.

[22] A. Natarajan, M. Motani, B. d. Silva, K. Yap, and K. Chua, "Investigating network architectures for body sensor networks," in *Proc. ACM SIGMOBILE 2007*, (San Juan, Puerto Rico), Jun. 2007.

[23] G. Bianchi, "Performance analysis of the IEEE 802.11 distributed coordination function," *IEEE Journal on Selected Areas in Communicatios*, vol. 18, no. 3, pp. 535–547, 2000.

[24] S. Marinkovic, E. Popovici, C. Spagnol, S. Faul, and W. Marnane, "Energy-efficient low duty cycle MAC protocol for wireless body area networks," *IEEE Transaction on Information Technology in Biomedicine*, vol. 13, no. 6, pp. 915–925, 2009.

[25] M. Cao, W. Ma, Q. Zhang, and X. Wang, "Analysis of IEEE 802.16 mesh mode scheduler performance," *IEEE Transaction on Wireless Communications*, vol. 6, no. 4, pp. 1455–1464, 2007.

[26] Y. Ge, C. Tham, P. Kong, and Y. Ang, "Dynamic end-to-end capacity in IEEE 802.16 wireless mesh networks," *Computer Networks Journal (Elsevier)*, vol. 54, no. 13, pp. 2147–2165, 2010.

[27] W. Ye, J. Heidemann, and D. Estrin, "Medium access control with coordinated adaptive sleeping for wireless sensor networks," *IEEE/ACM Transaction on Networking*, vol. 12, no. 3, pp. 493–506, 2004.

[28] A. Hoiydi, J. Decotignie, C. Enz, and E. Roux, "WiseMAC: an ultra low power MAC protocol for the wisenet wireless sensor networks," in *Proc. ACM SenSys*, (Los Angeles, CA), Apr. 2003.

[29] A. Annie Uthra and S. Kasmir Raja, "QoS routing in wireless sensor network-A survey," *ACM Computing Surveys*, vol. 45, no. 1, pp. 56–61, 2013.

[30] T. Wu and S. Biswas, "Minimizing inter-cluster interference by self-reorganizing MAC allocation in sensor networks," *Wireless Networks*, vol. 13, no. 5, pp. 691–703, 2007.

[31] A. Koubaa, A. Cunha, and M. Alves, "A time division beacon scheduling mechanism for IEEE 802.15.4/Zigbee cluster-tree wireless sensor networks," in *Proc. Euromicro Conference on Real-Time Systems 2007*, (Pisa, Italy), Oct. 2010.

[32] H. Eisawy, E. Hossain, and M. Haenggi, "Stochastic geometry for modeling, analysis, and design of multi-tier and cognitive cellular wiereless networks: a survey," *IEEE Communication Surveys and Tutorials*, vol. 15, pp. 996–1019, 2013.

[33] D. Renzo, M. Merola, A. Guidotti, F. Santucci, and G. Corazza, "Error performance of multi-antenna receivers in a poisson field of interfers: a stochastic geometry approach," *IEEE Transactions on Communications*, vol. 61, pp. 2025–2047, 2013.

[34] K. Huang and J. Andrew, "A stochastic-geometry approach to coverage in cellular networks with multi-cell cooperation," in *IEEE GLOBECOM*, pp. 1–5, 2011.

[35] H. Eisawy, E. Hossain, and S. Camorlinga, "Multi-channel design for random csma wireless networks: a stochastic geometry approach," in *IEEE ICC*, pp. 1656–1660, 2013.

[36] M. Haenggi, *Stochastic geometry for wireless networks*. Cambridge University Press, 2012.

[37] F. Baccelli, F. Blaszczyszyn, and P. Muhlethaler, "An aloha protocol for multihop mobile wireless networks," *IEEE Transaction on Information Theory*, vol. 52, pp. 421–436, 2006.

[38] Z. Gong and M. Haenggi, "Interference and outage in mobile random networks: expectation, distribution, and correlation," *IEEE Transaction on Mobile Computing*, vol. 1, pp. 1–14, 2012.

[39] H. Nguyen, F. Baccelli, and D. Kofman, "A stochastic geometry analysis of dense IEEE 802.11 networks," in *Proc. IEEE INFOCOM*, (Anchorage, USA), May 2007.

[40] C. Wu and Y. Tseng, "Data compression by temporal and spatial correlations in a body-area sensor network: a case study in pilates motion recognition," *IEEE Transaction on Mobile Computing*, vol. 10, pp. 1459–1472, 2011.

[41] R. Cavallari, F. Martelli, R. Rosini, C. Buratti, and R. Verdone, "A survey on wireless body area networks: technologies and design challenges," *IEEE Communications Surveys and Tutorials*, vol. 99, pp. 1–23, 2014.

[42] B. Liu, Z. Yan, and C. Chen, "Mac protocol in wireless body area networks for e-health: challenges and a context-aware design," *IEEE Wireless Communications*, vol. 20, pp. 64–72, 2013.

[43] L. Shi, M. Li, S. Yu, and J. Yuan, "Bana: body area network authentication exploiting channel characteristics," *IEEE Journal on Selected Areas in Communications*, vol. 31, no. 9, pp. 1803–1816, 2013.

[44] C. Ho, T. See, and M. Yuce, "An ultra-wideband wireless body area network: evaluation in static and dynamic channel conditions," *Sensors and Actuators A: Physical*, no. 180, pp. 137–147, 2012.

[45] R. Marin-Perianu, M. Marin-Perianu, P. Havinga, S. Taylor, R. Begg, M. Palaniswami, and D. Rouffet, "A performance analysis of a wireless body-area network monitoring system for professional cycling," *Journal of Personal and Ubiquitous Computing (Springer)*, vol. 17, no. 1, pp. 197–209, 2013.

[46] B. Shrestha, E. Hossain, and S. Camorlinga, "Ieee 802.15.4 mac with gts transmission for heterogeneous devices with application to wheelchair body-area sensor networks," *IEEE Transaction on Information Technology in Biomedicine*, vol. 15, pp. 767–777, 2011.

[47] F. Cuomo, A. Abbagnale, and E. Cipollone, "Cross-layer network formation for energy-efficient IEEE 802.15.4/ZigBee wireless sensor networks," *Ad Hoc Networks*, vol. 11, no. 2, pp. 672–686, 2013.

[48] W. Yuan, X. Wang, J. Linnartz, and I. Niemegeers, "Coexistence performance of IEEE 802.15.4 wireless sensor networks under IEEE 802.11 b/g interference," *Wireless Personal Communications*, vol. 68, no. 2, pp. 281–302, 2013.

[49] S. Jiang, Y. Cao, S. Lyengar, P. Kuryloski, R. Jafari, Y. Xue, R. Bajcsy, and S. Wicker, "CareNet: an integrated wireless sensor networking environment for remote healthcare," in *Proc. International conference on body area networks*, (Tempe, Arizona), Jun. 2008.

[50] K. Kwak, S. Ullah, and N. Ullah, "An overview of ieee 802.15. 6 standard," in *IEEE Symposium on Applied Sciences in Biomedical and Communication Technologies*, pp. 52–55, Jun. 2010.

[51] S. Rashwand and J. Misic, "Effects of access phases lengths on performance of ieee 802.15.6 csma/ca," *Computer Networks (Elsevier)*, vol. 56, pp. 2832–2846, 2012.

[52] M. Johann, C. Calafate, J. Cano, and P. Manzoni, "An overview of vertical handover techniques: algorithms, protocols and tools," *Computer Communications*, vol. 34, pp. 985–997, 2011.

[53] T. Rappaport, *Wireless Communications: Principles and Practice*. NJ: Prentice-Hall, 2001.

[54] D. Xenakis, N. Passas, L. Merakos, and C. Verikoukis, "Mobility management for femtocells in lte-advanced: key aspects and survey of handover decision algorithms," *IEEE Communications Survey and Tutorials*, vol. 16, pp. 64–91, 2014.

[55] M. Halgamuge, H. Vu, K. Ramamohanarao, and M. Zukerman, "Signal-based evaluation of handoff algorithms," *IEEE Communications Letters*, vol. 9, no. 9, pp. 790–793, 2005.

[56] R. Hansen, R. Wind, C. Jensen, and B. Thomsen, "Seamless indoor/outdoor positioning handover for location-based services in streamspin," in *IEEE Conference in Mobile Data Management: Systems, Services and Middleware*, pp. 267–272, 2009.

[57] T. Wu, C. Lai, and H. Chao, "Efficient ieee 802.11 handoff based on a novel geographical fingerprint scheme," *Wireless Communications and Mobile Computing*, vol. 6, pp. 127–135, 2006.

[58] J. Lee, S. Pack, T. Kwon, and Y. Choi, "Reducing handover delay by location management in mobile WiMAX multicast and broadcast services," *IEEE Transaction on Vehicular Technology*, vol. 60, no. 2, pp. 605–617, 2011.

[59] P. Tseng and K. Feng, "Location tracking assisted handover algorithms for broadband wireless networks," in *IEEE PIMRC*, pp. 1–5, 2008.

[60] M. Youssef and A. Agrawala, "Handling samples correlation in the horus system," in *IEEE INFOCOM*, pp. 1023–1031, 2004.

[61] C. Wu, Z. Yang, Y. Liu, and W. Xi, "Will: Wireless indoor localization without site survey," in *IEEE INFOCOM*, pp. 64–73, 2012.

[62] M. Almulla, Y. Wang, A. Boukerche, and Z. Zhang, "Design of a fast location-based handoff scheme for ieee 802.11 networks," *IEEE Transaction on Vehicle Technology*, vol. 52, no. 1, pp. 317–325, 2013.

[63] X. Yun, J. Calusdian, E. Bachmann, and R. McGhee, "Estimation of human foot motion during normal walking using inertial and magnetic sensor measurements," *IEEE Transaction on Instrumentation and Measurement*, vol. 61, no. 7, pp. 2059–2072, 2012.

[64] Y. Jin, H. Toh, W. Soh, and W. Wong, "A robust dead-reckoning pedestrian tracking system with low cost sensors," in *PerCom*, pp. 222–230, 2011.

[65] Y. Jin, W. Soh, M. Motani, and W. Wong, "A robust indoor pedestrian tracking system with sparse infrastructure support," *IEEE Transaction on Mobile Computing*, vol. 52, no. 1, pp. 317–325, 2013.

[66] L. Ni, D. Zhang, and M. Souryal, "RFID-based localization and tracking technologies," *IEEE Transaction on Fuzzy Systems*, vol. 18, no. 2, pp. 45–51, 2011.

[67] J. Rantakokko, J. Rydell, P. Stromback, P. Handel, J. Callmer, D. Tornqvist, F. Gustafsson, M. Jobs, and M. Gruden, "Accurate and reliable soldier and first responder indoor positioning: multisensor systems and cooperative localization," *IEEE Wireless Communications*, vol. 18, no. 2, pp. 10–18, 2011.

[68] Y. Chen, D. Lymberopoulos, J. Liu, and B. Priyantha, "Indoor localization using FM signals," *IEEE Transaction on Mobile Computing*, vol. 12, no. 8, pp. 1502–1517, 2013.

[69] T. Garcia-Valverde, A. Garcia-Sola, and J. Dooley, "A fuzzy logic-based system for indoor localization using WiFi in ambient intelligent environments," *IEEE Transaction on Fuzzy Systems*, vol. 21, no. 4, pp. 702–718, 2013.

[70] Y. Lin, C. Huang-Fu, and N. Alrajeh, "Predicting human movement based on telecom's handoff in mobile networks," *IEEE Transaction on Mobile Computing*, vol. 12, no. 6, pp. 1236–1242, 2013.

[71] S. Hasan, C. Schneider, S. Ukkusuri, and M. Gonzalez, "Spatiotemporal patterns of urban human mobility," *Journal of Statistical Physics (Springer)*, vol. 151, pp. 304–318, 2013.

[72] G. V. Sergio and M. Chen, "Mobility support for health monitoring at home using wearable sensors," *IEEE Transaction on Information Technology in Biomedicine*, vol. 15, no. 4, pp. 539–549, 2011.

[73] B. d. Silva, A. Natarajan, and M. Motani, "Inter-user interference in body sensor networks: preliminary investigation and an infrastructure-based solution," in *Proc. International Workshop on Wearable and Implantable Body Sensor Networks 2009*, (Berkeley, CA), Jun. 2009.

[74] S. Sengupta, M. Chatterjee, and K. Kwiat, "A game theoretic framework for power control in wireless sensor networks," *IEEE Transactions on Computers*, vol. 59, no. 2, pp. 231–242, 2010.

[75] G. Wu, J. Ren, F. Xia, L. Yao, and Z. Xu, "DISG: decentralized inter-user interference suppression in body sensor networks with non-cooperative game," in *Proc. ATC 2010*, (Xian, China), Jul. 2010.

[76] T. Kim, H. Lim, and J. Hou, "Improving spatial reuse through tuning transmit power, carrier sense threshold, and data rates in multihop wireless networks," in *Proc. ACM MOBICOM*, (Los Angeles, USA), Sep. 2006.

[77] Z. Zhang, H. Wang, C. Wang, and H. Fang, "Interference mitigation for cyber-physical wireless body area network system using social networks," *IEEE Transaction on Emerging Topics in Computing*, vol. 1, no. 1, pp. 121–134, 2013.

[78] N. A. Pantazis and D. D. Vergados, "A survey on power control issues in wireless sensor networks," *IEEE Communications Surveys and Tutorials*, vol. 9, no. 4, pp. 86–107, 2007.

[79] 2012. IEEE standard for local and metropolitan area networks–Part 15.6: Wireless body area networks, Available: http://ieee802.org/15/pub/TG6.html.

[80] S. Ulah and K. Kwak, "Throughput and delay limits of ieee 802.15.6," in *IEEE WCNC*, pp. 174–178, 2011.

[81] H. Li and R. Kohno, *Body area network and its standardization at IEEE 802.15 BAN*. Springer, 2008.

[82] S. Kim, J. W. Kim, and D. S. Eom, "Flexible beacon scheduling scheme for interference mitigation in body sensor networks 2012," in *Proc. IEEE SECON*, (Seoul, Korea), Jun. 2012.

[83] Y. Liang, Y. Zeng, E. Peh, and A. Hoang, "Sensing-throughput tradeoff for cognitive radio networks," *IEEE Transaction on Wireless Communications*, vol. 7, no. 4, pp. 1326–1337, 2008.

[84] R. Hekmat and P. Van Mieghem, "Interference in wireless multi-hop ad-hoc networks and its effect on network capacity," *Wireless Networks*, vol. 10, no. 4, pp. 389–399, 2004.

[85] P. Gupta and P. Kumar, "The capacity of wireless networks," *IEEE Transaction on Information Theory*, vol. 46, no. 2, pp. 388–404, 2000.

[86] P. Li and Y. Fang, "Impacts of topology and traffic pattern on capacity of hybrid wireless networks," *IEEE Transaction on Mobile Computing*, vol. 8, pp. 1585–1595, Dec. 2009.

[87] X. Wang and L. Cai, "Interference analysis of co-existing wireless body area networks," in *Proc. IEEE GLOBECOM*, (Houston, USA), Dec. 2011.

[88] R. Ganti, J. Andrews, and M. Haenggi, "High-SIR transmission capacity of wireless networks with general fading and node distribution," *IEEE Transaction on Information Theory*, vol. 57, no. 7, pp. 3100–3116, 2011.

[89] R. Giacomelli, R. Ganti, and M. Haenggi, "Outage probability of general ad hoc networks in the high-reliability regime," *IEEE/ACM Transaction on Networking*, vol. 9, no. 7, pp. 1151–1163, 2011.

[90] R. Ganti and M. Haenggi, "Interference in ad hoc networks with general motion-invariant node distributions," in *Proc. International Symposium on Information Theory*, pp. 1–6, Jul. 2008.

[91] P. Pinto, A. Giorgetti, M. Win, and M. Chiani, "A stochastic geometry approach to coexistence in heterogeneous wireless networks," *IEEE Journal on Selected Areas in Communications*, vol. 27, no. 7, pp. 1268–1282, 2009.

[92] F. Baccelli, F. Blaszczyszyn, and P. Muhlethaler, "An Aloha protocol for multihop mobile wireless networks," *IEEE Transaction on Information Theory*, vol. 52, no. 2, pp. 421–436, 2006.

[93] J. Andrew, F. Baccelli, and R. Ganti, "A tratable approach to coverage and rate in cellular networks," *IEEE Transaction on Communications*, vol. 59, pp. 3122–3134, 2011.

[94] D. Stoyan, W. Kendall, J. Mecke, and L. Ruschendorf, *Stochastic geometry and its applications*. Chichester: Wiley, 2013.

[95] R. Heath, M. Kountouris, and T. Bai, "Modeling heterogeneous network interference using Poisson point processes," *IEEE Transaction on Signal Processing*, vol. 61, no. 16, pp. 4114–4126, 2013.

[96] Z. Kong and E. Yeh, "On the latency for information dissemination in mobile wireless networks," in *Proc. ACM MobiHoc*, pp. 412–428, May 2008.

[97] M. Zignani, S. Gaito, and G. Rossi, "Extracting human mobility and social behavior from location-aware traces," *Wireless communications and mobile computing*, vol. 13, no. 3, pp. 313–327, 2013.

[98] J. Pansiot, B. Lo, and G. Yang, "Swimming stroke kinematic analysis with bsn," in *International Conference on Body Sensor Networks*, pp. 153–158, 2010.

[99] S. Sun, X. Meng, L. Ji, J. Wu, and W. Wong, "Adaptive sensor data fusion in motion capture," in *13th International Conference on Information Fusion*, pp. 1–8, 2010.

[100] D. Simon, "Kalman filtering," *Embedded Systems Programing*, vol. 14, pp. 72–79, 2001.

[101] X. Li and V. Jilkov, "Survey of maneuvering target tracking-part 1: dynamic models," *IEEE Transaction on Aerospace and Electronic Systems*, vol. 39, no. 4, pp. 1333–1364, 2003.

[102] J. S. John, *Probability, Random Variables, and Random Processes: Theory and Signal Processing Applications*. CRC, 2012.

[103] 2014. Matlab Simulator. Available: http://www.mathworks.com/products/matlab/.

[104] F. Bai and A. Helmy, "A survey of mobility models in wireless adhoc networks," *Wireless Adhoc Networks*, no. 206, pp. 1–30, 2004.

[105] Z. Xu, K. Sandrasegaran, X. Kong, X. Zhu, J. Zhao, B. Hu, and C. Lin, "Pedestrain monitoring system using Wi-Fi technology and RSSI based localization," *International Journal of Wireless and Mobile Networks*, vol. 5, no. 4, pp. 27–38, 2013.

[106] Y. Hao and R. Foster, "Wireless body sensor networks for health-monitoring applications," *Physiological Measurement*, vol. 29, no. 11, p. R27, 2008.

[107] E. Reusens, W. Joseph, G. Vermeeren, and L. Martens, "On-body measurements and characterization of wireless communication channel for arm and torso of human," in *Proc. International Workshop on Wearable and Implantable Body Sensor Networks*, (Aachen, Germany), Mar. 2007.

[108] Y. Zhao and Y. Hao, "A subject-specificity analysis of radio channels in wireless body area networks," *Engineering Journal*, vol. 15, pp. 40–47, 2011.

[109] A. EI Gamal and Y. Kim, *Network Information Theory*. Cambridge University Press, 2011.

[110] A. Molisch *et al.* IEEE 802.15.4a channel model-final report, IEEE P802.15.4: 0662, 2004.

[111] M. Chen, S. Gonzalez, A. Vasilakos, H. Cao, and V. C. M. Leung, "Body area networks: a survey," *ACM/Springer Mobile Networks and Applications*, vol. 16, no. 2, pp. 171–193, 2011.

[112] S. Kullback, *Information Theory and Statistics*. Courier Dover Publications, 2012.

[113] E. A. Lee and D. G. Messerschmitt, *Digital Communications*. Springer, 2004.

[114] D. W. Curtis, E. J. Pino, J. M. Bailey, E. I. Shih, J. Waterman, and S. A. Vinterbo, "SMART: an integrated wireless system for monitoring unattended patients," *Journal of the American Medical Informatics Association*, vol. 15, no. 1, pp. 44–53, 2008.

[115] D. Curtis, E. Pino, T. Stair, and L. Ohno-Machado, "Adding the human element: Experience with a wireless patient monitoring system," in *Wireless Sensor Networks Springer 2010*, (US), Aug. 2010.

[116] D. Curtis, E. Shih, J. Waterman, J. Guttag, J. Bailey, T. Stair, R. Greenes, and L. Ohno-Machado, "Physiological signal monitoring in the waiting areas of an emergency room," in *Proc. ACM BodyNets*, (Brussels, Belgium), Aug. 2008.

[117] E. Reusens, W. Joseph, and B. Latre, "Characterization of on-body communication channel and energy efficient topology design for wireless body area networks," *IEEE Transaction on Information Technology in Biomedicine*, vol. 13, no. 6, pp. 933–945, 2009.

[118] P. Park, S. Ergen, C. Fischione, and A. Sangiovanni-Vincentelli, "Duty-cycle optimization for IEEE 802.15.4 wireless sensor networks," vol. 10, no. 1, 2013.

[119] C. Li, H. Li, and R. Kohno, "Performance evaluation of IEEE 802.15.4 for wireless body area network (WBAN)," in *Proc. IEEE ICC Workshops*, (Dresden, Germany), Jun. 2009.

[120] C. Otto, A. Milenkovic, C. Sanders, and E. Jovanov, "System architecture of a wireless body area sensor network for ubiquitous health monitoring," *Journal of Mobile Multimedia*, vol. 1, no. 4, pp. 307–326, 2006.

[121] P. Baronti, P. Pillai, V. Chook, S. Chessa, A. Gotta, and Y. Hu, "Wireless sensor networks: A survey on the state of the art and the 802.15.4 and ZigBee standards," *Computer Networks Journal (Elsevier)*, vol. 30, no. 7, pp. 1655–1695, 2007.

[122] 2014. Qualnet Network. Available: http://www.qualnet.com.

[123] 2014. TelosB mote. Available: http://www.willow.co.uk.

[124] M. Patel and J. Wang, "Applications, challenges, and prospective in emerging body area networking technologies," *IEEE Wireless Communications*, vol. 17, no. 1, pp. 80–88, 2010.

[125] M. Seyedi, B. Kibret, D. Lai, and M. Faulkner, "A survey on intrabody communications for body area network applications," *IEEE Transaction on Biomedical Engineering*, vol. 60, no. 8, pp. 2067–2079, 2013.

[126] A. Michalopoulou, A. Alexandridis, K. Peppas, T. Zervos, F. Lazarakis, K. Dangakis, and D. Kaklamani, "Statistical analysis for on-body spatial diversity communications at 2.45 ghz," *IEEE Transactions on Antennas and Propagation*, vol. 60, no. 8, pp. 4014–4020, 2012.

[127] Z. Hu, Y. Nechayev, P. Hall, C. Constantinou, and Y. Hao, "Measurement and statistical analysis of on-body channel fading at 2.45 ghz," *IEEE Antennas and Wireless Propagation Letters*, vol. 6, pp. 612–616, 2007.

[128] D. Daley and D. Vere-Jones, *An Introduction to the Theory of Point Process: General Theory and Structure*. Springer, 2007.

[129] M. Haenggi, J. Andrew, F. Baccelli, O. Dousse, and M. Franceschitti, "Stochastic geometry and random graphs for the analysis and design of wireless networks," *IEEE Journal on Selected Areas in Communications*, vol. 27, no. 7, pp. 1029–1045, 2009.

[130] A. Busson, G. Chelius, and J. Gorce. "Interference modeling in CSMA multi-hop wireless networks", INRIA, France, Tech. Rep. 6624, Feb. 2009.

List of Publications

Journal papers

1. W. Sun, Y. Ge, and W. C. Wong, "A stochastic geometry analysis of inter-user interference in body sensor networks," submitted to *IEEE Transactions on Vehicular Technology*, Dec. 2013.

2. W. Sun, Y. Ge, and W. C. Wong, "A lightweight distributed scheme for mitigating inter-user interference in body sensor networks," *Computer Networks (Elsevier)*, vol. 57, no. 18, pp. 3885-3896, Dec. 2013.

3. W. Sun, Z. Zhang, L. Ji, and W.C. Wong, "An optimized handover scheme with movement trend awareness for body sensor networks," *Sensors,* vol. 13, no. 6, pp. 7308-7322, Jun. 2013.

Conference papers

1. W. Sun, Y. Ge, and W. C. Wong, "Performance analysis of body sensor networks using stochastic geometry in coexistence scenario," submitted to *GLOBECOM*, Mar. 2014.

2. W. Sun, Y. Ge, and W. C. Wong, "A lightweight inter-user interference mitigation method in body sensor networks," in *Proc. IEEE International Conference on Wireless and Mobile Computing, Networking and Communications (WiMob 2012),* pp. 34-40, Oct. 2012.

3. W. Sun, Y. Ge, and W. C. Wong, "Inter-user interference in body sensor networks: a case study in moderate-scale deployment in hospital environment," in *Proc. IEEE International Conference on E-health Networking, Applications, and Services (Healthcom 2012),* pp. 447-450, Oct. 2012.

4. W. Sun, L. Ji, and W. C. Wong, "Optimized handover strategy with movement trend awareness for body sensor networks," in *Proc. Elsevier International Conference on Ambient Systems, Networks and Technologies (ANT 2011),* pp. 255-263, Sep. 2011.